

ACOUSTIC NON-INVASIVE DIAGNOSIS OF
URINARY BLADDER OBSTRUCTION

Tim Idzenga

De omslagillustratie van de voorkaft is een replica van een erts van Rembrandt:

*B190, Het pissende mannetje, 1631
Ets, enige staat, 82 x 48 mm
Collectie Museum Het Rembrandthuis.*

Deze afbeelding geeft aan dat plassen (en dus ook plasklachten) iets is van alle lagen van de bevolking en dat een patiëntvriendelijke diagnose van plasklachten goed van pas zou komen.

This research is supported by the Dutch Technology Foundation STW, applied science division of NWO and the Technology Program of the Ministry of Economic Affairs.

De totstandkoming van het proefschrift werd mogelijk gemaakt met financiële ondersteuning van:

Technologiestichting STW
Stichting Urologisch Wetenschappelijk Onderzoek (SUWO)
Verathon Medical Europe BV
IQ+ Medical BV

© 2008 T. Idzenga, Breda, The Netherlands
ISBN 90-9022896-9

Printed by PrintPartners Ipskamp, Enschede, The Netherlands

Acoustic Non-invasive Diagnosis of Urinary Bladder Obstruction

Akoestische niet-invasieve diagnose van urineblaas obstructie

Proefschrift

ter verkrijging van de graad van doctor aan de
Erasmus Universiteit Rotterdam
op gezag van de
rector magnificus

Prof.dr. S.W.J. Lamberts

en volgens besluit van het College voor Promoties
De openbare verdediging zal plaatsvinden op

Woensdag 16 april 2008 om 15.45 uur

door

Tim Idzenga

geboren te Nijmegen



Promotiecommissie

Promotor: Prof.dr.ir. R. van Mastrigt

Overige leden: Prof.dr.ir. N. de Jong
Prof.dr. B.J.M. Heijmen
Prof.dr. W.L.C. Rutten

Copromotor: Dr.ir. J.J.M. Pel

Listen to the river and you will always catch a trout
–John 'Hannibal' Smith as *Sean O'Shay III* –

Contents

1	Introduction	11
2	Development of Perineal sound Recording as a non-invasive method for diagnosis of Bladder Outlet Obstruction	21
3	Perineal sound recording as a non-invasive diagnostic method of urinary bladder outlet obstruction: a study in Polyvinyl Alcohol and silicone model urethras	37
4	A biophysical model of the male urethra: comparing viscoelastic properties of PolyVinyl Alcohol urethras to male pig urethras	51
5	Is the impaired flow after hypospadias correction due to increased urethral stiffness?	69
6	Fluid perfused Urethral Pressure Profilometry and Valsalva Leak Point Pressure: a comparative study in a biophysical model of the urethra	79
7	Towards an acoustic non-invasive diagnosis of urinary bladder outlet obstruction	93
8	Variability and repeatability of perineal sound recording in a population of healthy male volunteers	109
9	General discussion	121
	Summary	131
	Samenvatting	137
	Nawoord	143
	Curriculum vitae	147

Chapter 1

Chapter 1

Introduction

Male urinary tract

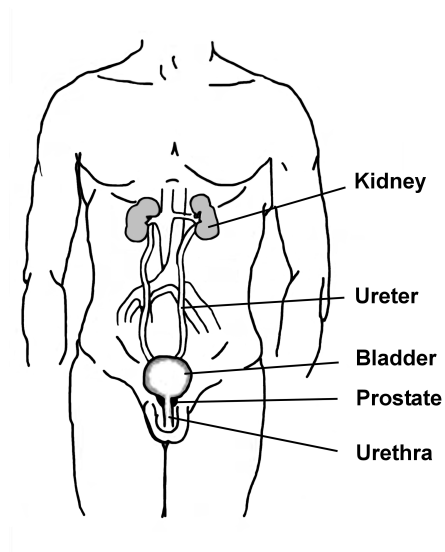


Figure 1.1: Schematic representation of the male urinary tract.

Elderly men often develop Lower Urinary Tract Symptoms (LUTS), such as a weak urinary stream, frequent (nocturnal) voiding and incomplete emptying of the bladder. These symptoms can be caused by an enlarged prostate, which is very common in elderly men, or a weakly contracting bladder muscle. The male urinary tract starts in the kidneys that filter toxic waste from the blood and excrete these in the form of urine. The urine is then transported via the ureters to the bladder, which is sealed by a circular striated muscle,

the sphincter. When a person feels the urge to void and voiding is socially acceptable, the sphincter relaxes and the urine is excreted via the urethra. Below the sphincter the male urethra passes through the prostate (see figure 1.1). The name prostate is derived from the Greek term *προσστημι* meaning “to stand before”³ (the bladder). The prostate is divided in two zones, namely the transitional zone and the peripheral zone. The transitional zone is the part of the prostate directly surrounding the urethra. The peripheral zone lies further outward and is encapsulated by a layer of muscular tissue and a fibrous capsule. The shape and size of the prostate are similar to a chestnut. In elderly men the prostate generally increases in size with age, most often as a result of Benign Prostatic Enlargement (BPE). More than two thirds (68%) of the men over the age of fifty have histological evidence of BPE^{1,2}. BPE mostly occurs in the transitional zone and refers to the overgrowth of prostatic tissue (see Figure 1.2), which can result in compression of the urethra and Bladder Outlet Obstruction (BOO). This is then usually followed by excessive growth of bladder muscle tissue⁵. Obstruction of the bladder outlet by an enlarged prostate can eventually result in LUTS. The first recorded attempts to relieve prostatic obstruction are documented in an Egyptian papyrus, which dates back to the fifteenth century BC⁴. This documents relates of a remedy, which involved tea brewed from the bark of juniper and cypress trees, and beer. In subsequent millenia there was little to no improvement in treating this urinary condition. It is said that in 1891 George Goodfellow performed the first perineal prostatectomy, i.e. removing the excess prostate tissue through an incision between the scrotum and rectum. In the following years this procedure was refined towards removal of the excess prostate tissue via the urethra (TransUrethral Resection of the Prostate or TURP), the currently most common surgical procedure in treatment of an enlarged prostate.

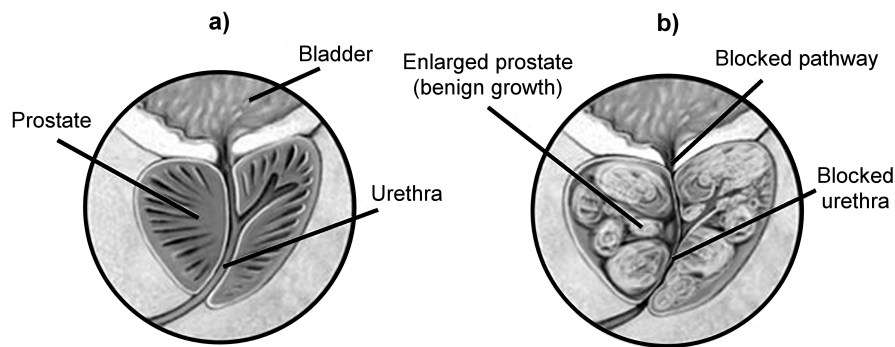


Figure 1.2: Cross-section of a normal prostate (a) and an enlarged prostate (b).

Urodynamic history

When a man suffers from voiding symptoms (LUTS), a diagnostic method is needed to distinguish between the two possible causes being either an enlarged prostate obstruc-

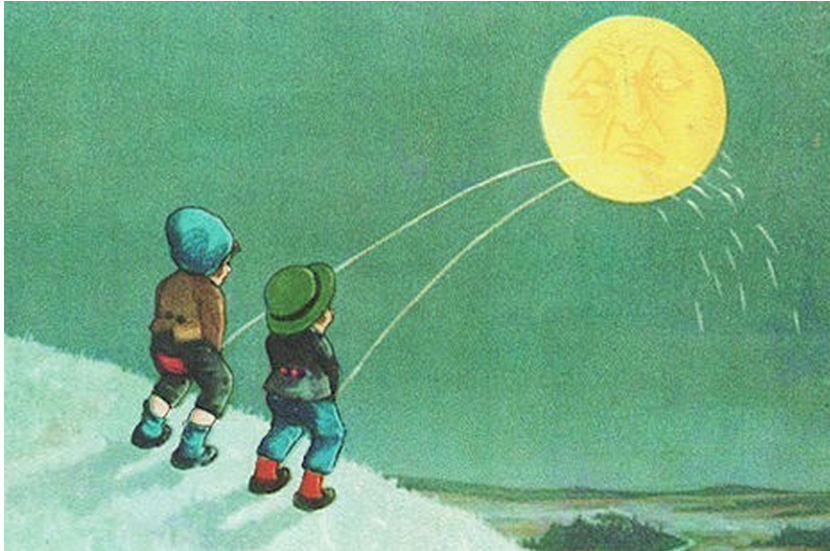


Figure 1.3: Basic urodynamics: “Who can pee the furthest?”

ting the bladder outlet or a weakly contracting bladder muscle (detrusor). The urinary stream is the most obvious parameter, which can be measured in patients suffering from LUTS. Attempts to quantify this urinary stream possibly started in ancient times with two small boys competing to see who can pee the furthest (see Figure 1.3). A pioneer in urophysiology, Havelock Ellis, measured his own urinary outflow with a primitive flowmeter in 1902. Ellis also performed the same experiment with women, placing them on their back 18 inches above the floor and measuring the flow, both with the labia in a closed position and open. His conclusions were rather remarkable: “The flow was the strongest in August and the weakest in October, strongest on Thursday and weakest on Sunday”⁶. Rehfisch⁷ whose technique was based on the displacement of air probably performed the first truly scientific measurement of urinary flow in 1897. In the 20th century many different ways to measure urinary flow were developed of which four ways are still in use. In 1948 W. Drake Jr. measured the urinary flow by continuously weighing urine collected in a beaker⁸. The flow is then calculated by differentiating the urine volume with respect to time. Around 1975 a device was manufactured which measured flow in a completely different way, the “rotating-disk flow meter”¹⁰. Urine hitting a rotating disk tends to slow the rotation of this same disk. The electrical energy that was needed to maintain a constant disk velocity is proportional to the mass flow rate of the urine. A third way to measure flow rate was the dropspectrometer, developed by Zinner¹¹. Zinner’s method was based on the idea that a urinary stream breaks up in droplets when it exits the meatus. The transit time of these droplets passing through two parallel planes was used to compute the velocity. In 1966 Keitzer and Huffman published a method of flow measurement based on sound measurements⁹.

Diagnosing Bladder Outlet Obstruction

Quantification of the urinary stream is not a conclusive measure for diagnosing BOO. The International Continence Society (ICS) developed a provisional method to diagnose BOO in patients with LUTS: an invasive pressure-flow study¹², which is currently most frequently used in the clinic. In an invasive pressure-flow study the urinary flow rate is measured in combination with invasive measurement of bladder pressure during voiding. The bladder and abdominal pressure are measured using one catheter that is inserted into the bladder via the urethra and one that is inserted in the rectum. The flow rate is recorded using e.g. an external rotating-disk flow meter. From the maximum flow rate and the detrusor pressure (i.e. bladder pressure minus the abdominal pressure) at this maximum flow rate the Bladder Outlet Obstruction Index (BOOI) is calculated as the detrusor pressure minus twice the flow rate. When BOOI is less than 20 the patient is diagnosed as non-obstructed. The patient is diagnosed as obstructed when BOOI is higher than 40. If BOOI is between 20 and 40 the patient is diagnosed as equivocal and further testing is advised. To illustrate the definition of BOOI: When a high bladder pressure is needed to produce a low urinary flow rate an obstruction of the bladder outlet (possibly an enlarged prostate) is the most probable cause of the symptoms. When a low flow rate is generated by low bladder pressure this can be caused by a weakly contracting bladder muscle. This method is effective, but it is also time-consuming, expensive, uncomfortable for the patient and the catheter may induce urethral trauma^{13,14}. Recently, non-invasive and more patient friendly measurement techniques for diagnosing BOO in patients with LUTS have been developed and tested: the condom-catheter method¹⁵, the cuff method¹⁶, Doppler flowmetry¹⁷, Penile Compression Release¹⁸ and ultrasonic measurement of bladder wall thickness¹⁹. The condomcatheter and the penile cuff method are based on non-invasive techniques to estimate bladder pressure. With the first technique an incontinence condom, with a pressure transducer attached to it, is fixed to the penis. During voiding the outflow of the condom is occluded, resulting in an open channel between the condom and the bladder. Thus the pressure that is measured in the condom is a measure of the bladder pressure. With the second technique a cuff is placed around the penis. During voiding this cuff is inflated until the urinary flow ceases. In this case the pressure in the cuff serves as a measure of the bladder pressure. Both techniques are non-invasive but require a manipulation/interruption of the urinary flow. Furthermore, both techniques require the patient to mentally continue voiding when the outflow tract is occluded. This requires a little practice. The penile compression-release technique also interrupts the urinary flow, by compressing the penile urethra, but does not measure bladder pressure. This technique measures the penile compression-release (PCR) index. With this technique the penis is occluded during voiding and then released. From the resulting flow rate surge after release and the steady flow rate, the PCR-index is calculated as a measure of BOO. Doppler flowmetry and the measurement of changes in bladder wall thickness both use ultrasound imaging and do not manipulate/interrupt the urinary flow. The first ultrasound technique measures the flow velocity in the prostatic urethra and in the bladder neck. The ratio of the two is taken as a measure of prostatic BOO. The second ultrasound technique measures a secondary effect of BOO, i.e. changes in bladder wall thickness. These changes, however, might have a number of different causes. All these non-invasive methods are still expensive or require manipulation/interruption

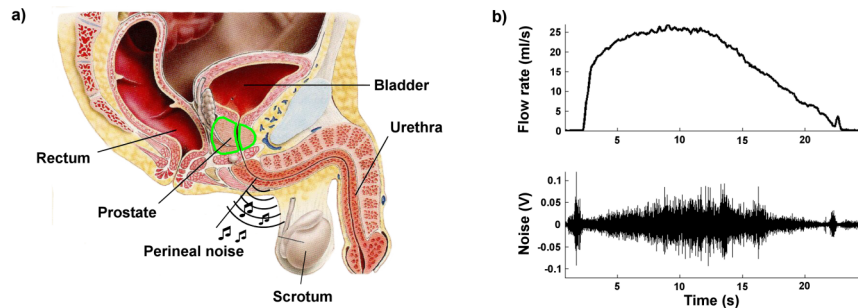


Figure 1.4: a) Cross-section of the lower urinary tract and b) an example of a perineal noise recording in a volunteer.

of the urinary flow. In cardiology the technique of sonography has been studied in patients^{20–23} and in models^{24–32} to relate spectral analysis of noise recorded at the vessel wall to the degree of arterial stenosis. This noise is allegedly produced by turbulence in the bloodstream as a result of the stenoses. In the midsixties a similar technique was introduced in urology with a voiding audiograph⁹. It was thought that the splashing noise of urine voided in a cup, recorded using a microphone and corrected for the voided volume, was a measure for bladder pressure. One decade later, the microphone was moved from the cup to the body at the level of the perineum (between scrotum and rectum) and the flow rate was recorded simultaneously with the noise produced in the urethra^{33–35}, see figure 1.4. However, no exact relationship or method to calculate the degree of obstruction from the noise recording was published. In this thesis we have related the recorded noise to the degree of obstruction. We have applied this relation in a simple, inexpensive and patient friendly method to potentially diagnose BOO in patients with LUTS. This non-invasive method is based on a recording of sound produced by urinary flow during voiding using a contact microphone placed at the perineum. In this thesis I intend to address three research questions. I will investigate whether the recorded sound is related to the degree of obstruction in a model urethra. And if so, I will attempt to define a relationship between the two. I will also look into the possibility of perineal sound recording being applied in a clinical setting as a non-invasive method to diagnose bladder outlet obstruction in patients with lower urinary tract symptoms.

Outline

In Chapter 1 I will briefly describe the development of two different models of the urethra that we have used for the development of perineal noise recording as a diagnostic method for BOO. One is a biophysical model constructed from PolyVinyl Alcohol (PVA) and the other is a computational model, which is constructed using Computational Fluid Dynamics (CFD). In Chapter 2 I will investigate whether the recorded noise is related to the degree of obstruction in the biophysical model urethra. This study includes variations in the viscoelastic properties of the model urethra, the microphone position and the de-

gree of obstruction. In Chapter 3 I will describe the development of a biophysical model of the urethra with viscoelastic properties comparable to the male pig urethra. In Chapter 4 I will use this model urethra as a bench model to test a hypothesis on impaired voiding in asymptomatic boys after hypospadias correction. I will assess the similarity of our model urethra and the human male urethra by measuring the pressure along its length, starting in the bladder (Urethral Pressure Profilometry or UPP) in Chapter 5. In Chapter 6 I will look further into the matter of the relation between the recorded noise and the degree of obstruction in the developed model urethra. And in the final chapter I will apply perineal sound recording in a population of healthy male volunteers and present the results. This thesis will be concluded with a general discussion, which intends to identify the position of perineal noise recording in the field of urodynamics.

Literature

1. S. J. Berry, D. S. Coffey, P. C. Walsh, and L. L. Ewing. The development of human benign prostatic hyperplasia with age. *J Urol*, 132(3):474–9, 1984.
2. H. B. Carter and D. S. Coffey. The prostate: an increasing medical problem. *Prostate*, 16(1):39–48, 1990.
3. H. Gray. *Gray's anatomy*. Barnes & Noble Books, New York, fifteenth edition, 1995.
4. P.T. Scardino and J. Kelman. *Prostate book, the complete guide to overcoming prostate cancer, prostatitis and BPH*. Penguin Group, New York, 2006.
5. W.A.D. Anderson. *Pathology*. The C. V. Mosby Company, St. Louis, 2nd edition edition, 1953.
6. J.J. Mattelaer. History of the urodynamics of the lower urinary tract. In J.J. Mattelaer, editor, *de Historia Urologiae Europaeae*, volume 5, pages 161–177. Historical Committee of the European Association Of Urology, Kortrijk - Belgium.
7. M. Rehfish. Ueber den mechanismus des harnblasenverschlusses und der harnentleerung. *Arch Pathol Anal Physiol*, 150:111, 1897.
8. W.M. Drake. Uroflowmeter: an aid to the study of the lower urinary tract. *Journal of Urology*, 59:650–658, 1948.
9. W.A. Keitzer and G.C. Huffman. The voiding audiograph: a new voiding test. *Journal of Urology*, 95:404–410, 1966.
10. D. Rowan, A. L. McKenzie, S. G. McNee, and E. S. Glen. A technical and clinical evaluation of the disa uroflowmeter. *Br J Urol*, 49(4):285–91, 1977.
11. N.R. Zinner and D.C. Harding. Velocity of the urinary stream, its significance and a method for its measurement. In F.J. Hinman, editor, *Hydrodynamics of micturition*. Charles C. Thomas, Springfield, IL, 1971.
12. D.J. Griffiths, K. Höfner, R. van Mastrigt, H.J. Rollema, A. Spångberg, and D.M. Gleason. Standardization of terminology of lower urinary tract: pressure-flow studies of voiding, urethral resistance and urethral obstruction. *Neurourology and Urodynamics*, 16:1–18, 1997.
13. H.C. Klingler, S. Madersbacher, B. Djavan, G. Schatzl, M. Marberger, and C.P. Schmidbauer. Morbidity of the evaluation of the lower urinary tract with transurethral multichannel pressure-flow studies. *Journal of Urology*, 159(1):191–194, 1998.
14. D. Porru, G. Madeddu, G. Campus, I. Montisci, R.M. Scarpa, and E. Usai. Evalua-

- tion of morbidity of multi-channel pressure-flow studies. *Neurourology and Urodynamics*, 18(6):647–652, 1999.
15. J.J.M. Pel and R. van Mastrigt. The variable outflow resistance catheter: a new method to measure bladder pressure noninvasively. *Journal of Urology*, 165:647–652, 2001.
 16. D.J. Griffiths, D. Rix, M. MacDonald, M.J. Drinnan, R.S. Pickard, and P.D. Ramsden. Noninvasive measurement of bladder pressure by controlled inflation of a penile cuff. *Journal of Urology*, 167:1344–1347, 2002.
 17. Y.Y. Ding, H. Ozawa, T. Yokoyama, Y. Nasu, M.B. Chancellor, and H. Kumon. Reliability of color doppler ultrasound urodynamics in the evaluation of bladder outlet obstruction. *Urology*, 56:967–971, 2000.
 18. M.P. Sullivan and V. S. Yalla. Penile urethral compression-release maneuver as a non-invasive screening test for diagnosing prostatic obstruction. *Neurourology and Urodynamics*, 19:657–669, 2000.
 19. C. Manieri, S. S. Carter, G. Romano, A. Trucchi, M. Valenti, and A. Tubaro. The diagnosis of bladder outlet obstruction in men by ultrasound measurement of bladder wall thickness. *J Urol*, 159(3):761–5, 1998.
 20. J.P. Kistler, R.S. Lees, J. Friedman, M. Pressin, J.P. Mohr, G. Roberson, and R.G. Ojemann. The bruit of carotid stenosis versus radiated basal heart murmurs. *Circulation*, 57(5):975–981, 1978.
 21. J.P. Kistler, R.S. Lees, A. Miller, R.M. Crowell, and G. Roberson. Correlation of spectral phonoangiography and carotid angiography with gross pathology in carotid stenosis. *New England Journal of Medicine*, 305(8):417–419, 1981.
 22. R.S. Lees and C. Forbes Dewey Jr. Phonoangiography: A new diagnostic method for studying arterial disease. *Proceedings of the National Academy of Sciences*, 67(2):935–942, 1970.
 23. G.W. Duncan, J.O. Gruber, C. Forbes Dewey Jr, G.S. Myers, and R.S. Lees. Evaluation of carotid stenosis by phonoangiography. *New England Journal of Medicine*, 27(Nov):1124–1128, 1975.
 24. J.J. Fredberg. Origin and character of vascular murmurs: Model studies. *Journal of Acoustic Society of America*, 61(4):1077–1085, 1977.
 25. S.A. Abdallah and N.H.C. Hwang. Arterial stenosis murmurs: An analysis of flow and pressure fields. *Journal of Acoustic Society of America*, 83(1):318–334, 1998.
 26. S.A. Jones and A. Fronek. Analysis of break frequency downstream of a constriction in a cylindrical tube. *Journal of Biomechanics*, 20(3):319–327, 1987.
 27. P.C. Lu, C.N. Hui, and N.H.C. Hwang. A model investigation of the velocity and pressure spectra in vascular murmurs. *Journal of Biomechanics*, 16(11):923–931, 1983.
 28. R.J. Tobin and I.D. Chang. Wall pressure spectra scaling downstream of stenoses in steady tube flow. *Journal of Biomechanics*, 9:633–640, 1976.
 29. P. C. Lu, D. R. Gross, and N. H. Hwang. Intravascular pressure and velocity fluctuations in pulmonic arterial stenosis. *J Biomech*, 13(3):291–300, 1980.
 30. W.H. Pitts and C.F. Dewey. Spectral and temporal characteristics of post-stenotic turbulent wall pressure fluctuations. *Journal of Biomechanical Engineering*, 101:89–95, 1979.
 31. P. Ask, B. Hok, D. Loyd, and H. Teriö. Bio-acoustic signals from stenotic tube flow:

- state of the art and perspectives for future methodological development. *Medical and Biological Engineering and Computing*, 33:669–675, 1995.
32. A. Miller, R.S. Lees, J.P. Kistler, and W.A. Abbott. Spectral analysis of arterial bruits (phonoangiography): Experimental validation. *Circulation*, 61(3):515–520, 1980.
 33. W.E. Bradley, B.P. Brockway, and G.W. Timm. Auscultation of urinary flow. *Journal of Urology*, 118:73–75, 1977.
 34. H. Teriö. Acoustic method for assessment of urethral obstruction: a model study. *Medical and Biological Engineering and Computing*, 29:450–456, 1991.
 35. A.J. van Koeveringe and R. van Mastrigt. A relation between the sound produced by urethral turbulence in patients and objectively assessed subvesical obstruction. *Neurourology and Urodynamics*, 10:442–443, 1991.

Chapter 2

Abstract

We are developing two models of the urethra to study perineal noise recording as a non-invasive method to diagnose Bladder Outlet Obstruction. In both models, a flexible model made from Polyvinyl Alcohol (PVA) and a computational model based on Computational Fluid Dynamics (CFD), we study the relation between the recorded noise and the degree of obstruction. In the PVA model we have confirmed the hypothesized relation between recorded noise and the degree of obstruction. In the CFD model we calculated that the location at which the amplitude of the noise is maximum mainly depends on the degree of obstruction.

Adapted from: T. Idzenga, J.J.M. Pel and R. van Mastrigt, "*Development of Perineal Noise Recording as a non-invasive method for diagnosis of Bladder Outlet Obstruction*", *Urodynamic* 16, 310-320, 2006.

Chapter 2

Development of Perineal sound Recording as a non-invasive method for diagnosis of Bladder Outlet Obstruction

Introduction

In ageing males, lower urinary tract symptoms (LUTS), for example a poor flow rate, possibly result from an obstructed urethra caused by an enlarged prostate. In some cases, however, a weakly contracting bladder also causes a poor flow rate. At present the International Continence Society (ICS) recommends a provisional method for diagnosing bladder outlet obstruction on the basis of the maximum flow rate and the associated detrusor pressure, graphically represented in a pressure-flow plot¹, see figure 2.1. The transurethral catheters used for such a pressure flow study induce the risk of urinary tract infection and urethral trauma^{2,3}. Recently, non-invasive (and more patient friendly) measurement techniques have been developed and tested to diagnose bladder outlet obstruction in patients with LUTS: the condom-catheter method⁴, the cuff method⁵ and Doppler flowmetry⁶. Alternatively, a non-invasive measurement technique may be based on urethral sound recording, i.e. voiding with a microphone pressed against the perineum (between scrotum and anus). An example of such a sound recording is shown in figure 2.2. A major advantage of such a diagnostic method is its simplicity. The patient can void freely without interruptions, there is no contact between penis and equipment and it is specifically directed towards diagnosing Bladder Outlet Obstruction (BOO). The development of this non-invasive technique for diagnosing LUTS started in the mid-sixties with a voiding audiograph⁷. It was thought that the splashing sound of urine voided in a cup, recorded with a microphone and corrected for the voided volume, was a measure for bladder pressure. One decade later, the microphone was moved from the cup to the body at the level of the perineum and the sound produced in the urethra and the flow

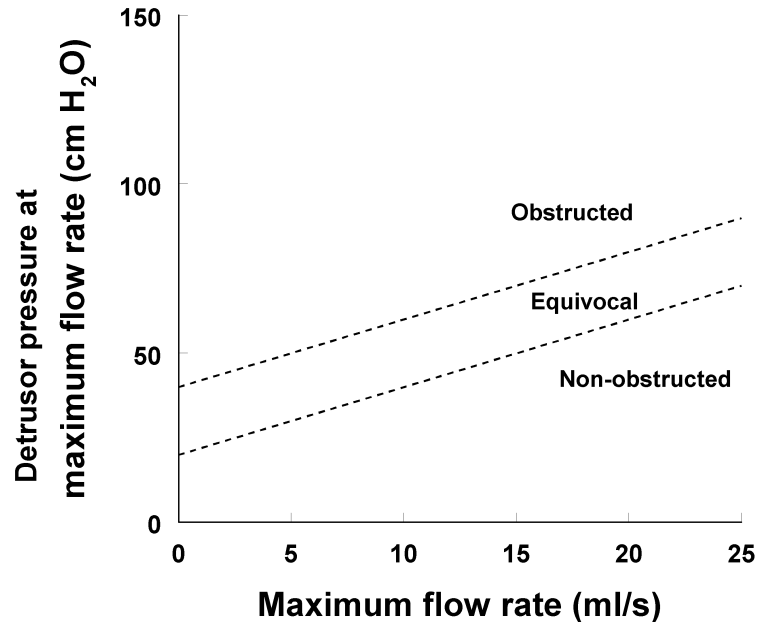


Figure 2.1: The provisional ICS method for definition of obstruction. Classification of bladder outlet obstruction is based on a combination of maximum flow rate and the simultaneously measured detrusor pressure value during a pressure-flow study. A voiding with low flow rate, e.g. 8 ml/s, may either be obstructed or unobstructed depending on the detrusor pressure.

rate were recorded⁸. It was hypothesized that urinary flow is turbulent at the bladder neck. These turbulences cause pressure fluctuations on the wall of the urethra that can be recorded as sound transmitted via the urethra to the skin. It was also hypothesized that this perineal sound is related to the degree of prostatic obstruction. In latex^{9,10} or silicone¹¹ test tubes it has been shown that pressure fluctuations are indeed induced by flow and that the power spectrum of the recorded sound depends among others on the degree of obstruction applied.

The precise relation between perineally recorded sound during voiding and the degree of obstruction is not obvious. There are many factors besides the degree of obstruction that could influence the recorded sound, e.g. viscoelastic properties and thickness of the urethral wall and tissue surrounding the urethra. This review presents the development of two models of the urethra to study how perineally recorded sound relates to the degree of prostatic obstruction. The first model is a highly flexible and extensible tube made of a 10% aqueous solution of the polymer Polyvinyl Alcohol (PVA). This cryogel behaves like rubber after a freezing/thawing process that controls the viscoelastic properties. The second model is based on Computational Fluid Dynamics (CFD). In the last two decades the application of this computational technique has been extended to biological systems including the peripheral circulation¹²⁻¹⁵, the respiratory tract¹⁶ and the

male urinary tract^{17,18}. It enables simulations of (urinary) flow through complexly shaped tubes.

PolyVinyl Alcohol model urethra

As mentioned, in recent decades latex and silicone tubing has been used as a model of blood vessels^{9,10} and the urethra¹¹. These tubes are considerably stiffer than arteries and the urethra. A more flexible and extensible tube can be made from PVA cryogel¹⁹, see figure 2.3. This polymer-solution (liquid at room temperature) was poured in a mould; storage in a freezer overnight and thawing at room temperature during the day completed one freeze/thaw cycle and stiffened the PVA cryogel. The number of freeze/thaw cycles, the rate of freezing/thawing and the concentration of the cryogel control the viscoelastic properties of this PVA cryogel.

In a number of model urethras we studied the relation between the recorded sound and the degree of obstruction of the urethra²⁰. We constructed three models with different viscoelastic properties; applied three degrees of obstruction by inflating a blood pressure cuff placed around the urethral model and recorded the sound at three positions distal to the applied obstruction (see figure 2.4). The flow rate was kept constant and was

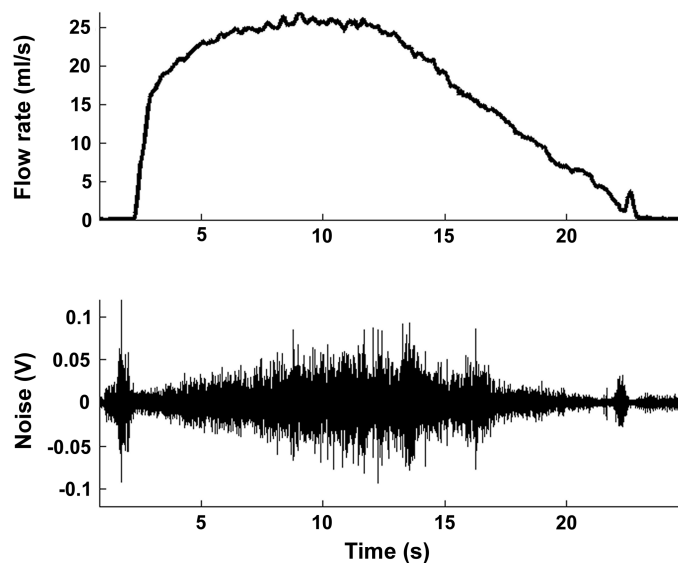


Figure 2.2: An example of simultaneously measured urine flow rate (top panel) and perineal sound (lowest panel). The sound was recorded using a microphone pressed against the perineum. The peaks in the sound recording before voiding commences and at the end of voiding are probably caused by a contraction of the pelvic floor muscles.



Figure 2.3: Cross section and side-view of a PVA model urethra (reproduced from NeuroUrol. Urodyn. 24(4): 381-388, 2005, with kind permission of John Wiley & Sons, Inc.).

identical in all recordings. We analysed the recordings by calculating the average sound-amplitude of the recorded sound signals and the weighted average frequency of its power spectrum. We found that both depended significantly (ANOVA, $p < .05$) on the degree of obstruction (see figure 2.5). Both increased with increasing degree of obstruction. This result supports the hypothesis that there is a relation between the recorded sound and the degree of obstruction. It also supports the hypothesis that a non-invasive method for diagnosing bladder outlet obstruction might be based on perineal sound recording. However, we found that the two studied parameters of the recorded sound also depended on the distance between microphone and obstruction and on the viscoelastic properties of the model urethra. The three factors were found to be independent of each other.

In order to relate the recorded sound unambiguously to the degree of obstruction, despite differences in viscoelastic properties and position of the microphone, we have fine-tuned the model urethra to match the viscoelastic properties of the human male urethra. As a model for the viscoelastic properties of the human male urethra we used the pig urethra because of the similarities between pig and human physiology²¹. We made bladder/urethra preparations from 8 male and 10 female pigs sacrificed at the department of Experimental Cardiology (Erasmus MC, Rotterdam, the Netherlands). The part of the urethra closest to the bladder was selected for the measurements (distal to the prostate for the male pigs). An example of a cross-section of the male and female pig urethra is shown in figure 2.6a. We used Elastic von Gieson staining²² to mark elastin, collagen and muscle tissue in these cross-sections, which show a difference in tissue composition of the urethral wall between male and female pig urethras. We also made 12 different model

urethras²¹. Half of the model urethras had a circular-shaped flow-channel and the other half a Y-shaped channel. Within each group four model urethras were freeze-thawed 1, 2, 3, and 4 times and two consisted of a once or twice freeze-thawed cylinder in a separate shell that was freeze-thawed 3 times. Each model was placed in a water-filled container (approx. 1 cm below the water-surface) at room temperature and each pig urethra was placed in a container (approx. 1 cm below the solution-surface) filled with a cold (10°C) modified Krebs solution. One side of the model or pig urethra was connected to a 5 ml syringe to manually inject a known volume of water in a very short time. The pressure response was recorded using a disposable pressure transducer connected to the other side of the urethra. Increasing volumes were injected and the pressure response was recorded. To derive the viscoelastic properties the simplified analytical solution of the step-response of a mechanical model was fitted to 1000 samples (equivalent of 1 sec.) of the pressure signal. The fit-procedure resulted in 6 coefficients, three coefficients accounted for the amount of stress in the urethral wall, two accounted for the relaxation of the urethral wall in time and one accounted for vibration of the wall upon stepwise-applied strain.

We found a difference in viscoelastic properties between male and female pigs²³. In female pig urethras the same stress-values could be achieved as in male pig urethras but at significantly higher strain than in male pig urethras (see figure 2.6b). This difference in viscoelastic properties was supported by the difference in muscular tissue surrounding

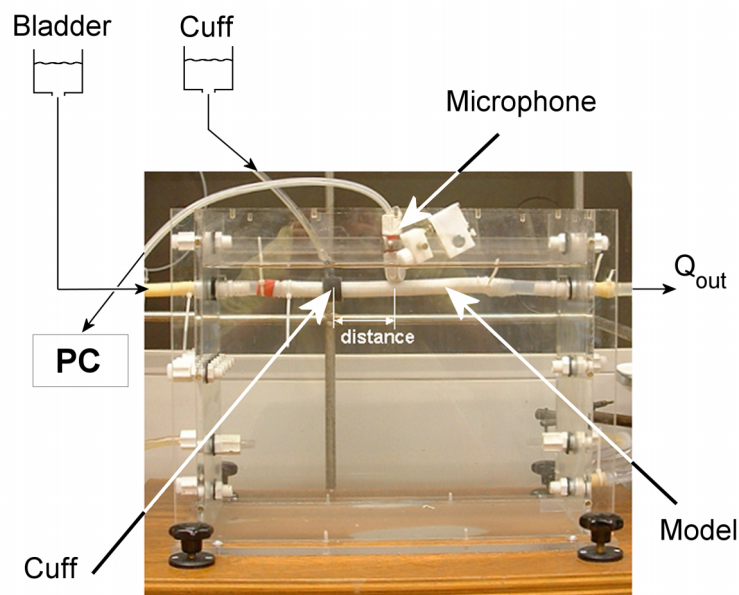


Figure 2.4: The measurement setup (reproduced from *Neurourol. Urodyn.* 24(4): 381-388, 2005, with kind permission of John Wiley & Sons, Inc.). Changing the combination of 'bladder pressure' and 'cuff pressure' varied the degree of obstruction urethra.

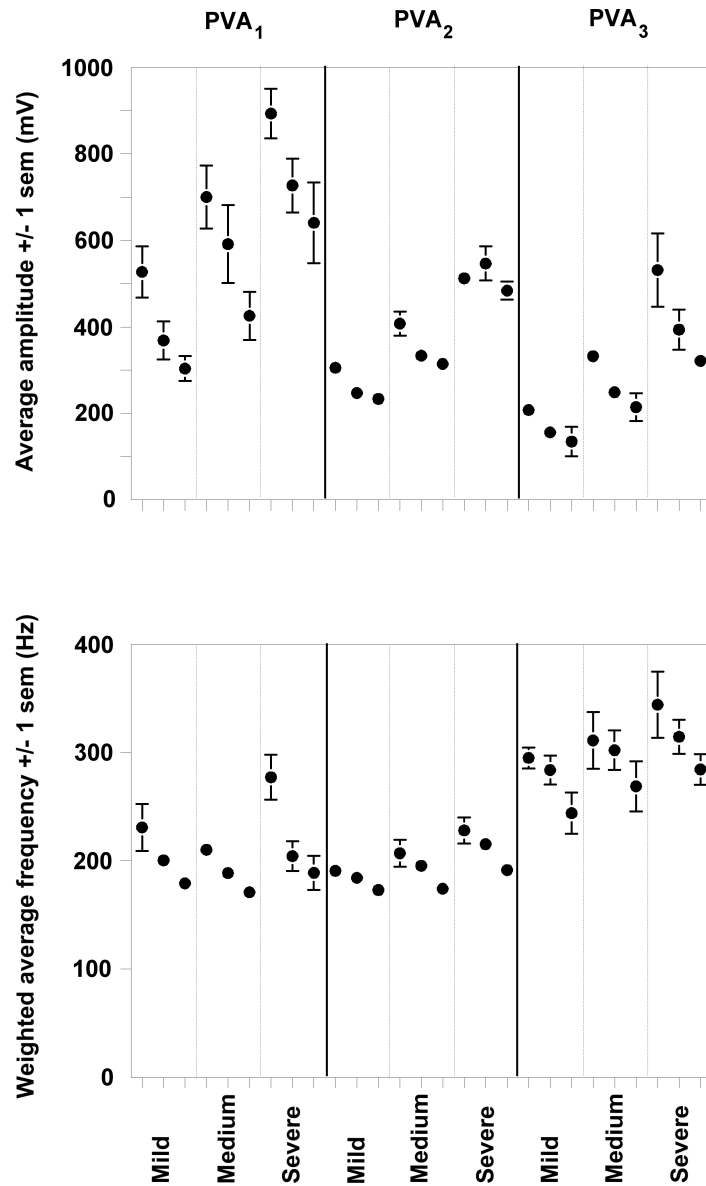


Figure 2.5: Mean (± 1 standard error of the mean) average amplitude and weighted average frequency of five sound recordings done at nine different combinations of degree of obstruction and microphone position in three PVA-urethras with different wall stiffness (PVA₁, PVA₂ and PVA₃). The degrees of obstruction are separated by dotted lines and displayed on the X-axis. Within each degree of obstruction the distance from the obstruction increases from left to right (3, 5 and 7 cm). This graph is reproduced from *Neurourol. Urodyn.* 24(4): 381-388, 2005, with kind permission of John Wiley & Sons, Inc.

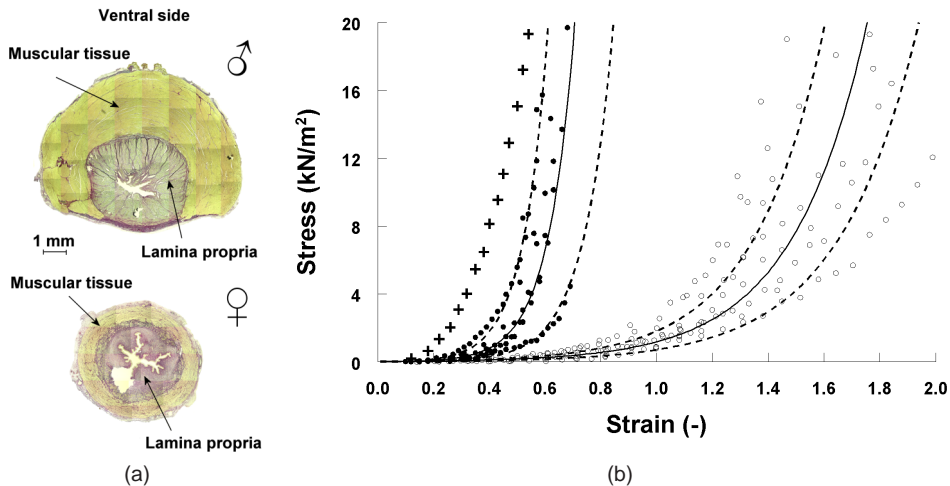


Figure 2.6: a) Cross-section of the proximal part of the male (top) and the female (bottom) pig urethra. We stained elastin, collagen (both dark grey) and muscle tissue (light grey) using Elastic von Gieson staining. In the male cross-section the lamina propria is surrounded by muscular tissue with a horseshoe-like shape. In the female cross-section the lamina propria is surrounded by muscular tissue with a circular shape. The top part of this figure is reproduced from *Neurourol. Urodyn.* 25(5): 451-460, 2006, with kind permission of John Wiley & Sons, Inc. b) Stress in the urethral wall of male (●) and female (○) pig urethras as a function of the applied strain with fitted exponential functions (solid lines) and 95% CI of these functions (dashed lines). The stress-strain relation for the selected model urethra (Y-shaped channel, freeze-thawed 3 times) is plotted in this graph as +. This graph is reproduced from *Neurourol. Urodyn.* 25(5): 451-460, 2006, with kind permission of John Wiley & Sons, Inc.

the lamina propria in male and female pig urethra shown in figure 2.6a. Based on the comparison between the model urethras and the male pig urethra²¹ a model urethra with a Y-shaped flow channel that was uniformly freeze-thawed three times was chosen as the best model of the human male urethra for studying the relation between sound recording during urine flow and the degree of bladder outlet obstruction.

To further test how well this model urethra represents the male urethra, we have done urethral pressure measurements (to be published). We created three different continence zones in the model urethra by applying three different blood-pressure cuffs around the model and inflated them to different pressures using a water column. At each cuff pressure we measured a quasi-static approximation of the Valsalva Leak-Point-Pressure (VLPP). We also recorded a Urethral Pressure Profile (UPP) by withdrawing a fluid perfused catheter at different withdrawal rates and with different perfusion rates through the urethral model. From each UPP, corrected for the pressure loss in the catheter, the maximum was denoted as the Maximum Urethral Closure Pressure (MUCP). We found that with increasing cuff pressure the measured VLPP as well as the MUCP increased. VLPP, however, was found to be a more accurate measure than MUCP. We also found that MUCP depended significantly on the perfusion and withdrawal rate of the catheter and

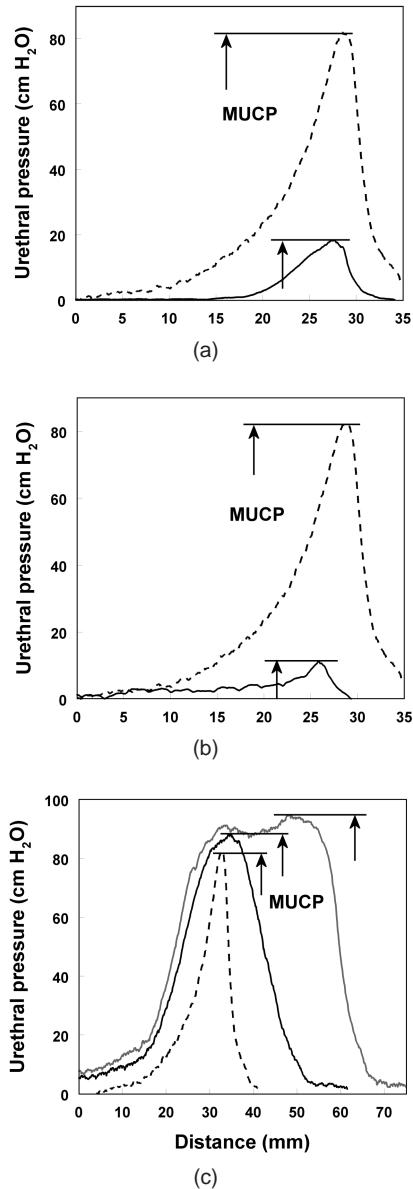


Figure 2.7: Examples of UPP-recordings at a cuff pressure of 150 cm H₂O. The recordings were done with: a) a constant withdrawal rate (0.5 mm/s) in combination with two different perfusion rates (— = 0.5 ml/min and - - - = 10 ml/min) and b) a constant perfusion rate (10 ml/min) in combination with two different withdrawal rates (- - - = 0.5 mm/s and — = 2 mm/s) using the single Tricomed-cuff. In c) the recordings were done with a constant withdrawal rate (0.5 mm/s) and a constant perfusion rate (10 ml/min) using the three different cuff-types (- - - = single Tricomed, — = Critikon 5 and — = double Tricomed). The horizontal axis represents distance measured from the proximal end of the model urethra.

on the type of continence zone. In figure 2.7 examples of recorded pressure profiles are presented that demonstrate the dependence we found. Similarities between the urethral pressure profiles in a model urethra and those in a male urethra support the model urethra as a good representation of the human male urethra.

Our next aim in development of perineal sound recording as a non-invasive technique is studying the relation between recorded sound and obstruction in detail. This will be done in the three times freeze-thawed model urethra by varying the degree of obstruction and record the sound between 1 and 12 cm, at intervals of 1 cm, downstream of the obstruction. Inflating a blood pressure cuff around the model urethra will create the obstruction and by connecting a water-column to one side of the model urethra a bladder will be simulated. Varying the pressure in the cuff and in the 'bladder' will result in a flow rate between 0 and 35 ml/s and a bladder pressure ranging from 45 to 130 cm H₂O.

Computational Fluid Dynamics model urethra

The second model we have developed to study perineal sound recording as a non-invasive diagnostic method for BOO is based on Computational Fluid Dynamics (CFD). Theoretical and experimental fluid dynamics studies have shown that flow passing an obstruction starts recirculating in vortices and further downstream restores to forward flow²⁴⁻²⁶. The point at which flow restores is called the reattachment point. Since at this point the maximum r.m.s. wall pressure and thus the maximum urethral sound amplitude is found^{9,12,27,28}, the reattachment point may be the best location to non-invasively record perineal sound. We studied some of the parameters that influence the location of this point in a simple two-dimensional computational model of the prostatic urethra²⁹. Figure 2.8a, top panel, shows the computational model, consisting of the bladder, the bladder neck, the prostatic urethra and a posterior part of the urethra. Each model was divided in ~2200 fluid elements, see the second panel. Some boundary conditions were applied to the model, and the fluid was given the properties of water. Calculations were carried out at 4 different bladder pressures, 5 degrees of obstruction and 3 obstruction shapes. In each simulation, the velocity (third panel) and pressure (lowest panel) distributions and the wall shear stresses were calculated (see figure 2.8b). The model calculations showed that recirculation of urine may occur above a certain degree of obstruction. This recirculation is related to decreased pressure (below atmospheric level) at the obstruction outlet. The location of the reattachment point depended primarily on the degree and secondarily on the shape of the obstruction and it was independent of the applied bladder pressure. This finding led us to the hypothesis that two diagnostic parameters may be derived from perineal sound. The first is the location of the maximum sound amplitude as a measure for the degree of prostatic obstruction. The higher the degree of obstruction, the more distal this point is located. Since the sound amplitude is highest at the reattachment point, perineal sound should simultaneously be recorded at a number of locations along the urethral wall to identify this location. The second diagnostic parameter, the frequency of the perineal sound, may be a measure for the bladder pressure. The dominant mechanism generating sound at the reattachment point is the frequency of passing fluid vortices travelling from the obstruction to the reattachment point via streamlines. The frequency of newly developed vortices depends on the fluid velocity¹². Based on physi-

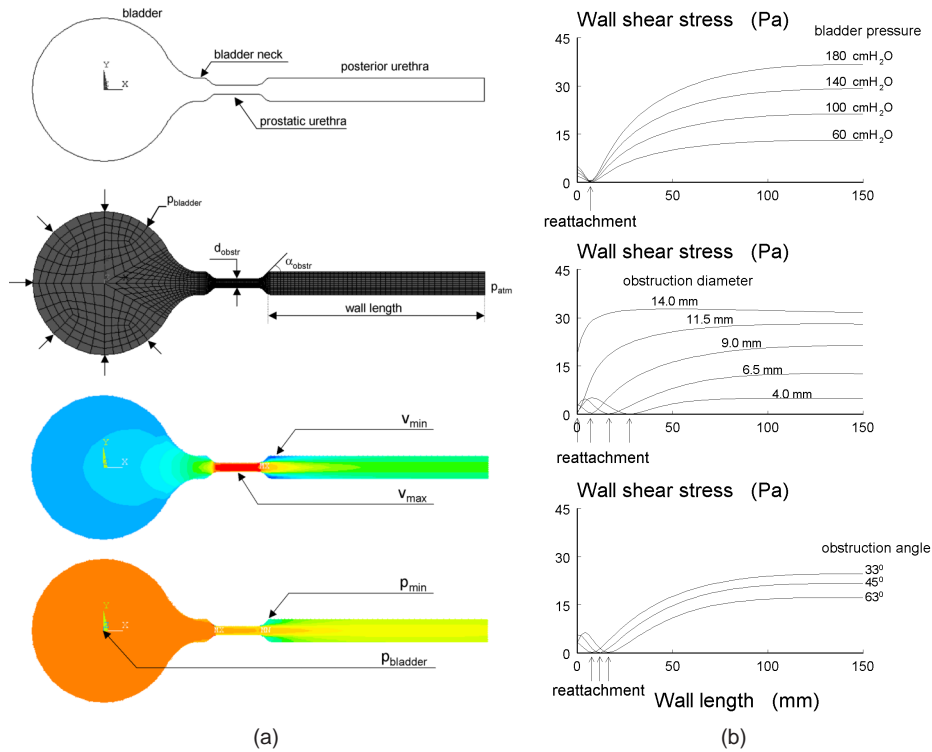


Figure 2.8: a) The bladder-urethra complex was modelled as a bladder, connected via a bladder neck to the urethra with a proximally narrowed prostatic part and a posterior part of 150 mm in length, see the top panel. This cross section was divided in ~ 2200 fluid elements, see the second panel. For each simulation the following parameters were set: the bladder wall pressure (P_{bladder}), the obstruction diameter (d_{obstr}) and the in- and outflow obstruction angle (α_{obstr}). The third panel shows the velocity distribution of fluid flow through the model urethra with P_{bladder} of 180 cm H₂O, d_{obstr} of 9 mm and α_{obstr} of 45 degrees. The maximum velocity, v_{max} , is found in the obstruction, the (negative) minimum velocity, v_{min} , at the obstruction outlet. The lowest panel shows the pressure distribution of the fluid flow, with the maximum pressure in the bladder, P_{bladder} , and the minimum pressure, P_{min} , again at the obstruction outlet. b) Each panel shows wall shear stress along the urethral wall with a total length of 150 mm, starting from the obstruction outlet to the end of the urethra, see also figure 2.3, top panel. The location of the reattachment point did not depend on bladder pressure (top panel), but did depend on the degree of obstruction (middle panel) and on the obstruction shape (lowest panel).

cal principles, it may be expected that the obstruction diameter and the bladder pressure influence the maximum fluid velocity the most. The model calculations showed that with varying degree of obstruction from low ($d_{\text{obs}} = 14$ mm) to severe ($d_{\text{obs}} = 4$ mm) at any bladder pressure value, the maximum fluid velocity increased with only 20%. Varying the bladder pressure from 60 to 180 cm H₂O at any obstruction diameter, led to an increase in the fluid velocity with 75%. We therefore hypothesise that the frequency of sound (i.e.

frequency of passing fluid vortices) depends primarily on the bladder pressure.

Discussion

At present the International Continence Society (ICS) recommends a provisional invasive method for diagnosing bladder outlet obstruction on the basis of the maximum flow rate and the associated detrusor pressure. Recently non-invasive techniques are developed to diagnose BOO. In this review the development of a non-invasive technique based on perineal sound recording is described. Based on differences in spectral intensities it was shown that the recorded sound correlated with flow rate⁸. Experimental^{11,30} and clinical studies^{30,31} were published on the relation between sound recordings and BOO. The test tubes used in these experiments were rather stiff compared to the more flexible and distensible blood vessel or urethra. In the same period of time studies were done on vascular murmurs caused by stenoses, a method referred to as phonoangiography^{9,10,32–35}. It was shown that based on either the mean power frequency¹¹, the break frequency of the sound spectrum^{9,10,35}, the shape of the recorded sound signal³⁰ or a combination of the average power amplitude in a specific frequency band with the simultaneously measured flow rate³¹ diagnosing arterial stenosis and BOO could be possible.

In a review on bio-acoustic signals it was noted that the phonoangiographic methods might be non-invasive and inexpensive, but that clinical application of these methods has been overtaken by large-scale application of ultrasound Doppler³⁶. Nevertheless, over the years attempts have been made to relate sound recordings from biological fluids (e.g. blood, urine) to the obstruction passed (stenosis or prostatic obstruction). And despite encouraging results, a non-invasive measurement device based on sound recordings is not yet available.

In this review we have presented two models of the human male urethra for studying perineal sound recording as a non-invasive technique for diagnosing males with LUTS, caused by an enlarged prostate. We have shown in the Polyvinyl Alcohol (PVA) model urethra that the recorded sound indeed depends on the degree of obstruction, but also on the viscoelastic properties of the model wall. Therefore we have developed a PVA model urethra with viscoelastic properties comparable to the male pig urethra. The advantage of such a model is the ability to physically control the various factors that influence the recorded sound, e.g. the viscoelastic properties and the degree of obstruction. The PVA model can be used to record sound that is presumably produced by the flow through an obstructed urethra. We also developed a model urethra based on Computational Fluid Dynamics (CFD). In the CFD model urethra the various factors can be controlled mathematically and it can be used to visualize the flow through the obstruction and urethra.

Future aims are studying the relation between sound and the degree of obstruction in more detail, as mentioned, and development of a measurement-setup for validating the perineal sound recording technique in male volunteers. This measurement-setup is then to be used to test the developed diagnostic method in a patient population. Eventually this method is intended to diagnose obstruction in patients with impaired voiding.

Literature

1. D.J. Griffiths, K. Höfner, R. van Mastrigt, H.J. Rollema, A. Spångberg, and D.M. Gleason. Standardization of terminology of lower urinary tract: pressure-flow studies of voiding, urethral resistance and urethral obstruction. *Neurourology and Urodynamics*, 16:1–18, 1997.
2. H.C. Klingler, S. Madersbacher, B. Djavan, G. Schatzl, M. Marberger, and C.P. Schmidbauer. Morbidity of the evaluation of the lower urinary tract with transurethral multichannel pressure-flow studies. *Journal of Urology*, 159(1):191–194, 1998.
3. D. Porru, G. Madeddu, G. Campus, I. Montisci, R.M. Scarpa, and E. Usai. Evaluation of morbidity of multi-channel pressure-flow studies. *Neurourology and Urodynamics*, 18(6):647–652, 1999.
4. J.J.M. Pel and R. van Mastrigt. The variable outflow resistance catheter: a new method to measure bladder pressure noninvasively. *Journal of Urology*, 165:647–652, 2001.
5. D.J. Griffiths, D. Rix, M. MacDonald, M.J. Drinnan, R.S. Pickard, and P.D. Ramsden. Noninvasive measurement of bladder pressure by controlled inflation of a penile cuff. *Journal of Urology*, 167:1344–1347, 2002.
6. Y.Y. Ding, H. Ozawa, T. Yokoyama, Y. Nasu, M.B. Chancellor, and H. Kumon. Reliability of color doppler ultrasound urodynamics in the evaluation of bladder outlet obstruction. *Urology*, 56:967–971, 2000.
7. W.A. Keitzer and G.C. Huffman. The voiding audiograph: a new voiding test. *Journal of Urology*, 95:404–410, 1966.
8. W.E. Bradley, B.P. Brockway, and G.W. Timm. Auscultation of urinary flow. *Journal of Urology*, 118:73–75, 1977.
9. R.J. Tobin and I.D. Chang. Wall pressure spectra scaling downstream of stenoses in steady tube flow. *Journal of Biomechanics*, 9:633–640, 1976.
10. S.A. Jones and A. Fronek. Analysis of break frequency downstream of a constriction in a cylindrical tube. *Journal of Biomechanics*, 20(3):319–327, 1987.
11. H. Teriö. Acoustic method for assessment of urethral obstruction: a model study. *Medical and Biological Engineering and Computing*, 29:450–456, 1991.
12. S.A. Abdallah and N.H.C. Hwang. Arterial stenosis murmurs: An analysis of flow and pressure fields. *Journal of Acoustic Society of America*, 83(1):318–334, 1998.
13. C. Skilbeck, S.M. Westwood, P.G. Walker, T. David, and G.B. Nash. Population of the vessel wall by leukocytes binding to p-selectin in a model of disturbed arterial flow. *Arterioscler Thromb Vasc Biol*, 21(8):1294–300, 2001.
14. X. Song, A.L. Throckmorton, H.G. Wood, P.E. Allaire, and D.B. Olsen. Transient and quasi-steady computational fluid dynamics study of a left ventricular assist device. *Asaio J*, 50(5):410–7, 2004.
15. J.J. Wentzel, F.J. Gijssen, J.C. Schuurbijs, R. Krams, P.W. Serruys, P.J. De Feyter, and C.J. Slager. Geometry guided data averaging enables the interpretation of shear stress related plaque development in human coronary arteries. *J Biomech*, 38(7):1551–5, 2005.
16. C. Xu, S. SangHun, J.M. McDonough, J.K. Udupa, A. Guez, R. Arens, and D.M. Wootton. Computational fluid dynamics modelling of the upper airway of children with obstructive sleep apnea syndrome in steady flow. *Journal of Biomechanics*,

- 39(11):2043–54, 2006.
17. Z. Tonar, F. Zat'ura, and R. Grill. Surface morphology of kidney, ureters and urinary bladder models based on data from the visible human male. *Biomed Pap Med Fac Univ Palacky Olomouc Czech Repub*, 148(2):249–51, 2004.
 18. J. Kren, M. Horak, F. Zat'ura, and M. Rosenberg. Mathematical model of the male urinary tract. *Biomed Pap Med Fac Univ Palacky Olomouc Czech Repub*, 145(2):91–6, 2001.
 19. K.C. Chu and B.K. Rutt. Polyvinyl alcohol cryogel: an ideal phantom material for mr studies of flow and elasticity. *MRM*, 37:314–319, 1997.
 20. T. Idzenga, J.J.M. Pel, R. A. Baldewising, and R. van Mastrigt. Perineal noise recording as a non-invasive diagnostic method of urinary bladder outlet obstruction: a study in polyvinyl alcohol and silicone model urethras. *Neurourology and Urodynamics*, 24(4):381–8, 2005.
 21. T. Idzenga, J.J.M. Pel, and R. van Mastrigt. A biophysical model of the male urethra: Comparing viscoelastic properties of polyvinyl alcohol urethras to male pig urethras. *Neurourology and Urodynamics*, 25(5):451–460, 2006.
 22. J.D. Bancroft and A. Stevens. Theory and practice of histological techniques. Churchill Livingstone, New York, 4th edition, 1996.
 23. T. Idzenga, J.J.M. Pel, and R. van Mastrigt. Compliance of the urethra: a possible contribution to the difference in maximum flow rate between men and women? In *International Continence Society 35th Annual meeting*, Montreal, Canada, 2005.
 24. R.W. Fox and A.T. MacDonald. *Introduction to fluid mechanics*. John Wiley & Sons, New York, 3rd edition, 1985.
 25. R.S. Reneman, T. van Merode, P. Hick, and A.P. Hoeks. Flow velocity patterns in and distensibility of the carotid artery bulb in subjects of various ages. *Circulation*, 71(3):500–9, 1985.
 26. H.L. Goldsmith and V.T. Turitto. Rheological aspects of thrombosis and haemostasis: basic principles and applications. ict-report–subcommittee on rheology of the international committee on thrombosis and haemostasis. *Thromb Haemost*, 55(3):415–35, 1986.
 27. P.C. Lu, C.N. Hui, and N.H.C. Hwang. A model investigation of the velocity and pressure spectra in vascular murmurs. *Journal of Biomechanics*, 16(11):923–931, 1983.
 28. C. Clark. Turbulent wall pressure measurements in a model of aortic stenosis. *J Biomech*, 10(8):461–72, 1977.
 29. J.J.M. Pel and R. van Mastrigt. Development of a computational model urethra to study perineal noise as a diagnostic marker to prostatic obstruction. *Journal of Biomechanics*, 39(Suppl. 1):S390, 2006.
 30. K. Koiso, R. Nemoto, and M. Ohtani. Urographic studies of benign prostatic hypertrophy. *Journal of Urology*, 145:1071–1077, 1991.
 31. A.J. van Koevinge and R. van Mastrigt. A relation between the sound produced by urethral turbulence in patients and objectively assessed subvesical obstruction. *Neurourology and Urodynamics*, 10:442–443, 1991.
 32. R.S. Lees and C. Forbes Dewey Jr. Phonoangiography: A new diagnostic method for studying arterial disease. *Proceedings of the National Academy of Sciences*, 67(2):935–942, 1970.

33. G.W. Duncan, G.O. James, C. Forbes Dewey Jr, G.S. Myers, and R.S. Lees. Evaluation of carotid stenosis by phonoangiography. *New England Journal of Medicine*, 27(Nov):1124–1128, 1975.
34. W.H. Pitts and C.F. Dewey. Spectral and temporal characteristics of post-stenotic turbulent wall pressure fluctuations. *Journal of Biomechanical Engineering*, 101:89–95, 1979.
35. J.J. Fredberg. Origin and character of vascular murmurs: Model studies. *Journal of Acoustic Society of America*, 61(4):1077–1085, 1977.
36. P. Ask, B. Hok, D. Loyd, and H. Teriö. Bio-acoustic signals from stenotic tube flow: state of the art and perspectives for future methodological development. *Medical and Biological Engineering and Computing*, 33:669–675, 1995.

Chapter 3

Abstract

Aims: At present, an invasive pressure flow study is recommended to diagnose urinary bladder outlet obstruction. This method induces the risk of urinary tract infection and urethral trauma. We studied perineal noise recording as an alternative, non-invasive diagnostic method in three flexible/extensible model urethras and two silicone tubes. **Methods:** The flexible/extensible model urethras were made of a 10% aqueous solution of polyvinyl alcohol (PVA) and differed in wallstiffness, the silicone tubes differed in diameter and wall-thickness. Three degrees of obstruction were applied by inflating a cu placed around the PVA-urethras and by compressing the silicone tubes with an adjustable clamp. Noise, produced during flow, was recorded at three positions distal to the obstruction using a piezoceramic contact microphone. **Results:** The average amplitude of the noise and the essential frequency of the power spectrum of each noise recording depended significantly on the degree of obstruction, the position of the microphone and the wall-stiffness in PVA-urethras and the diameter in silicone tubes. **Conclusions:** Based on the results of this study perineal noise recording shows good potential as an alternative method for diagnosing bladder outlet obstruction.

Adapted from: T. Idzenga, J.J.M. Pel, R. Baldewsing and R. van Mastrigt, "Perineal noise recording as a non-invasive diagnostic method of urinary bladder outlet obstruction: a study in Polyvinyl Alcohol and silicone model urethras", *Neurourology and Urodynamics* 24, 381-388, 2005.

Chapter 3

Perineal sound recording as a non-invasive diagnostic method of urinary bladder outlet obstruction: a study in Polyvinyl Alcohol and silicone model urethras

Introduction

In most ageing males, lower urinary tract symptoms, for example a poor flow rate, result from an obstructed urethra caused by an enlarged prostate. In some cases, however, a weakly contracting bladder also causes a poor flow rate. At present the International Continence Society (ICS) recommends a provisional method for diagnosing bladder outlet obstruction on the basis of the maximum flow rate and the associated detrusor pressure¹. The transurethral catheters used for such a pressure flow study induce the risk of urinary tract infection and urethral trauma^{2,3}. Recently, non-invasive (and more patient friendly) measurement techniques have been developed and tested to diagnose bladder outlet obstruction in patients with lower urinary tract symptoms: the Doppler flowmetry method⁴, the condom-catheter method⁵ and the cuff method⁶. Another non-invasive measurement technique may be based on urethral sound recording. The development of this technique started in the mid-sixties with a voiding audiograph⁷. It was thought that the splashing sound of urine voided in a cup, recorded with a microphone and corrected for the voided volume, was a measure for bladder pressure. One decade later, the microphone was moved from the cup to the body at the level of the perineum (between scrotum and anus) and the sound produced in the urethra and the flow rate were recorded⁸. It was hypothe-

sised that urinary flow is turbulent at the bladder neck. These turbulences cause pressure fluctuations on the wall of the urethra that can be recorded as sound transmitted via the urethra to the skin. In silicone⁹ or latex^{10,11} test tubes it has been shown that pressure fluctuations are indeed induced by flow and that the power spectrum of the recorded sound depends among others on the degree of obstruction applied.

Based on differences in spectral intensities it was shown that the recorded sound correlated with flow rate⁸. Another decade later, experimental^{9,12} and clinical studies^{12,13} were published on the relation between sound recordings and bladder outlet obstruction. In the same period of time studies were done on vascular murmurs caused by stenoses, a method referred to as phonoangiography^{10,11,14–17}. It was shown that based on either the mean power frequency⁹, the break frequency of the sound spectrum^{10,11,17}, the shape of the recorded sound signal¹² or a combination of the average power amplitude in a specific frequency band with the simultaneously measured flow rate¹³ diagnosing arterial stenosis and bladder outlet obstruction could be possible.

In a review on bio-acoustic signals it was noted that the phonoangiographic methods might be non-invasive and inexpensive, but that clinical application of these methods has been overtaken by large-scale application of ultrasound Doppler¹⁸. Nevertheless, over the years attempts have been made to relate sound recordings from biological fluids (e.g. blood, urine) to the obstruction passed (stenosis or prostatic obstruction). And despite encouraging results, a non-invasive measurement device based on sound recordings is not yet available. The test tubes used in earlier experiments are rather stiff compared to the more flexible and distensible blood vessel or urethra. Recently, it was reported that flexible and distensible tubes could easily be constructed using a 10% aqueous solution of Polyvinyl Alcohol (PVA) cryogel¹⁹. The number of freeze-thaw cycles, the rate of freezing and thawing and the concentration of the PVA control the elastic properties of this gel. The aim of the present study is to establish the relation between the recorded sound and the degree of obstruction. Using model urethras made of PVA cryogel (in this paper referred to as PVA-urethras) in an experimental setup we were able to independently vary the large number of parameters (i.e. degree of obstruction, bladder pressure, microphone position and wall-stiffness of the urethra) that influence the produced sound. Direct measurements in volunteers, without preceding model studies would make deciphering of the recorded sound virtually impossible as a result of the large number of factors influencing it. The results of this study provide us with tools to interpret sound recordings in volunteers.

We constructed three PVA-urethras with different wall-stiffness, applied three degrees of obstruction by inflating a cuff placed around the PVA-urethra and recorded the sound at three positions distal to the applied obstruction. The flow rate was kept constant and was identical in all recordings. We analysed the recordings by calculating the average sound-amplitude of the recorded sound signals and the weighted average frequency of its power spectrum. For a comparison with earlier work⁹ we repeated the measurements in two silicone tubes with different diameters.



Figure 3.1: Cross section of a PVA model urethra.

Materials & Methods

PVA- and silicone tubes The PVA cryogel, a 10% aqueous solution of PVA (Chu, Kingston, USA), was heated in boiling water for 30 min. and poured in a cylindrical mould (450 mm in length, 16 mm in diameter). A Y-shaped copper strip (legs of 4 mm) was placed along the centre of the mould to create a channel allowing flow through the PVA-urethra (see figure 3.1). The exposure of the cryogel to air was minimized to prevent evaporation of water. Some free space was maintained at the top of the mould to allow air bubbles to escape and to allow expansion of the frozen cryogel. After 6 hours of rest at room temperature (21°C), the mould was stored in a freezer at -20°C. After 14 hours in the freezer the mould was stored at room temperature for 10 hours. That completed one freeze-thaw cycle. Three PVA-urethras were made with 2, 3 and 4 freeze-thaw cycles (PVA₂, PVA₃ and PVA₄ respectively). Increasing the number of freeze-thaw cycles resulted in a PVA-urethra with increased wall-stiffness. We characterized the wall-stiffness of our PVA-urethras by their elastic moduli. We estimated that in the human urethral wall in vivo strain varies between 0-0.5. In this range the elastic moduli of the PVA-urethras were approximately 2×10^4 , 4×10^4 and 7×10^4 N/m². All PVA-urethras were kept in demineralized water to prevent dehydration.

The silicone tubes (Rubber BV, Hilversum, The Netherlands) used had an inner diameter of 6.0 and 9.6 mm (S₁ and S₂ respectively), and an outer diameter of 8.0 and 12.8 mm. The elastic modulus was in the order of 10^6 N/m².

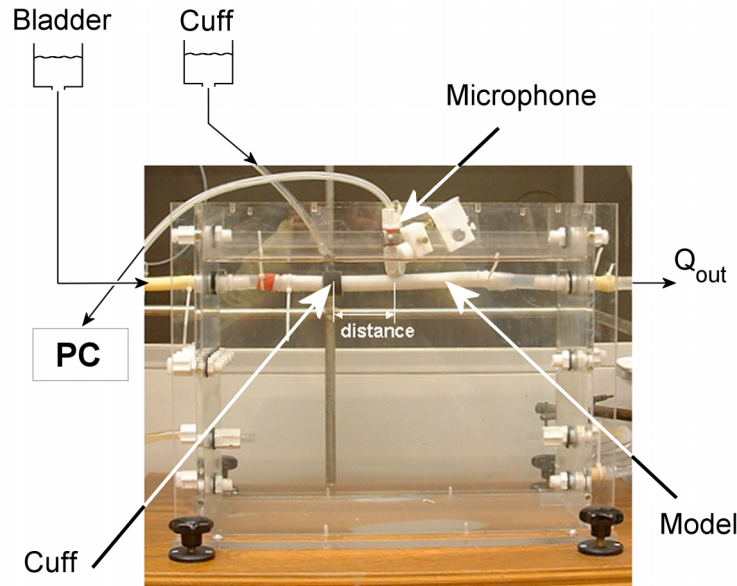


Figure 3.2: The measurement setup. Changing the combination of 'bladder pressure' and 'cuff pressure' varied the degree of obstruction. For all combinations the flow rate was 6 ml/s.

Measurement set-up The PVA-urethras (160 mm in length) and the silicone tubes were placed 5 cm below the water surface in a self-made container filled with demineralized water (see figure 3.2). Polyurethane tubing was used to connect one side of the PVA-urethras or tubes via a turbine flow meter (Flo-sensor 101, McMillan Company, USA) to a water column representing the bladder. The water level in this column was kept constant using a floating device to mimic a constant bladder pressure, which was measured with a pressure transducer at the entrance of the container. The other side of the PVA-urethras/tubes was connected to a polyurethane outflow tube draining into a sink. An inflatable cuff, controlled by a second water column (cuff pressure) was placed around each PVA-urethra to create an obstruction. In the silicone tubes compressing the tubes with an adjustable clamp created the different degrees of obstruction.

sound was recorded with a waterproofed microphone (Electret, a flat frequency response between 20 and 18000 Hz) that was placed against the wall of each urethra/tube. The sound signal was amplified 10 times using an amplifier (constructed at the department of Experimental and Medical Instrumentation, Erasmus MC, Rotterdam, The Netherlands). To reduce environmental sound the signal was band-pass filtered between 50-5000 Hz using a 4-pole Butterworth-filter (Krohn-Hite 3944, Krohn-Hite Corporation, USA). The filtered signal was sampled at a rate of 10 kHz and stored in a PC using an Analog-Digital Converter (PCL-818, Advantech, Taiwan) for further analysis with self-made programs in Matlab® (The Mathworks, Inc., USA).

Three degrees of obstruction were applied to each PVA-urethra and silicone tube. These

degrees of obstruction were obtained by applying bladder pressures of 75, 100 and 150 cm H₂O. In the PVA-urethras the cuff pressure at each bladder pressure was adjusted to ~ 60, ~90 and ~140 cm H₂O respectively to attain a constant flow rate of 6 ml/s. The corresponding Bladder Outlet Obstruction Indices (BOOI²⁰) were 63, 88 and 138 (all in the 'obstructed' region) and the corresponding Bladder Contractility Indices (BCI²⁰) were 105, 130 (both 'normal' contractility) and 180 ('strong' contractility). In the silicone tubes, the clamp was adjusted to attain the same flow rate at the three applied bladder pressures. We labeled the three degrees of obstruction as mild, medium and severe. The microphone was positioned at three positions (3, 5 and 7 cm) from the midpoint of the cuff/clamp. 9 Recordings (sound recorded at 3 locations for 3 degrees of obstruction) of approximately 80 s each were done in each PVA-urethra, resulting in a total of 27 recordings. This series of 27 recordings was repeated five times. Next 9 recordings were done in each silicone tube, resulting in a series of 18 recordings. This series of 18 recordings was also repeated five times. To prevent bias, the order of the measurements was varied: starting at the mild degree of obstruction and increasing the degree of obstruction or vice versa. Finally, the ambient sound was recorded 5 times in each PVA-urethra and silicone tube at a flow rate of 6 ml/s without obstruction.

Data analysis From each recording we selected 2¹⁹ samples (~50 sec.) to calculate the average sound-amplitude (A) by taking the sum of the absolute values and dividing by the number of samples. A power spectrum of each recording was calculated using a Fast Fourier Transform after multiplying the selected part with a Hanning window. The power spectrum of each recording was quantified by its weighted average frequency (f_c) calculated as the sum of frequencies (f) times the corresponding power ($P(f)$) divided by the sum of the power, for frequencies between 100 and 1000 Hz. In the literature this weighted average frequency has also been referenced to as the Mean Power Frequency⁹.

The dependence of A and f_c on the degree of obstruction, the position of the microphone and the wall-stiffness (for PVA-urethras) or radial dimensions (for silicone tubes) was statistically tested using a multivariate analysis of variance and a multiple linear regression analysis in SPSS®.

Results

An example of a sound recording on a PVA-urethra is presented in figure 3.3a. The top-panel shows the sound signal ($A = 293$ mV with amplification factor of 10) and the lower panel shows its power spectrum ($f_c = 390$ Hz). Figure 3.3b shows an example of a recording on a silicone tube under approximately the same conditions as in figure 3.3a. In the top-panel the recorded sound signal ($A = 44$ mV with an amplification factor of 20) and in the lower panel the power spectrum of the sound signal ($f_c = 602$ Hz) are presented. The ambient sound amplitude at 6 ml/s without obstruction was approximately 25 mV in PVA₂, 50 mV in PVA₃ and PVA₄ and 5 mV in S₁ and S₂.

The means (± 1 standard error of the mean) of A recorded in each PVA-urethra, at three degrees of obstruction (mild, medium and severe) and at three positions of the

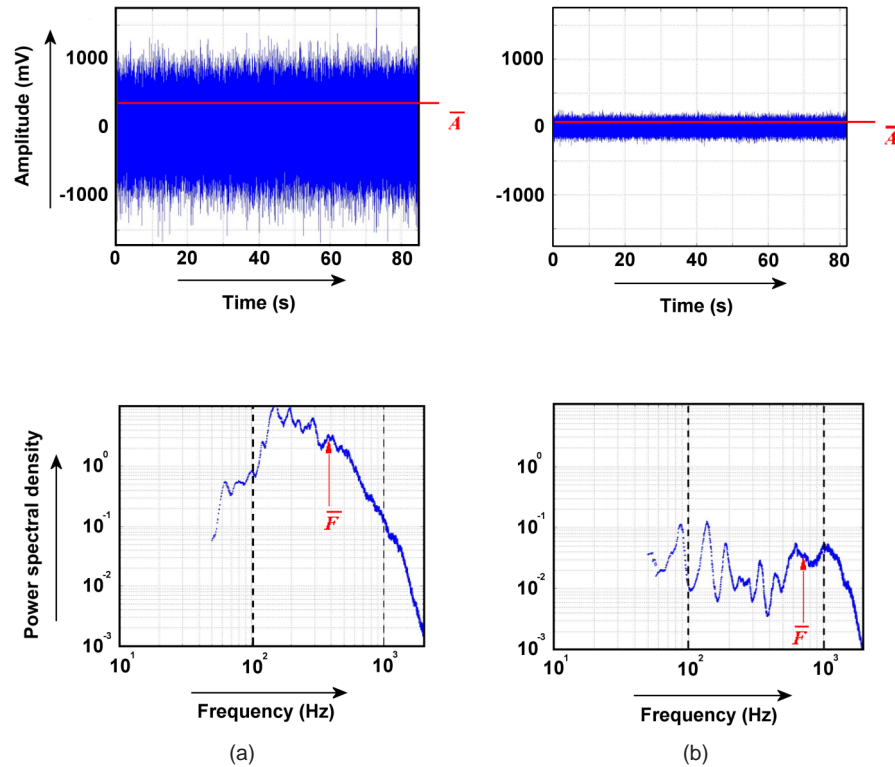


Figure 3.3: Example of a sound recording at 3 cm from the midpoint of the cuff in a medium obstructed PVA-urethra (a) and in a silicone tube (b). With an amplification factor of 10, the average amplitude was 293 mV in the PVA-urethra. And with an amplification factor of 20 the average amplitude was 44 mV in the silicone tube. The power spectra are plotted in the two lower panels; weighted average frequencies of the power spectrum were 390 Hz for the PVA-urethra and 602 Hz for the silicone tube. Both axes of the lower panels are logarithmic and the dotted vertical lines are the boundaries for calculation of the weighted average frequency.

microphone (3, 5 and 7 cm from the obstruction) are shown in figure 3.4a and 3.4c. For silicone tubes the means (± 1 standard error of the mean) of \bar{A} are presented in figure 3.4b and 3.4d. The thick black lines separate the model urethras and the dotted lines separate the degrees of obstruction. Between the dotted lines the distance between microphone and obstruction increases from left to right. Variance analysis of the data set in PVA-urethras (see table 3.1) showed that degree of obstruction, position of the microphone and wall-stiffness contributed significantly to the variation of \bar{A} ($p < .05$). In the silicone tubes (see table 3.2) degree of obstruction, position of the microphone and inner diameter (or wall-thickness) of the tube contributed significantly to the variation of \bar{A} ($p < .05$). Regression analysis of the two data sets showed that \bar{A} significantly increased with increasing degree of obstruction and decreased with increasing distance

Table 3.1: Variance analysis of the average amplitude and the essential frequency of the power spectrum of sound recordings in PVA-urethras.

Source	Dependent variable	Degrees of freedom	F	<i>p</i>
Stiffness	<i>A</i>	2	96.989	< .001
	<i>f_c</i>	2	128.412	< .001
Obstruction	<i>A</i>	2	88.802	< .001
	<i>f_c</i>	2	10.899	< .001
Distance	<i>A</i>	2	24.511	< .001
	<i>f_c</i>	2	23.618	< .001
Stiffness × Obstruction	<i>A</i>	4	1.406	.237
	<i>f_c</i>	4	1.099	.361
Stiffness × Distance	<i>A</i>	4	3.252	.015
	<i>f_c</i>	4	1.473	.215
Obstruction × Distance	<i>A</i>	4	.256	.905
	<i>f_c</i>	4	.853	.495
Stiffness × Obstruction × Distance	<i>A</i>	8	.561	.808
	<i>f_c</i>	8	.300	.965

Table 3.2: Variance analysis of the average amplitude and the essential frequency of the power spectrum of sound recordings performed on silicone tubes.

Source	Dependent variable	Degrees of freedom	F	<i>p</i>
Stiffness	<i>A</i>	1	9.339	.003
	<i>f_c</i>	1	2.516	.117
Obstruction	<i>A</i>	2	50.603	< .001
	<i>f_c</i>	2	4.594	.013
Distance	<i>A</i>	2	32.322	< .001
	<i>f_c</i>	2	5.026	.009
Stiffness × Obstruction	<i>A</i>	2	.511	.602
	<i>f_c</i>	4	.831	.440
Stiffness × Distance	<i>A</i>	2	.219	.804
	<i>f_c</i>	4	.594	.555
Obstruction × Distance	<i>A</i>	4	4.219	.004
	<i>f_c</i>	4	.013	1.000
Stiffness × Obstruction × Distance	<i>A</i>	8	.360	.836
	<i>f_c</i>	8	.414	.798

between microphone and obstruction in PVA-urethras (see table 3.3) as well as in silicone tubes (see table 3.4). In the PVA-urethras *A* significantly decreased with increasing wall-stiffness. In silicone tubes *A* significantly increased with increasing inner diameter (or wall-thickness).

The means (± 1 standard error of the mean) of *f_c* recorded in each PVA-urethra and silicone tube, at the three degrees of obstruction and at the three positions of the microphone are presented in figure 3.4. Variance analysis of the data set in PVA-urethras (see table 3.1) showed again that degree of obstruction, position of the microphone and wall-stiffness all contributed significantly to the variation of the *f_c* of the recorded sound ($p < .05$). In the silicone tubes variance analysis (see table 3.2) also showed that degree of

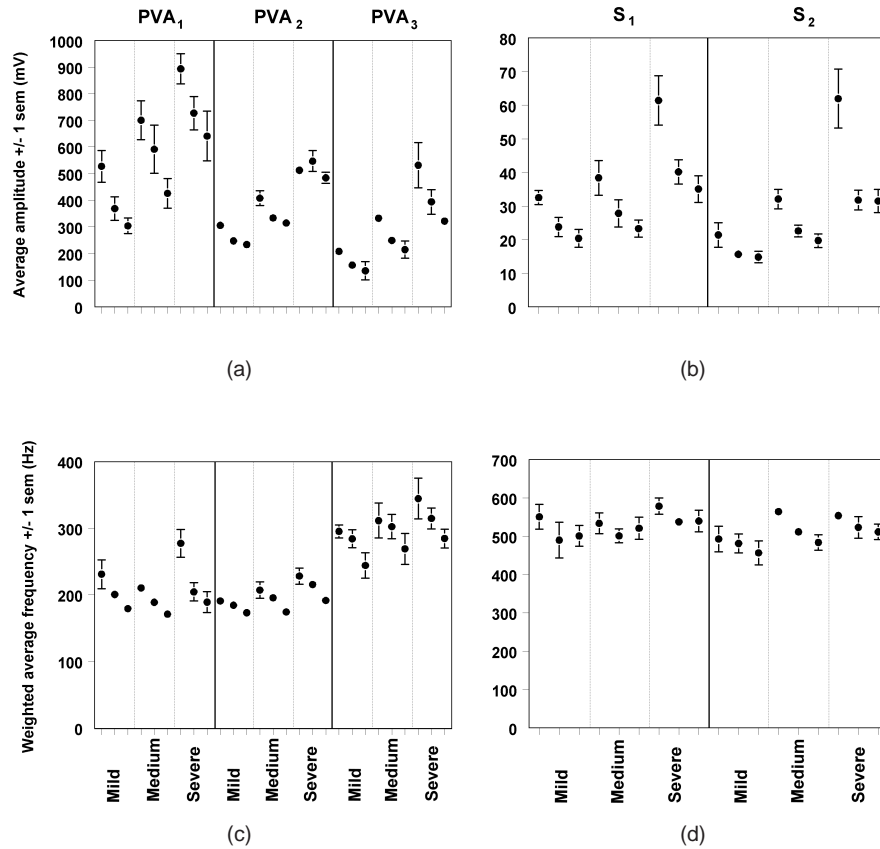


Figure 3.4: Mean (± 1 sem) average amplitude (a and b) and weighted average frequency (c and d) of five sound recordings done at nine different combinations of obstruction, position and wall-stiffness in three different PVA-urethras (PVA₂, PVA₃ and PVA₄ and two different silicone tubes (S₁ and S₂). The degrees of obstruction are separated by dotted lines and displayed on the X-axis. Within each degree of obstruction the distance from the obstruction increases from left to right (3, 5 and 7 cm). The ambient sound amplitude at 6 ml/s without obstruction was approximately 25 mV in PVA₂ and 50 mV in PVA₃ and PVA₄.

obstruction and distance between microphone and obstruction contributed significantly to the variation of f_c of the recorded sound ($p < .05$). The inner diameter (or wall-thickness) however did not contribute significantly. Regression analysis of the two data sets showed that f_c significantly increased with increasing degree of obstruction and decreased with increasing distance between microphone and obstruction in PVA-urethras as well as in silicone tubes. Regression analysis also showed that f_c significantly increased with increasing wall-stiffness of the PVA-urethra.

f_c Did not depend significantly on interactions between degree of obstruction, position of the microphone and (for PVA-urethras) wall-stiffness (for p-values see table 3.1 and 3.2).

Table 3.3: Coefficients of linear regression analysis of the average amplitude and the essential frequency of the power spectrum of the sound recorded in PVA urethras on stiffness of the model wall, the degree of obstruction and the distance between microphone and obstruction. The last two columns are the results of a t-test performed on the regression-coefficients.

		Unstandardized coefficient		t	p
		β	Std. Error		
A	Constant	606.143	43.247	14.016	< .001
	Stiffness	-146.547	11.197	-13.088	< .001
	Obstruction	142.652	11.197	12.740	< .001
	Distance	-37.381	5.599	-6.677	< .001
f_c	Constant	171.715	16.696	10.285	< .001
	Stiffness	44.340	4.323	10.257	< .001
	Obstruction	14.842	4.323	3.433	.001
	Distance	-11.656	2.161	-5.393	< .001

Table 3.4: Coefficients of linear regression analysis of the average amplitude and the essential frequency of the power spectrum of sound recorded in silicone tubes on dimensions of silicone tubes, degree of obstruction and the distance between microphone and obstruction. The last two columns are the results of a t-test performed on the regression-coefficients.

		Unstandardized coefficient		t	p
		β	Std. Error		
A	Constant	55.753	10.293	5.417	< .001
	Dimension	5.713	2.086	-2.739	.007
	Obstruction	11.116	1.277	8.702	< .001
	Distance	-4.293	.639	-6.721	< .001
f_c	Constant	614.393	54.447	10.695	< .001
	Dimension	-19.369	11.643	-1.664	.100
	Obstruction	22.656	7.130	3.178	.002
	Distance	-10.849	3.565	-3.043	.003

This means that when using f_c as a parameter the degree of obstruction, the position of the microphone and the wall-stiffness were not correlated. A However depended significantly on two interactions: in PVA-urethras A depended significantly on the interaction of position of the microphone and wall-stiffness ($p < .05$) and in silicone tubes A depended significantly on the interaction of degree of obstruction and the distance between microphone and the obstruction ($p < .05$).

Discussion

In the present study we have shown that the average amplitude (A) and the weighted average frequency (f_c) of the recorded sound-signal in PVA-urethras depend significantly on the degree of obstruction. Both increase with increasing degree of obstruction. This result supports the hypothesis that a non-invasive method for diagnosing bladder outlet obstruction might be based on perineal sound recording.

A And f_c also depend significantly on the distance between the microphone and the ob-

struction. In PVA-urethras as well as in silicone tubes A and f_c decrease with increasing distance. The changes that we applied to the microphone-position are however rather large. In an earlier study in silicone tubes, a more accurate (steps of 5 mm between microphone-positions) relation between the mean power frequency and the distance between microphone and obstruction was presented⁹. An increase was found in mean power frequency, followed by a decrease, and finally a slight increase again with increasing distance between microphone and obstruction. Since the relations between sound recording and distance between microphone and obstruction in PVA-urethras and silicone tubes show good correlation we assume that a similar relation exists in the PVA-urethra.

We also found that the wall-stiffness of the PVA-urethra significantly influenced A and f_c of the recorded sound. Therefore a urethral model with viscoelastic properties as close as possible to those of the human male urethral wall needs to be used to study the relation between sound recording and degree of obstruction as well as between sound recording and position of the microphone in detail. The viscoelastic properties of the PVA cryogel can be varied by the number of freeze-thaw cycles and this gives PVA an advantage over the silicone and latex tubes used in earlier studies^{9-11,17}.

It was also shown that obstruction, microphone-position and wall-stiffness are not correlated. This means that varying one parameter does not change the relation between A or f_c and the other two parameters. However there are two exceptions: A does depend on the interaction between microphone-position and wall-stiffness in PVA-urethras and it depends on the interaction between microphone-position and degree of obstruction in silicone tubes. The first exception suggests that when the viscoelastic properties of the wall vary, sound with the same amplitude can be found at a different microphone-position. The second exception suggests that in silicone tubes, when the degree of obstruction varies, sound with the same amplitude can be found at a different microphone-position. Therefore the microphone-position seems to be an important parameter influencing the relation between sound recordings and degree of obstruction. Also the shape and length of the obstruction and the geometry of the PVA-urethra are important parameters to be studied. Between PVA-urethras and silicone tubes a difference was observed in sound recordings (compare figure 3.4a and 3.4c to figure 3.4b and 3.4d). In silicone tubes A was a factor of about ~ 20 smaller and f_c a factor of about ~ 2 larger than in PVA-urethras. Also between the PVA-urethras with increasing stiffness A was smallest and f_c was largest in the PVA-urethra with the highest stiffness. Therefore it can be said that in general an increase in wall-stiffness led to a decrease in A and an increase in f_c . Between the two silicone tubes the inner diameter as well as the wall-thickness differed, therefore it is not really clear which of the two (or both) contributes to the variation of A . Also the shape of the power spectrum differed between PVA-urethras and silicone tubes (see figure 3.3a and 3.3b).

In the past sound recordings have been done in obstructed males. The mean power frequency⁹ (equivalent of the weighted average frequency with different cut-off frequencies) varied between 150-450 Hz and average power was found between 300-750 Hz¹³. In males with BPH and in males after prostatectomy, power was found between 500-650 Hz¹². In our present study we calculated weighted average frequencies between 150-400 Hz in PVA-urethras. In silicone tubes we calculated weighted average frequencies between 340-650 Hz. Our results appear to be comparable to the mean power frequency

measured in obstructed males. This comparison might be slightly biased by the different frequency-boundaries used by Teriö for the calculation of his mean power frequency. The values found however are lower than those measured in males with BPH and in males who underwent prostatectomy. This difference may be explained by the higher flow rate (in the order of 14 ml/s) measured in the males with BPH and after prostatectomy as opposed to the flow rate of 6 ml/s in our model, which could lead to a difference in power spectrum. A second possible explanation for the difference in spectral characteristics is the difference in viscoelastic properties of the tube-wall and the human male urethral wall (including the surrounding tissue).

Conclusions

The diagnosis of bladder outlet obstruction is presently based on the pressure flow study, an invasive method. There are also non-invasive methods to diagnose bladder outlet obstruction: using Doppler flowmetry⁴ to measure flow velocity or using either condom type catheters⁵ or inflatable cuffs⁶ to measure the bladder pressure. Although all three non-invasive techniques are very patient friendly, the last two methods require the flow rate to be manipulated during voiding, and the first method requires expensive equipment. Based on the results of this study and the earlier work of Teriö⁹ an alternative method for diagnosing bladder outlet obstruction based on perineal sound recording seems to show good potential. For development of such an alternative method the relation between sound recordings and degree of obstruction needs to be studied more extensively. Therefore sound recordings need to be done at more than one flow rate and with a wider range of bladder pressures.

Literature

1. D.J. Griffiths, K. Höfner, R. van Mastrigt, H.J. Rollema, A. Spångberg, and D.M. Gleason. Standardization of terminology of lower urinary tract: pressure-flow studies of voiding, urethral resistance and urethral obstruction. *Neurourology and Urodynamics*, 16:1–18, 1997.
2. H.C. Klingler, S. Madersbacher, B. Djavan, G. Schatzl, M. Marberger, and C.P. Schmidbauer. Morbidity of the evaluation of the lower urinary tract with transurethral multichannel pressure-flow studies. *Journal of Urology*, 159(1):191–194, 1998.
3. D. Porru, G. Madeddu, G. Campus, I. Montisci, R.M. Scarpa, and E. Usai. Evaluation of morbidity of multi-channel pressure-flow studies. *Neurourology and Urodynamics*, 18(6):647–652, 1999.
4. Y.Y. Ding, H. Ozawa, T. Yokoyama, Y. Nasu, M.B. Chancellor, and H. Kumon. Reliability of color doppler ultrasound urodynamics in the evaluation of bladder outlet obstruction. *Urology*, 56:967–971, 2000.
5. J.J.M. Pel and R. van Mastrigt. The variable outflow resistance catheter: a new method to measure bladder pressure noninvasively. *Journal of Urology*, 165:647–652, 2001.

6. D.J. Griffiths, D. Rix, M. MacDonald, M.J. Drinnan, R.S. Pickard, and P.D. Ramsden. Noninvasive measurement of bladder pressure by controlled inflation of a penile cuff. *Journal of Urology*, 167:1344–1347, 2002.
7. W.A. Keitzer and G.C. Huffman. The voiding audiograph: a new voiding test. *Journal of Urology*, 95:404–410, 1966.
8. W.E. Bradley, B.P. Brockway, and G.W. Timm. Auscultation of urinary flow. *Journal of Urology*, 118:73–75, 1977.
9. H. Teriö. Acoustic method for assessment of urethral obstruction: a model study. *Medical and Biological Engineering and Computing*, 29:450–456, 1991.
10. R.J. Tobin and I.D. Chang. Wall pressure spectra scaling downstream of stenoses in steady tube flow. *Journal of Biomechanics*, 9:633–640, 1976.
11. S.A. Jones and A. Fronek. Analysis of break frequency downstream of a constriction in a cylindrical tube. *Journal of Biomechanics*, 20(3):319–327, 1987.
12. K. Koiso, R. Nemoto, and M. Ohtani. Urographic studies of benign prostatic hyper-trophy. *Journal of Urology*, 145:1071–1077, 1991.
13. A.J. van Koeveringe and R. van Mastrigt. A relation between the sound produced by urethral turbulence in patients and objectively assessed subvesical obstruction. *Neurourology and Urodynamics*, 10:442–443, 1991.
14. R.S. Lees and C. Forbes Dewey Jr. Phonoangiography: A new diagnostic method for studying arterial disease. *Proceedings of the National Academy of Sciences*, 67(2):935–942, 1970.
15. G.W. Duncan, G.O. James, C. Forbes Dewey Jr, G.S. Myers, and R.S. Lees. Eval-uation of carotid stenosis by phonoangiography. *New England Journal of Medicine*, 27(Nov):1124–1128, 1975.
16. W.H. Pitts and C.F. Dewey. Spectral and temporal characteristics of post-stenotic turbulent wall pressure fluctuations. *Journal of Biomechanical Engineering*, 101:89–95, 1979.
17. J.J. Fredberg. Origin and character of vascular murmurs: Model studies. *Journal of Acoustic Society of America*, 61(4):1077–1085, 1977.
18. P. Ask, B. Hok, D. Loyd, and H. Teriö. Bio-acoustic signals from stenotic tube flow: state of the art and perspectives for future methodological development. *Medical and Biological Engineering and Computing*, 33:669–675, 1995.
19. K.C. Chu and B.K. Rutt. Polyvinyl alcohol cryogel: an ideal phantom material for mr studies of flow and elasticity. *MRM*, 37:314–319, 1997.
20. P Abrams. Bladder outlet obstruction index, bladder contractility index and bladder voiding efficiency: three simple indices to define bladder voiding function. *BJU International*, 84:14–15, 1999.

Chapter 4

Abstract

Aims: We aim at developing a non-invasive method for grading and diagnosing urinary bladder outlet obstruction, based on noise recording with a perineal contact microphone during voiding. We found that the noise production during voiding depends amongst others on the viscoelastic properties of the urethral wall. To further test our method, we need a realistic biophysical model of the male urethra. **Methods:** We made various model urethras with different viscoelastic properties from a 10% aqueous solution of polyvinyl alcohol cryogel. We measured the viscoelastic properties of each model and compared them to those of the male pig urethra. The male pig urethra was used, as it is physiologically comparable to the human male urethra. The viscoelastic properties of both model and pig urethras were measured by applying strain to the urethral wall in a stepwise manner and recording the pressure response. We fitted the step-response of a mechanical model to this pressure response and derived the viscoelastic properties from the coefficients of this response. **Results:** A uniform model urethra that was freeze-thawed three times, with a Y-shaped flow channel was found to best represent the male pig urethra. **Conclusions:** We consider the three times freeze-thawed model urethra with a Y-shaped flow channel the best model of the human male urethra. And we therefore use this model urethra for studying the relation between noise recording during urine ow and the degree of bladder outlet obstruction.

Adapted from: T. Idzenga, J.J.M. Pel and R. van Mastrigt, "A biophysical model of the male urethra: comparing viscoelastic properties of PolyVinyl Alcohol urethras to male pig urethras", *Neurourology and Urodynamics* 25, 451-460, 2006.

Chapter 4

A biophysical model of the male urethra: comparing viscoelastic properties of PolyVinyl Alcohol urethras to male pig urethras

Introduction

At present a pressure-flow study is the standard method used in urology to diagnose urinary bladder outlet obstruction. An enlarged prostate may cause such an obstruction. For a pressure-flow study a catheter is inserted via the urethra into the bladder. During voiding the urinary flow-rate and the pressure in the bladder are measured and the combination of these two indicates whether the bladder outlet is obstructed or not. This method is time-consuming, and it may also induce urethral trauma^{12,14}. We are developing an alternative non-invasive method that is based on the turbulent flow-pattern in the male urethra during voiding⁹. This flow pattern causes pressure fluctuations at the urethral wall that can be measured by placing a piezoelectric microphone against the perineum, between scrotum and anus^{2,13}.

In recent decades the relationship between audible sound and the degree of obstruction has been studied with the aim of diagnosing cardiovascular stenosis^{8,11} and bladder outlet obstruction^{13,17}. Latex tubing^{10,16} has been used as a model of blood vessels, and silicone tubing to model the urethra¹⁵. However, these types of tubing are considerably stiffer than arteries and the male urethra. A more flexible and extensible tube can be made from a Polyvinyl Alcohol (PVA) cryogel³. The number of freeze/thaw cycles, the rate of freezing/thawing and the concentration of the cryogel control the viscoelastic properties of this PVA cryogel. For studying the relationship between sound and degree of obstruction, such a PVA tube could be used as a realistic model of the male urethra. To establish which model urethra best represents the male urethra we have measured viscoelastic properties of different model urethras and tuned these to those measured

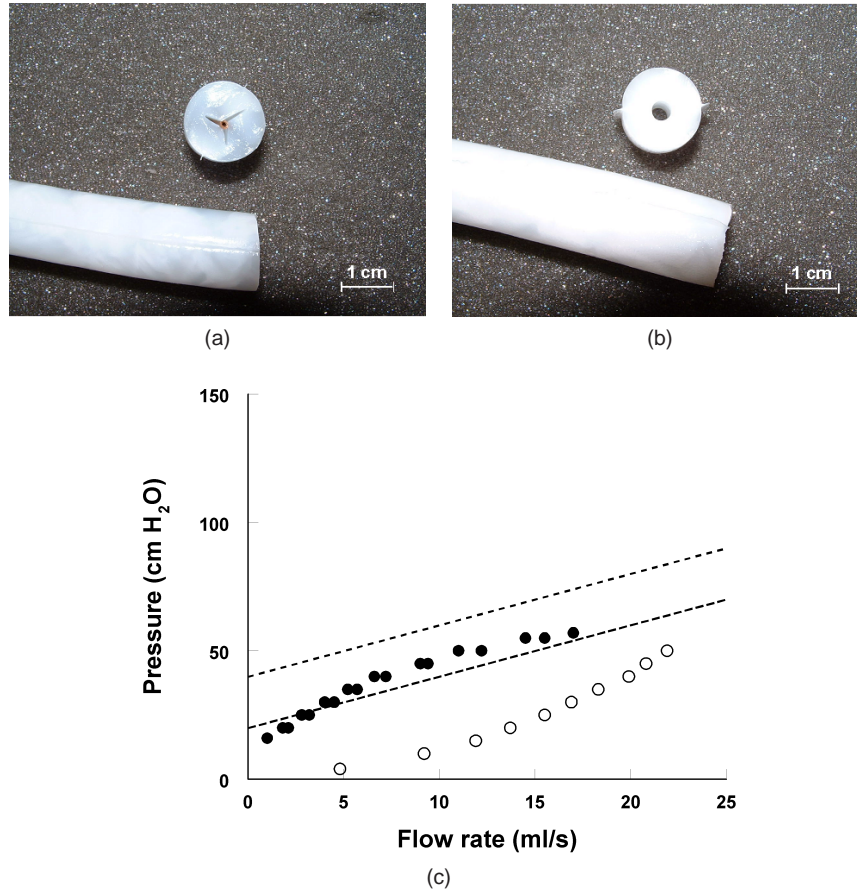


Figure 4.1: Cross-sections of a PVA model urethra with a Y-shaped (a) and with an O-shaped opening (b). c) Typical pressure-flow curve for unobstructed model urethras with a Y-shaped profile and with a circular profile. The flow rate is measured at discrete values of driving pressure. The dotted lines discriminate unobstructed, equivocal and obstructed curves according to the provisional ICS method for diagnosing intravesical obstruction.

in pig urethras. To this end, we varied the number of freeze-thaw cycles, the profile of the flow channel in the model and the number of cross-sectional layers. The rate of freezing/thawing and the concentration of the PVA cryogel were the same in all models. We used the male pig urethra as a reference for the development of a model urethra because of the similarities between pig and human physiology⁷. To measure the viscoelastic properties we used the method developed by Coolsaet et al.⁴⁻⁶, adapting it for use in cylindrical structures. This method involves the stepwise application of strain to the urethral wall by rapidly injecting known volumes of water into the urethra and recording the pressure response.

Materials & Methods

We made 12 different model urethras by pouring a 10% aqueous solution of PVA into a cylindrical mould. After 6 hours of rest at room temperature (21°C), the mould was stored in a freezer at -20°C. After 14 hours in the freezer the mould was stored at room temperature for 10 hours. That completed one freeze-thaw cycle. To create a channel allowing flow through the models, we placed either a strip with a Y-profile (with legs 5 mm wide) or a circular rod (diameter 4 mm) along the central axis of the mould (see figure 4.1).

The Y-profile reflects the lumen of a male pig urethra without flow of urine (see figure 4.2) and the circular profile reflects the expected profile of a male pig urethra during urine flow. Four models were uniform solid cylinders (outer diameter 16 mm) with a Y-profile; these were freeze-thawed one, two, three and four times respectively (indicated as Y₁, Y₂, Y₃ and Y₄). Four more models were also uniform solid cylinders (outer diameter 16 mm) and

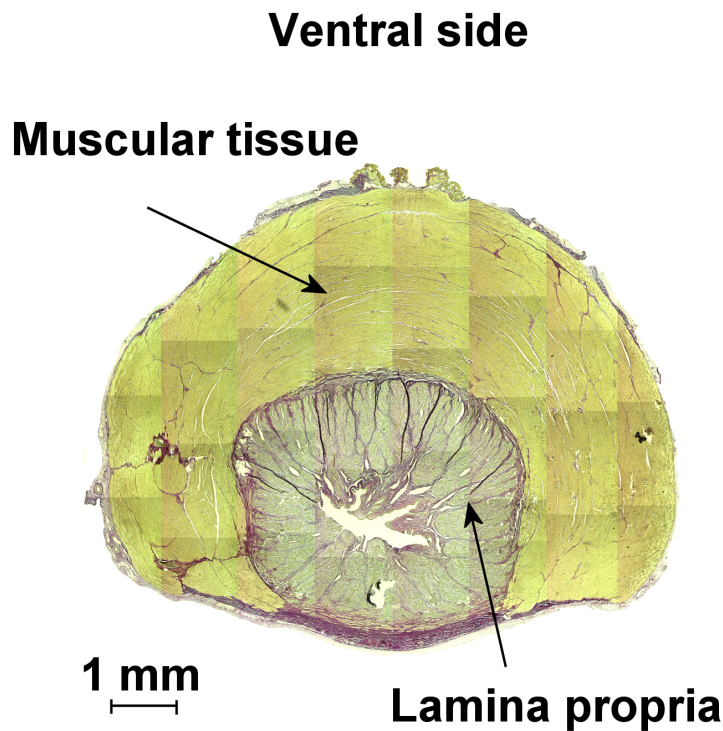


Figure 4.2: Cross-section of the proximal part of the male pig urethra. We stained elastin, collagen (both dark grey) and muscle tissue (light grey) using Elastic von Gieson staining. The lamina propria is surrounded by muscular tissue with a horseshoe-like shape.

freeze-thawed one, two, three and four times but these had a circular profile (indicated as O_1 , O_2 , O_3 and O_4). Another four models consisted of cylinders similar to those described above (but with an outer diameter of 12 mm) inside a separate shell. Two of the cylinders had a Y-profile and two had a circular profile. For each profile one cylinder was freeze-thawed once the other was freeze-thawed twice. All four cylinders were placed in a PVA shell (inner diameter 12 mm, outer diameter 16 mm) that was freeze-thawed three times. These models are indicated as $Y_{1/3}$, $Y_{2/3}$, $O_{1/3}$ and $O_{2/3}$. Typical pressure-flow curves for model urethras with a Y-shaped profile and with a circular profile are shown in figure 4.1c. In the human urethra hysteresis causes the pressure flow curves to take the form of a loop. This is by variation in the degree of urethral relaxation during voiding. In the model urethras no hysteresis loop is observed, as there is no such relaxation mechanism. We made bladder/urethra preparations from 8 male pigs sacrificed at the department of Experimental Cardiology (Erasmus MC, Rotterdam, the Netherlands). The part of the urethra closest to the bladder (proximal part), distal to the prostate was selected for the measurements. The prostate of the pig is located just under the bladder. The average (± 1 sd) length of the sections was 65 ± 16 mm. An example of a cross-section is shown in figure 4.2. We used Elastic von Gieson staining¹ to mark elastin, collagen and muscle tissue in this cross-section.

Each model was placed in a water-filled container (approx. 1 cm below the water-surface) at room temperature and each pig urethra was placed in a container (approx. 1 cm below the solution-surface) filled with a cold (10°C) modified Krebs solution (118 mM NaCl; 4.7 mM KCl; 25 mM NaHCO₃; 1.2 mM KH₂PO₄; 1.8 mM CaCl₂; 1.2 mM MgSO₄ and 11 mM glucose aerated with 95% O₂ and 5% CO₂ (pH of 7.4)). One side of the model or pig urethra was connected to a 5 ml syringe to manually inject a known volume of water in a very short time. The pressure response was recorded using a disposable pressure transducer connected to the other side of the urethra. The pressure transducer was zeroed to the atmosphere at the level of the pig or model urethra. Increasing volumes were injected, starting at 0.2 ml with increments of 0.2 ml to a maximum of 5 ml, or to the volume at which the range of the pressure transducer (~ 250 cm H₂O) was exceeded. After each measurement the injected water was extracted. The transducer signal was sampled at a frequency of 1000 Hz using an AD-converter (PCL-818, Advantech[®]) and stored in a PC for further analysis using custom-written programs in Matlab[®].

For an approximate calculation of the viscoelastic properties of the model and pig urethras from the recorded pressure response we made a mechanical model of the urethral wall consisting of springs, dashpots and a mass (see Appendix). The simplified analytical solution for the step-response (Eqn. A-6) was fitted to 1000 samples (equivalent of 1 sec.) of the pressure signal. These 1000 samples were selected from the maximum in the pressure signal onwards (see figure 4.3). The fit-procedure resulted in 6 coefficients: $a_{0,1,2}$, $b_{1,2}$ and c_2 . The coefficients $a_{0,1,2}$ were converted from units of pressure into units of stress ($\sigma_{0,1,2}$) using Laplace's Law⁶, see Appendix. The coefficients b_1 and b_2 were converted into the time-constants τ_1 and τ_2 (the reciprocals of b_1 and b_2). The oscillation frequency f of the mass in the mechanical model was derived from c_2 .

Differences in the three time-related parameters (i.e. τ_1 , τ_2 and f) between each model urethra and the pig urethras were tested using a Mann-Whitney U-test. The stress-parameters (i.e. σ_0 , σ_1 and σ_2) in pig urethras were found to depend on the applied strain. The stress-strain functions of each pig urethra were fitted with an exponential

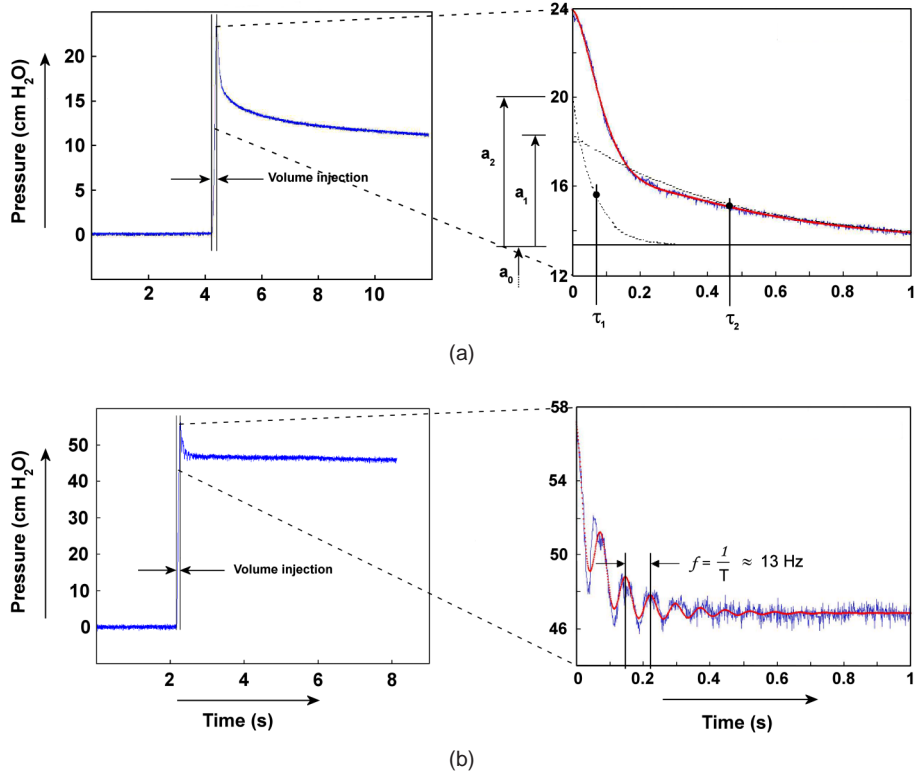


Figure 4.3: Examples of the selected part of the measured pressure response and the fitted function in a pig urethra (a) and model urethra Y_2 (b). The step response of the mechanical model was fitted to a 1000 samples (equivalent to 1 second of the pressure signal) from the maximum pressure onwards. The solid line represents the analytical solution of the mechanical model (with a low frequent oscillation of approx. 2 Hz) fitted to the recorded data. In (a) the two dotted lines represent the two exponential terms without taking the multiplicative oscillation term into account. The amplitudes and time-constants of the exponentials are indicated by $a_{0,1,2}$ and $\tau_{1,2}$. In (b) a high frequent oscillation in one of the model urethras is shown.

function and the average exponential function and its approximate 95% Confidence Interval (CI) were calculated. As a measure of agreement, we used the overlap between the stress-parameters measured in the models and the 95% CI calculated for the pig urethras.

Results

An example of the pressure response to injection of water in a pig urethra is shown in figure 4.3. The injection time was kept short (~ 0.1 s) to induce a step-response. Figure 4.3, top panel, shows the selected part of the pressure response measured in a

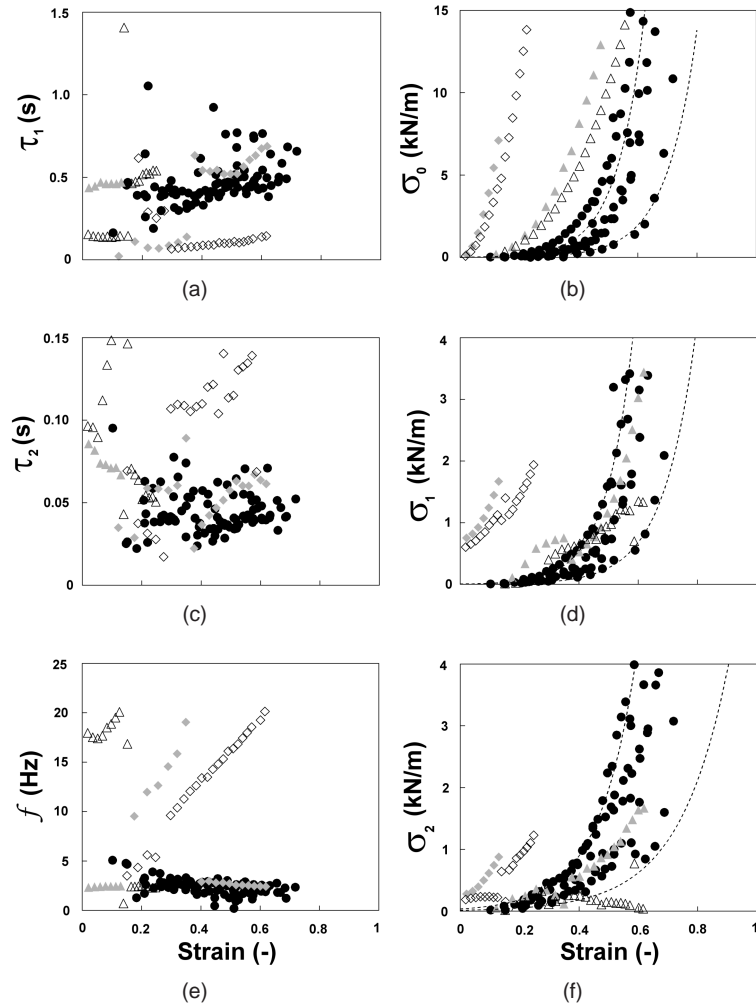


Figure 4.4: Viscoelastic parameters as a function of the applied strain measured in male pig urethras (\bullet) and in model urethras Y_3 (\blacktriangle), $Y_{2/3}$ (\triangle), O_2 (\diamond) and O_3 (\blacklozenge). In panel (a) and (c) τ_1 and τ_2 are plotted. The scale of the Y-axis in panel (c) is a factor 10 smaller than that of the top panel. Some of the models (e.g. Y_3 and O_2) have a discontinuity in τ_1 and τ_2 at a certain level of strain. The oscillation frequency is plotted in panel (e). In model O_3 the oscillation frequency was found not to be significantly different from the frequencies measured in the male pig urethra. Y_3 is an example of a model in which the oscillation frequency equaled that of the pig urethras, but only at higher strain levels. $Y_{2/3}$ shows oscillation frequencies higher than those measured in the male pig urethras. The parameters σ_0 , σ_1 and σ_2 are plotted in panels (b), (d) and (f). The dotted lines represent the 95% CI of the fitted function.

pig urethra. Upon injection of the volume the pressure increased rapidly and then decreased bi-exponentially (τ_1 and τ_2) to an equilibrium pressure. In the bottom panel the pressure response measured in a model urethra is shown. Again, pressure decreased bi-exponentially, but in most of the models the pressure signal showed a more distinct oscillation (f) than in pig urethras. The wall of the model with a Y-shaped channel that was freeze-thawed one time was not strong enough to withstand the induced stress.

Table 4.1 summarizes the mean (\pm SD) values of f , τ_1 and τ_2 measured in pig and model urethras, including the results of the Mann-Whitney U-test. Figure 4.4e shows the oscillation frequency measured in the male pig urethras and in some of the models with different cross-sectional layers, number of freeze-thaw cycles and channel shapes. The models for which f was not significantly different from that measured in the pig urethras were Y_4 and O_3 . In some of the models a discontinuity in the frequency of oscillation was observed at a certain level of strain: Y_3 (at $\epsilon \sim 0.37$), Y_4 (at $\epsilon \sim 0.2$), O_2 (at $\epsilon \sim 0.15$) and $O_{2/3}$ (at $\epsilon \sim 0.18$). The models with an oscillation frequency that was not significantly different from that in male pig urethras, but only at the higher levels of strain were: Y_3 , O_2 and $O_{2/3}$.

The top left panel of figure 4.4 shows the time-constant τ_1 measured in the pig urethras and some of the model urethras. The models for which τ_1 was not significantly different from τ_1 in the male pig urethra were: Y_3 , Y_4 , O_2 and O_3 . The models that showed a discontinuity in f also showed a discontinuity in τ_1 at the same level of strain.

All model urethras had a time-constant τ_2 that was significantly different from that in the male pig urethra. However, the model with τ_2 closest to the one measured in male pig urethras was Y_3 ($p < .05$), see table 4.1 and figure 4.4c. Also in the time-constant τ_2 the same four models showed a discontinuity at the same level of strain as for f and τ_1 .

Figure 4.4 shows the stress-parameter σ_0 in the male pig urethra as a function of the applied strain and data of some model urethras with different cross-sectional layers, number of freeze-thaw cycles and channel shapes. The solid line represents the average of the exponential functions fitted to the data in each pig urethra and the dotted lines represent the 95% CI of this average. In the model urethras stress increased more rapidly as a

Table 4.1: Time-parameters f , τ_1 and τ_2 (mean \pm SD) and the number of measurements that were done in the male pig urethra (indicated by σ) and in the different model urethras. The results of the Mann-Whitney U-tests are noted by the p-values between brackets.

	N	τ_1 (s)	τ_2 (s)	f (Hz)
σ	88	0.47 \pm 0.30	0.046 \pm 0.026	2.9 \pm 1.8
Y_2	20	0.09 \pm 0.06 ($p < .001$)	0.141 \pm 0.055 ($p < .001$)	12.4 \pm 3.5 ($p < .001$)
Y_3	19	0.40 \pm 0.25 ($p = .735$)	0.054 \pm 0.015 ($p < .050$)	6.6 \pm 5.9 ($p < .010$)
Y_4	16	0.41 \pm 0.14 ($p = .690$)	0.062 \pm 0.016 ($p < .001$)	4.9 \pm 5.1 ($p = .215$)
$Y_{1/3}$	24	0.07 \pm 0.03 ($p < .001$)	0.161 \pm 0.040 ($p < .001$)	7.2 \pm 1.8 ($p < .001$)
$Y_{2/3}$	24	0.17 \pm 0.15 ($p < .001$)	0.105 \pm 0.044 ($p < .001$)	12.1 \pm 5.8 ($p < .001$)
O_1	24	0.12 \pm 0.05 ($p < .001$)	0.216 \pm 0.036 ($p < .001$)	10.7 \pm 0.9 ($p < .001$)
O_2	18	0.38 \pm 0.32 ($p = .141$)	0.093 \pm 0.045 ($p < .001$)	10.2 \pm 8.3 ($p < .010$)
O_3	7	0.46 \pm 0.01 ($p = .428$)	0.075 \pm 0.007 ($p < .001$)	2.4 \pm 0.05 ($p = .743$)
O_4	5	0.20 \pm 0.01 ($p < .001$)	0.122 \pm 0.013 ($p < .001$)	12.7 \pm 0.8 ($p < .001$)
$O_{1/3}$	24	0.09 \pm 0.04 ($p < .001$)	0.123 \pm 0.013 ($p < .001$)	12.1 \pm 1.7 ($p < .001$)
$O_{2/3}$	17	0.30 \pm 0.19 ($p < .050$)	0.099 \pm 0.052 ($p < .001$)	12.5 \pm 7.5 ($p < .001$)

Table 4.2: Comparison of viscoelastic parameters between the different model urethras and the male pig urethra. The agreement between the male pig urethra and the different model urethras is depicted as good (+), adequate (\pm) or bad (-).

	τ_1 (s)	τ_2 (s)	f (Hz)	σ_0 (kN/m)	σ_1 (kN/m)	σ_2 (kN/m)
Y ₂	-	-	-	-	-	-
Y ₃	+	+	\pm	-	+	+
Y ₄	+	+	+	-	-	+
Y _{1/3}	-	-	-	\pm	-	\pm
Y _{2/3}	-	-	-	-	\pm	-
O ₁	-	-	-	-	+	+
O ₂	+	\pm	\pm	-	-	-
O ₃	+	-	+	-	-	-
O ₄	-	-	-	-	-	-
O _{1/3}	-	-	-	-	-	-
O _{2/3}	\pm	\pm	\pm	-	-	-

function of strain with increasing number of freeze-thaw cycles. The increase in stress as a function of strain appeared to be higher in models with a circular opening than in model urethras with a Y-shaped opening. The stress-strain plots for the stress-parameters σ_1 and σ_2 were similar, except that the range of these stress-values was smaller than that of σ_0 , see figure 4.4b, 4.4d and 4.4f.

An overall comparison of the viscoelastic properties of the different model urethras and the male pig urethra, based on level of agreement, is presented in table 4.2. From table 4.2 it can be concluded that models Y₃ and Y₄ best represent the male pig urethra.

Discussion

In order to study the relation between sound recorded at the perineum and urinary bladder outlet obstruction we have developed a biophysical model of the male urethra. To develop such a model we measured the viscoelastic properties of different model urethras made from PVA cryogel. The intended location of sound recording (i.e. perineum) is distal to the obstruction. Therefore, only the viscoelastic properties of the normal male urethra distal to the obstruction are relevant and we compared the properties of the model urethras to those measured in normal pig urethras. We varied three properties of the model urethras: the number of freeze-thaw cycles, the shape of the flow channel and the number of cross-sectional layers. It is known that during freezing and thawing the PVA solution forms cross-links through hydrogen bonding with hydroxyl groups on the PVA molecules³. When the number of freeze-thaw cycles is increased more cross-links are formed and thus the strength and stiffness increases. Also with increasing number of freeze-thaw cycles the PVA gets more and more compact and the outer diameter of the model urethra decreases slightly (approx. 1 mm). This is not expected to significantly change the values of the parameters. The increase in stiffness with increasing number of

freeze-thaw cycles was best demonstrated by the stress parameter σ_0 of the model urethras. With a larger number of freeze-thaw cycles the stress-parameter increased more rapidly with strain (which implies an increase in stiffness). The increase in stiffness with the number of freeze-thaw cycles was also found by Chu³. In figure 4.4b only data of a few models has been plotted but this effect was found in all models. In models with a circular shaped opening the increase in stress, as a function of strain, appeared to be slightly higher than in models with a Y-shaped opening. In calculating the applied strain in models it was assumed that the injected volume in the model had a circular cross section. This is not exactly the case when the opening is Y-shaped initially. This might lead to a shift of the horizontal axis and cause the difference in stress-increase that was found. The models that consisted of two layers, one softer layer surrounded by a stiffer shell were thought to mimic the stress-strain plot of the pig urethras, i.e. a small increase in stress at low strain due to the soft inner layer and a steep increase in stress at high strain due to the stiffer shell. This however did not turn out to be the case. Application of strain to the soft inner layer by injecting a volume of water probably simultaneously applied strain to the outer shell, resulting in an interaction.

Viscoelastic properties of male pig urethras and model urethras were compared by fitting a mathematical model. When interpreting the estimated parameters it should be kept in mind that these are only one set of possible parameters in the modeling of the viscoelastic properties. The sensitivity of these parameters needs to be assessed in future studies. In the male pig urethras we found that the two time-constants τ_1 and τ_2 differed a factor of ~ 10 from each other, which supports the assumption that two independent relaxation processes (indicated by the two exponential terms, see Appendix) are activated after stepwise straining of the pig urethral wall. Four model urethras (Y_3 , Y_4 , O_2 and O_3) had a time-constant τ_1 that was not significantly different from that in male pig urethras. The agreement of τ_1 between these four models and the male pig can therefore be considered as good. In all models the second time-constant τ_2 measured in model urethras was statistically different from that of the male pig urethra. However, two model urethras with τ_2 close to the range of values in male pig urethras were Y_3 and Y_4 . Since the absolute difference between the τ_2 -means of pigs and models was quite small the agreement was considered good. There were two models with τ_2 close to the range of values measured in pigs, but only at high strain: O_2 and $O_{2/3}$. The agreement of these models was considered adequate.

The oscillation frequency f in most of the model urethras was higher than that in male pig urethras. In some of the models there was a discontinuity in the oscillation frequency with increasing strain: above a certain level of strain the frequency suddenly dropped to a lower level (e.g. see model Y_3 in figure 4.4). Such a discontinuity was also observed in the time-constants τ_1 and τ_2 . At the lower level of strain the τ - and σ -values of the second and third term of the step response (Eqn. A-6) are of approximately the same order (see figure 4.4). At these levels of strain a high frequency oscillation (i.e. relative to the oscillation found in pig urethras) was found in the pressure response (see example in figure 4.3). At the higher level of strain the τ - and σ -values of the second term of equation A-6 (see Appendix) are larger than those in the third term and therefore the oscillation in the third term was outdone by the second term. In models with a high oscillation frequency at each applied strain level the τ - and σ -values of the two terms are approximately of the same order over the whole range of applied strain. Two models (Y_4 and O_3) how-

ever had an oscillation frequency that was not significantly different from the male pig urethras over the full range of applied strains and we therefore considered the agreement between the frequency measured in these models and those in pigs to be good. Three model urethras (Y_3 , O_2 and $O_{2/3}$) had an oscillation frequency not significantly different from the male pig urethras, in the higher region of applied strain only. Therefore, in these three models the agreement with pig urethras on the basis of the oscillation frequency is considered adequate.

The intended application of the model urethra we have developed is studying the relation between pressure fluctuations at the urethral wall, caused by a turbulent flow pattern, and the degree of bladder outlet obstruction. These pressure fluctuations are time-related and therefore the viscoelastic parameters f , τ_1 and τ_2 are the most important parameters in comparing the different models to the male pig urethra. Based on these parameters there are four models that best represent the male urethra, i.e. O_2 , O_3 , Y_3 and Y_4 . When the associated amplitudes σ_1 and σ_2 are also taken into account only two models remain, i.e. Y_3 and Y_4 . Adding up good and adequate agreement considerations model Y_3 shows the best agreement with the male pig urethra.

Conclusions

We aim at developing a non-invasive method for grading and diagnosing urinary bladder outlet obstruction, based on sound recording with a perineal contact microphone during voiding. The recorded sound depends (among others) on the viscoelastic properties of the urethra. We therefore developed a biophysical model to study the relation between recorded sound and degree of bladder outlet obstruction. We measured the viscoelastic properties of different model urethras and compared them to the viscoelastic properties measured in male pig urethras. Based on this comparison a model urethra with a Y-shaped flow channel that was uniformly freeze-thawed three times showed best agreement with the male pig urethra. We therefore consider this model urethra the best model of the human male urethra for studying the relation between sound recording during urine flow and the degree of bladder outlet obstruction.

Literature

1. J.D. Bancroft and A. Stevens. Theory and practice of histological techniques. Churchill Livingstone, New York, 4th edition, 1996.
2. W.E. Bradley, B.P. Brockway, and G.W. Timm. Auscultation of urinary flow. *Journal of Urology*, 118:73–75, 1977.
3. K.C. Chu and B.K. Rutt. Polyvinyl alcohol cryogel: an ideal phantom material for mr studies of flow and elasticity. *MRM*, 37:314–319, 1997.
4. B.L.R.A. Coolsaet, W.A. van Duyl, R. van Mastrigt, and A. van der Zwart. Step-wise cystometry of urinary bladder. new dynamic procedure to investigate viscoelastic behavior. *Urology*, 2(3):255–257, 1973.
5. B.L.R.A. Coolsaet, W.A. van Duyl, R. van Mastrigt, and A. van der Zwart. Viscoelastic properties of the bladder wall. *Urologia Internationalis*, 30(1):16–26, 1975.

6. B.L.R.A. Coolsaet, W.A. van Duyl, R. van Mastrigt, and J.W. Schouten. Visoelastic properties of bladder wall strips. *Investigative Urology*, 12(5):351–356, 1975.
7. W.R. Douglas. Of pigs and men and research. *Space Life Sciences*, 3:226–234, 1972.
8. G.W. Duncan, G.O. James, C. Forbes Dewey Jr, G.S. Myers, and R.S. Lees. Evaluation of carotid stenosis by phonoangiography. *New England Journal of Medicine*, 27(Nov):1124–1128, 1975.
9. T. Idzenga, J.J.M. Pel, R. A. Baldewsing, and R. van Mastrigt. Perineal noise recording as a non-invasive diagnostic method of urinary bladder outlet obstruction: a study in polyvinyl alcohol and silicone model urethras. *Neurourology and Urodynamics*, 24(4):381–8, 2005.
10. S.A. Jones and A. Fronek. Analysis of break frequency downstream of a constriction in a cylindrical tube. *Journal of Biomechanics*, 20(3):319–327, 1987.
11. J.P. Kistler, R.S. Lees, A. Miller, R.M. Crowell, and G. Roberson. Correlation of spectral phonoangiography and carotid angiography with gross pathology in carotid stenosis. *New England Journal of Medicine*, 305(8):417–419, 1981.
12. H.C. Klingler, S. Madersbacher, B. Djavan, G. Schatzl, M. Marberger, and C.P. Schmidbauer. Morbidity of the evaluation of the lower urinary tract with transurethral multichannel pressure-flow studies. *Journal of Urology*, 159(1):191–194, 1998.
13. K. Koiso, R. Nemoto, and M. Ohtani. Urographic studies of benign prostatic hyper trophy. *Journal of Urology*, 145:1071–1077, 1991.
14. D. Porru, G. Madeddu, G. Campus, I. Montisci, R.M. Scarpa, and E. Usai. Evaluation of morbidity of multi-channel pressure-flow studies. *Neurourology and Urodynamics*, 18(6):647–652, 1999.
15. H. Teriö. Acoustic method for assessment of urethral obstruction: a model study. *Medical and Biological Engineering and Computing*, 29:450–456, 1991.
16. R.J. Tobin and I.D. Chang. Wall pressure spectra scaling downstream of stenoses in steady tube flow. *Journal of Biomechanics*, 9:633–640, 1976.
17. A.J. van Koevinge and R. van Mastrigt. A relation between the sound produced by urethral turbulence in patients and objectively assessed subvesical obstruction. *Neurourology and Urodynamics*, 10:442–443, 1991.
18. R. van Mastrigt, B.L.R.A. Coolsaet, and W.A. van Duyl. Passive properties of the urinary bladder in the collection phase. *Medical and Biological Engineering and Computing*, 16:471–482, 1978.

Appendix

The flow of urine through the urethra during voiding causes pressure-fluctuations on the urethral wall, which induce displacement. The urethral wall behaves like a flexible tube and has viscoelastic properties that affect the displacement. Viscoelasticity is a combination of both elastic and viscous properties of a material. Elasticity describes the relation between stress and strain and viscosity describes the resistance of a material to a change in form, i.e. the relation between stress and the change in strain. As a linear approximation of the viscoelastic properties of a urethra we have developed a mechanical model of the urethral wall consisting of springs, dashpots and a mass (see figure 4.5).

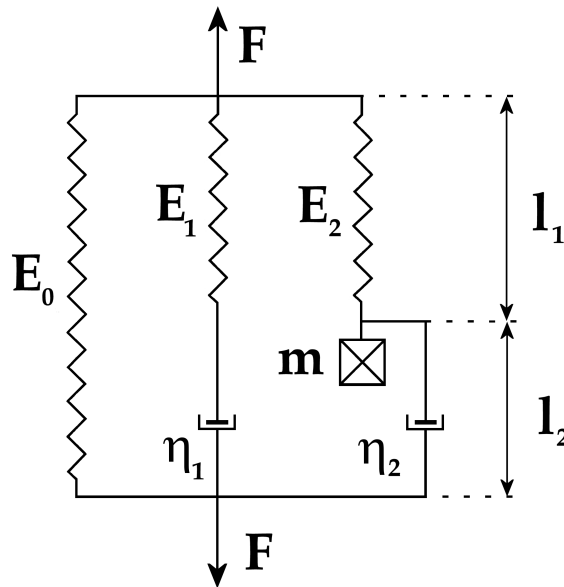


Figure 4.5: Mechanical model of the urethral wall consisting of springs ($E_{0,1,2}$), dashpots ($\eta_{1,2}$)⁶ and a mass (m). The step-response function of this mechanical model was fitted to (a part of) the pressure-response of the model and pig urethras to stepwise application of strain

A change in length ℓ of the model equally stretches each series of elements thereby generating a force in each series. These forces (F) can be calculated from the general equations for each element:

$$F = E \cdot \ell \quad (\text{Spring}) \quad (4.1)$$

$$F = \eta \cdot \frac{\partial \ell}{\partial t} \quad (\text{Dashpot}) \quad (4.2)$$

$$F = m \cdot \frac{\partial^2 \ell}{\partial t^2} \quad (\text{Mass}) \quad (4.3)$$

With E the elastic modulus of the spring, ℓ the length of each element, η the viscosity of

the dashpot and m the mass of the mass element.

When the model is strained stepwise:

$$\ell = H(t) \cdot \Delta\ell, \text{ with } H(t) = \begin{cases} 0 & t < 0 \\ 1 & t \geq 0 \end{cases} \text{ (Heaviside function)} \quad (4.4)$$

with $\Delta\ell$ the change in length.

From the Laplace-transformation of the sets of equations the Laplace-transform of the overall solution can be calculated. Inverse Laplace transformation of the overall solution results in an equation for the overall force that is generated by the mechanical model in response to stepwise straining:

$$F(t) = \Delta\ell \cdot \left(E_0 + E_1 \cdot e^{-\frac{E_1}{\eta_1} \cdot t} + E_2 \cdot e^{-\frac{\eta_2}{2m} \cdot t} \cdot [g(t)] \right) \quad (4.5)$$

With,

$$g(t) = \cos\left(\sqrt{\frac{4mE_1 - \eta_2^2}{4m^2}} \cdot t\right) + \frac{\eta_2}{\sqrt{4mE_1 - \eta_2^2}} \cdot \sin\left(\sqrt{\frac{4mE_1 - \eta_2^2}{4m^2}}\right)$$

This equation can be simplified for each length displacement of to:

$$F(t) = a_0 + a_1 \cdot e^{-b_1 \cdot t} + a_2 \cdot e^{-b_2 \cdot t} \cdot \left[\cos(c_2 t) + \frac{b_2}{c_2} \cdot \sin(c_2 t) \right] \quad (4.6)$$

With:

- a_0 = equilibrium amplitude;
- $a_{1,2}$ = amplitudes of the exponential terms;
- $b_{1,2}$ = relaxation-constants of the exponential terms;
- c_2 = oscillation frequency.

In an idealized thin-walled urethra the tension T in the urethral wall can be calculated from the recorded pressure response of the urethra using Laplace's Law, written in a cylindrical form:

$$T = P \cdot R \quad (4.7)$$

With R the radius of the urethra. As the urethra does have a thick wall we calculated stress in units of force per unit surface by dividing Laplace's Law by the wall thickness d ¹⁸:

$$\sigma = \frac{T}{d} = \frac{P \cdot R}{d} \quad (4.8)$$

With σ stress in the urethral wall and R the average of the inner and outer diameter of the urethra. The inner and outer diameter can be calculated from the injected volume V_{inj} ,

the tissue-volume V_t and the initial volume V_i . In the model urethras without a circular channel-profile $V_i = 0$. With the inner and outer diameter after injection of the volume written in terms of injected, tissue and initial volumes Laplace's Law can be rewritten in terms of volumes, corrected for the state before injection of the volume:

$$\sigma = \left(\frac{2 \cdot (V_{inj} - \sqrt{V_i} \cdot \sqrt{V_t + V_i} + \sqrt{V_{inj} + V_i} \cdot \sqrt{V_{inj} + V_t + V_i})}{V_t} \right) \cdot P \quad (4.9)$$

The applied strain ϵ can be calculated from the change in average circumference of the cross-sections before and after injection. The average circumference is calculated from the averages of the inner and outer radius before ($R_{avg,0}$) and after (R_{avg}) injection and rewritten in terms of the above mentioned volumes:

$$\epsilon = \frac{\ell - \ell_0}{\ell_0} = \frac{2\pi R_{avg} - 2\pi R_{avg,0}}{2\pi R_{avg,0}} = \frac{\sqrt{V_i + V_t + V_{inj}} + \sqrt{V_i + V_{inj}}}{\sqrt{V_i + V_t} + \sqrt{V_i}} - 1 \quad (4.10)$$

Using the rewritten Laplace's Law (Eqn. A-8) the coefficients a_n ($n = 0, 1, 2$) in Eqn. A-6 can be written in terms of stress. The time-constants τ_1 and τ_2 of the decay in stress can be calculated as the inverse of the coefficients b_m ($m = 1, 2$). And the oscillation frequency f is the coefficient c_2 .

Chapter 5

Abstract

Purpose: A low flow rate without clinical symptoms is commonly found in boys after hypospadias correction. Urethral calibration usually shows no abnormalities. We investigated whether this impairment might be caused by increased neo-urethral wall stiffness. **Methods:** From polyvinyl alcohol cryogel two models of the urethra were made, hypospadias and control; both had a constant and equal inner diameter and equal compliance. The hypospadias model had a less compliant distal segment mimicking the distal neo-urethra after hypospadias correction. In both models, flow rate was recorded as a function of bladder pressure. To test whether the length of the less compliant segment had an effect on the flow rate, both models were shortened by cutting off 1-cm segments. **Results:** In a physiological range of bladder pressures (10-130 cm H₂O) the mean flow rate (± 1 sem) in the hypospadias model was 2.8 ± 0.3 ml/s, significantly lower ($p < 0.05$) than in the control model (5.4 ± 0.6 ml/s). Shortening of the hypospadias model showed some increase in flow rate, but this was not statistically significant. In the control model there was also no significant variation in flow rate. **Conclusion:** A low-compliant segment of a urethral model reduced the flow rate. Extrapolating these results to asymptomatic boys with a low urinary flow rate after hypospadias repair might justify a watchful waiting policy.

Adapted from: T. Idzenga, D.J. Kok, J.J.M. Pel, R. van Mastrigt and K.P. Wolffenbuttel, "Is the impaired flow after hypospadias correction due to increased urethral stiffness?", *Journal of Pediatric Urology* 2, 299-303, 2006.

Chapter 5

Is the impaired flow after hypospadias correction due to increased urethral stiffness?

Introduction

Hypospadias is a congenital malformation with an incidence of up to 0.73% in the general population¹. Treatment and follow up of hypospadias patients forms a large part of the work of pediatric urologists. Surgical repair of hypospadias comprises lengthening of the urethra to obtain a normally placed meatus, chordee correction and remodelling of the abnormal penile skin. Probably the most frequently used technique for the correction of hypospadias is the tubularized incised plate correction (TIP or Snodgrass procedure²). In the short term complications like fistula and urethral stricture formation occur in 5% (primary cases³) to 17.5% (proximal hypospadias⁴) of the cases. An impaired flow rate is often observed in asymptomatic boys after hypospadias correction. A urethral stricture is, however, rarely found. An open question is whether the neo-urethra will function adequately throughout adult life.

Recently we reported on the urine flow characteristics of boys with hypospadias before and after correction of hypospadias⁶. The cause of the impaired flow rate in hypospadias patients is unknown. Two factors might play a role in this impaired flow rate: narrowing of the urethral lumen or stricture (intraluminal factor) and diminished compliance (i.e. increased stiffness) of the urethral wall or the surrounding tissue surrounding (extraluminal factor). In this study we tested the hypothesis that an impaired urinary flow rate may be caused by a low compliance of the neo-urethral wall. We therefore constructed two models of the urethra from Polyvinyl Alcohol: one model in which the distal segment had low compliance, mimicking a urethra after hypospadias correction, and one control model (see figure 5.1). We measured the flow rate in the hypospadias model and compared this to the flow rate in the control model. We also tested the influence of the length of the low compliant segment on the flow rate.

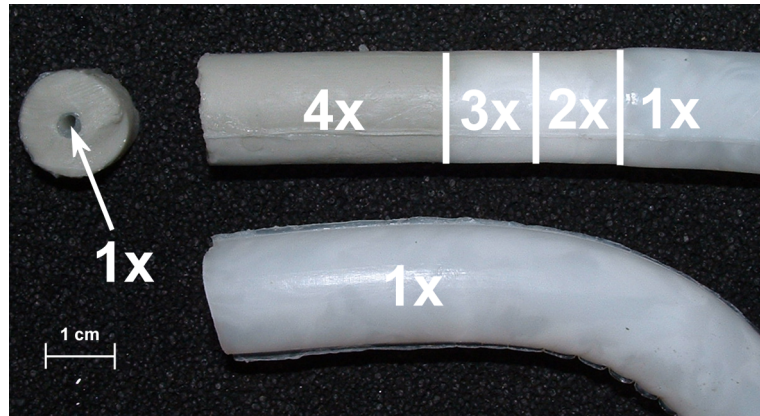


Figure 5.1: Model of the human male urethra after hypospadias correction (upper model) and control model (bottom model), both made from Polyvinyl Alcohol. On the left a cross section is shown of the hypospadias model. This model had a segment (grey) with diminished compliance (freeze-thawed four times) and two segments that were freeze-thawed three or two times mimicking the neo-urethra. The control model had uniform compliance (freeze-thawed once).

Materials & Methods

We constructed 2 model urethras from Polyvinyl Alcohol (PVA) cryogel. Repeated freezing and thawing of the PVA controls its elastic properties. With increasing number of freeze/thaw cycles the stiffness of the PVA increases. We made the models by pouring a 10% aqueous solution of PVA into a cylindrical mould (400 mm in length, 16 mm in diameter⁵). To create a part with low compliance we placed a circular rod along the central axis with a diameter of 4 mm and poured PVA (mixed with Carborundum particles of 3-10 μm for contrast between stiff and normal tissue) into the mould until approximately 3 cm of the mould was filled. After one freeze-thaw cycle we added a segment of approximately 1 cm length and once again freeze-thawed the mould. We added another 1 cm segment of PVA and again repeated the freeze-thaw cycle. After these three freeze-thaw cycles we removed the 4 mm diameter rod and replaced it with a rod with a diameter of 2 mm. We completely filled up the mould with PVA and repeated the freeze-thaw cycle once more. We removed the model from the mould and cut off excess PVA resulting in a model urethra freeze-thawed once (Elastic modulus $\sim 2 \times 10^4 \text{ N/m}^2$) with a total length of 30 cm including a 3 cm long distal segment that was freeze-thawed four times (Elastic modulus $\sim 5.9 \times 10^4 \text{ N/m}^2$) and two 1 cm long parts that were freeze-thawed respectively three and two times. To obtain a control model we cut off 15 cm of the once freeze-thawed segment. This resulted in two models of 15 cm length each with equal stiffness except for the distal segment of the hypospadias model (see figure 5.1). Both models had an inner diameter of 2 mm.

Each model was placed in a custom-made container⁵. Polyurethane tubing was used to connect the models via a turbine flow meter (Flo-sensor 101, McMillan Company, USA) to a water column representing the bladder. The water level in this column was kept con-

stant using a floating device to maintain a constant pressure. To exclude errors due to the pressure loss caused by connective tubing we measured the resulting bladder pressure with a pressure transducer at the entrance of the container (see figure 5.2). The measured bladder pressure and the resulting flow rate were recorded on a personal computer using an A/D-converter (PCI-6221, National Instruments, Woerden, The Netherlands) in combination with a custom-written Labview-program (National Instruments, Woerden, The Netherlands).

We applied increasing levels of bladder pressure to both models and measured the resulting flow rate. We increased the level of the water column from 10 to 170 cm H₂O in steps of 10 cm H₂O. Due to pressure loss in the turbine flow meter and the connective tubing this resulted in a bladder pressure range from 10 to 130 cm H₂O. To test the influence of the length of the least compliant segment on the flow rate we decreased the length of both models from 15 to 14, 13, 12.5 and 12 cm by cutting off distal sections. At each length we repeated the pressureflow measurements.

In each set of pressureflow measurements we calculated the mean (± 1 sem) flow rate at the bladder pressure values between 10 and 130 cm H₂O. At each length of the models we compared the mean flow rates between the two models using an independent samples t-test. We tested whether the length of the least compliant segment affected the mean flow rate using Analysis of Variance.

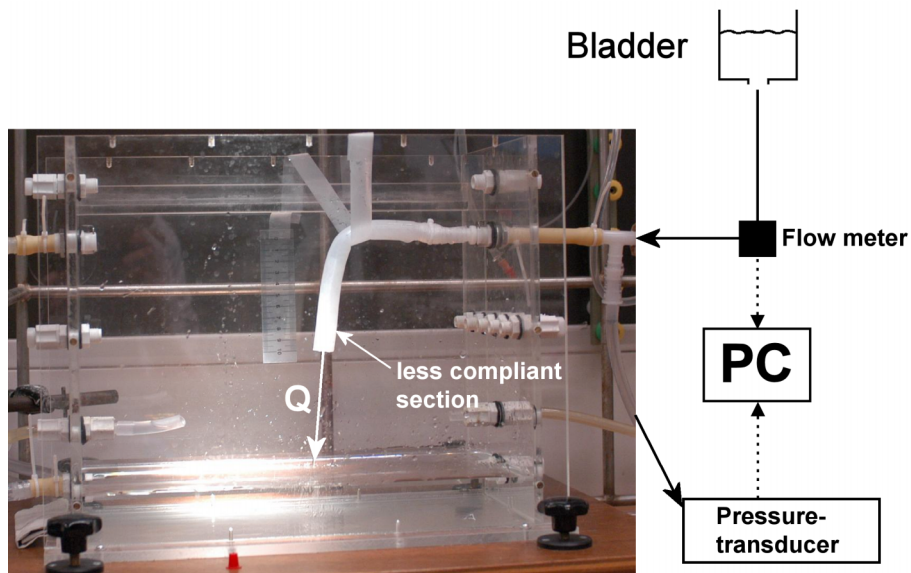


Figure 5.2: Measurement setup for recording of flow through the hypospadias model and the control model. Both were placed in a custom made container and connected via a turbine flow meter to a water column. The bladder pressure was recorded at the entrance of the container.

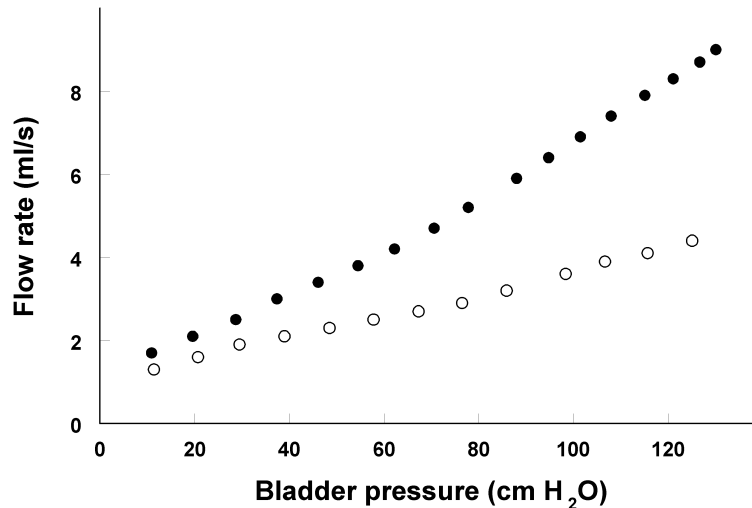


Figure 5.3: Flow rate through the two model urethras (○ = hypospadias model, ● = control model) as a function of the applied bladder pressure. Due to the higher flow rate in the control model the bladder pressure values in the control model are shifted to the left with respect to the bladder pressure values in the hypospadias model. This is caused by increased pressure loss over the connective tubing and the turbine flow meter at the higher flow rate.

Results

Figure 5.3 shows the urine flow rate in the two models as a function of the applied bladder pressure at maximum length of the models. In the hypospadias model the mean (± 1 sem) flow rate (2.8 ± 0.3 ml/s) was significantly lower ($p < .05$) than the mean flow rate in the control model (5.4 ± 0.6 ml/s). The measured bladder pressures in the control model are shifted to the left relatively to the hypospadias model. This shift is due to the increased pressure loss in turbine flow meter and connective tubing caused by the higher flow rate in the control model.

The mean (± 1 s.e.m.) flow rates through both models are plotted in figure 5.4 as a function of the length of the models. At 15, 14 and 13 cm there was a significant difference in flow rate between the hypospadias and the control model. Shortening of both models did not affect the flow rate significantly. In the hypospadias model the flow rate seemed to increase a little when the least compliant segment (freeze-thawed four times) was shortened to approximately 0.5 cm, but this increase was not significantly different ($p = .973$). In the control model the flow rate did not increase upon shortening of the model ($p = .998$).

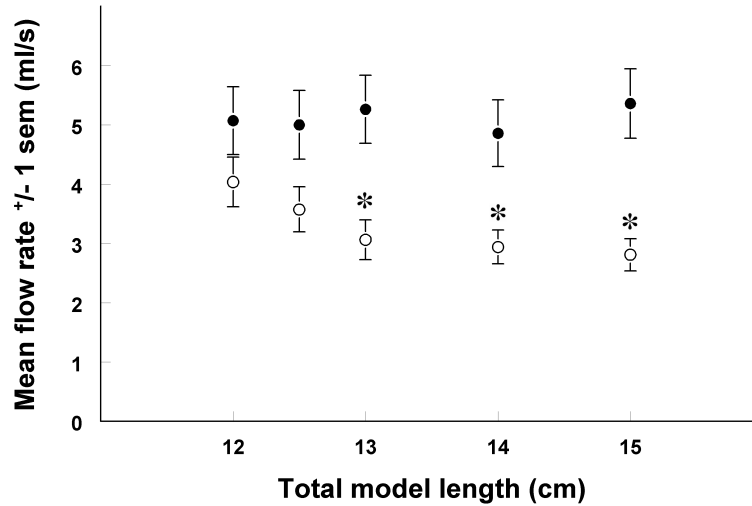


Figure 5.4: Mean (± 1 sem) flow rate between 10 and 130 cm H₂O bladder pressure as a function of the length of the model (○ = hypospadias model, ● = control model). At the lengths marked * the difference is significant at the .05 level.

Discussion

We constructed a model urethra with a low compliant distal segment, mimicking a male urethra with low compliance of the urethral wall after hypospadias correction and a control model mimicking a normally developed male urethra. The compliance of the used PVA decreased with increasing number of freeze-thaw cycles. The control model was freeze-thawed once, whereas the hypospadias model was freeze-thawed once with a distal segment that was freeze-thawed four times. The added segments of 1 cm length in the hypospadias model were necessary to firmly connect the once freeze-thawed segment to the four times freeze-thawed segment. Both models had equal inner diameter. The pressure-flow measurements in the two models showed that the mean flow rate in the hypospadias model with the low compliant distal segment was significantly lower than the flow rate in the control model (see figure 5.4). They also showed that a decrease in length of the low compliant segment did not have a significant effect on the flow rate. In general, these results show that low compliance of a segment of the urethral wall is able to diminish the flow rate.

The lower flow rate in a urethra with a segment of low compliance can be explained as follows. The pressure generated in the bladder by contraction of the detrusor muscle drives the urine through the urethra. To this end the urine opens the urethra. When the urethral wall is more compliant it can be opened wider, i.e. to a larger cross sectional area. Consequently at a given bladder pressure the urethra can accommodate a larger flow rate. When a segment of the urethra has lower compliance it is opened less wide, i.e. to a smaller cross sectional area. Therefore a urethra with a less compliant segment

can accommodate a lower flow rate at the same given bladder pressure. Shortening the least compliant segment of the hypospadias model had no significant effect on the flow rate. When the length of the distal segment approached zero a small increase in flow rate was observed. This small increase in flow rate is due to the increase in compliance. With the increase in compliance the hypospadias model can accommodate a larger flow rate. Whether the compliance of the newly constructed urethra after hypospadias correction is actually lower than normal remains to be established. Two possible mechanisms could diminish the compliance. The first is fibrosis around the suture line of the new urethra. The excess collagen or the scar tissue increases the stiffness of the new urethral wall resulting in diminished compliance in comparison to a normally developed urethra. Careful histological analysis of the urethral wall after a TIP procedure in an animal model, however, did not show excess collagen deposition or scarring⁷. A second possible mechanism is lack of tissue development around the new urethra resulting in lower compliance of the surrounding tissue than normal. Elastic fibers are a major component of the extracellular matrix of this surrounding tissue⁸. In this recent study the authors hypothesised that in utero biomechanical processes such as voiding, erection and amniotic pressure are closely related to development of the foetal urethral extracellular matrix. As the new urethra after hypospadias correction was not exposed before to these biomechanical processes this may explain the lack of compliance.

In conclusion we have shown in our hypospadias model that lack of compliance of a segment of the urethra results in a low flow rate. The length of the low compliant segment had little to no effect on the flow rate. Extrapolated to patients after hypospadias correction, an impaired flow rate could be caused by low compliance of the newly constructed urethra due to a local aberration of the surrounding tissue. The length of this low compliant newly constructed urethra does not affect the flow rate significantly. Thus, when an impaired urinary flow rate is observed in asymptomatic boys after hypospadias correction low compliance of the newly constructed urethra has to be considered, warranting a watchful waiting policy.

Literature

1. F.H. Pierik, A. Burdorf, J.M. Nijman, S.M. de Muinck Keizer-Schrama, R.E. Juttman, and R.F. Weber. A high hypospadias rate in the netherlands. *Hum Reprod*, 17(4):1112–5, 2002.
2. W. Snodgrass. Tubularized, incised plate urethroplasty for distal hypospadias. *J Urol*, 151(2):464–5, 1994.
3. J.G. Borer, S.B. Bauer, C.A. Peters, D.A. Diamond, A. Atala, Jr. Cilento, B.G., and A.B. Retik. Tubularized incised plate urethroplasty: expanded use in primary and repeat surgery for hypospadias. *J Urol*, 165(2):581–5, 2001.
4. S.C. Chen, S.S. Yang, C.H. Hsieh, and Y.T. Chen. Tubularized incised plate urethroplasty for proximal hypospadias. *BJU Int*, 86(9):1050–3, 2000.
5. T. Idzenga, J.J.M. Pel, R.A. Baldewsing, and R. van Mastrigt. Perineal noise recording as a non-invasive diagnostic method of urinary bladder outlet obstruction: a study in polyvinyl alcohol and silicone model urethras. *Neurourol Urodyn*, 24(4):381–8, 2005.

6. K.P. Wolffenbuttel, N. Wondergem, J.J. Hoefnagels, G.C. Dieleman, J.J.M. Pel, B.T. Passchier, B.W. de Jong, W. van Dijk, and D.J. Kok. Abnormal urine flow in boys with distal hypospadias before and after correction. *J Urol*, 176(4 Pt 2):1733–6; discussion 1736–7, 2006.
7. J.F. Lopes, A. Schned, P.I. Ellsworth, and M. Cendron. Histological analysis of urethral healing after tubularized incised plate urethroplasty. *J Urol*, 166(3):1014–7, 2001.
8. A.L. Bastos, E.A. Silva, W. Silva Costa, and F.J. Sampaio. The concentration of elastic fibres in the male urethra during human fetal development. *BJU Int*, 94(4):620–3, 2004.

Chapter 6

Abstract

In patient studies the correlation between maximum urethral closure pressure (MUCP) and Valsalva leak point pressure (LPP) is meagre at best ($r = 0.22-0.50$). We therefore studied the relation between MUCP and LPP in a flexible and extensible model urethra. We applied differently sized pressure zones and different degrees of resistance to a biophysical model urethra by stepwise inflating three types of blood pressure cuff placed around the model. At each degree of resistance we measured detrusor LPP, an in vitro equivalent of Valsalva LPP. Subsequently, we recorded the Urethral Pressure Profile using a water-perfused 5F end-hole catheter at four withdrawal rates and five perfusion rates and calculated MUCP. We tested the dependence of LPP on pressure zone length and MUCP on perfusion rate, withdrawal rate and pressure zone length using analysis of variance. We tested the correlation between LPP and MUCP using Pearson's correlation coefficient and Linear Regression. LPP did not significantly depend on the pressure zone length ($p = 0.80$) and increased linearly with increasing cuff pressure. MUCP also increased with increasing cuff pressure, however, MUCP significantly depended ($p < 0.01$) on perfusion rate, withdrawal rate and pressure zone length. MUCP increased with increasing perfusion rate, and decreased with increasing withdrawal rate. In our model urethra MUCP only accurately reflected urethral resistance for a very limited number of combinations of perfusion rate and withdrawal rate. LPP reflected urethral resistance independent of the type of pressure zone.

Adapted from: T. Idzenga, J.J.M. Pel and R. van Mastrigt, "Fluid perfused Urethral Pressure Profilometry and Valsalva Leak Point Pressure: a comparative study in a biophysical model of the urethra", World Journal of Urology 25(4), 423-429, 2007.

Chapter 6

Fluid perfused Urethral Pressure Profilometry and Valsalva Leak Point Pressure: a comparative study in a biophysical model of the urethra

Introduction

Leak Point Pressure (LPP) and Urethral Pressure Profilometry (UPP) are both methods that aim at measuring the maximum bladder pressure the urethra can withstand without leakage¹. With LPP the intravesical pressure is increased by either increasing the abdominal pressure (Valsalva manoeuvre or coughing) or the detrusor pressure. When leakage is visually observed the intravesical pressure is noted as LPP¹. With UPP pressure along the urethra is recorded, starting in the bladder. The maximum difference between urethral and bladder pressure is denoted as the Maximum Urethral Closure Pressure (MUCP)¹.

The two most frequently used techniques to perform UPP in the clinic are micro-tip transducers and fluid perfused catheters with side-/end-hole. Micro-tip transducers are very sensitive and give good quality recordings. However, they are expensive and fragile², require proper positioning in the urethra^{3,4} and are prone to artifacts caused by the sensor touching the urethral wall⁵. Also micro-tip transducers are found to have a larger standard deviation in measuring MUCP than fluid perfused catheters⁶. Fluid perfused catheters are inexpensive, disposable and easy to use in the clinic, although care must be taken to prevent air bubbles. Artifacts may be induced by motion, and the signals of fluid perfused catheters with side-holes depend on rotational positioning in the urethra. An end-hole catheter eliminates this problem and is therefore considered the best fluid per-



Figure 6.1: Cross-section and side view of a PVA model urethra with a Y-shaped channel to allow flow through the model.

fused catheter for performing a UPP-measurement³. Reproducibility of the UPP-method is poor, which is possibly caused by lack of standardization of the procedure⁷. Using the perfusion technique, the investigator has to choose catheter type, perfusion rate and withdrawal rate of the catheter. Perfusion rates between 2 and 5 ml/min and withdrawal rates between 2 and 7 mm/s have been reported in the literature⁸⁻¹². The correlation between UPP and Valsalva LPP has been studied in female patients with stress urinary incontinence. It was found that the correlation was meagre at best ($r = 0.22-0.50$)¹³⁻¹⁵. It was also found that contraction and relaxation of pelvic floor muscles influence UPP¹⁶. Valsalva LPP measurements on the other hand depend on the vesical volume^{17,18}, catheter size¹⁹ and patient position²⁰. Also the time-delay between observation of leakage and pressure recording affects the leak point pressure.

Many studies on the correlation between MUCP and LPP have been done in patients. Measurements in patients can easily vary. Therefore we objectively compared the two measurement techniques in a 'static' urethra, a flexible and collapsible urethral model made from PolyVinyl Alcohol (PVA). We developed this urethral model to study perineal recording of sound as a non-invasive diagnostic method for diagnosing bladder outlet obstruction. In a separate study we confirmed a relation between this recorded sound and the degree of prostatic obstruction in the model²¹. Three types of inflatable blood-pressure cuffs placed around the model and inflated stepwise, simulated three different types of pressure zones. We measured detrusor LPP at different cuff pressures by increasing the pressure at the entrance of the urethral model until leakage was observed.

The pressure at which leakage occurred may be considered a quasi-static approximation of the Valsalva Leak Point Pressure. In this paper it will be denoted LPP. We performed UPP at five different perfusion and four different withdrawal rates and calculated MUCP.

Materials & Methods

We made a flexible and distensible model urethra by pouring a 10% aqueous solution of PVA into a cylindrical mould with a diameter of 16 mm and a length of 150 mm. To create a channel allowing flow through the model, we placed a strip with a Y-profile (with legs 5 mm wide) along the central axis of the mould (see figure 6.1). After 6 hours of rest at room temperature (21°C), the mould was stored in a freezer at -20°C. After 14 hours in the freezer the mould was stored at room temperature for 10 hours. This freeze-thaw cycle was repeated three times. The urethral model had viscoelastic properties comparable to the male pig urethra²². It was placed approximately 1 cm below the water level in a water-filled container to prevent dehydration of the PVA.

Three types of inflatable blood pressure cuffs were placed around the model as three different types of pressure zones. A 28 mm wide single cuff (Tricomed, EME Ltd., Brighton,

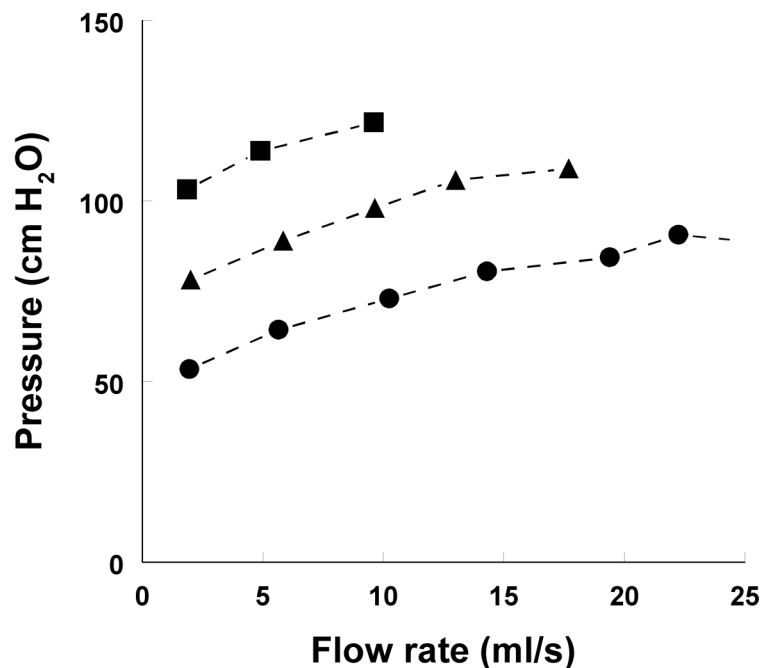


Figure 6.2: Pressure-flow measurements in the urethral model using the Tricomed cuff at pressures of 60 (●), 100 (▲) and 140 (■) cm H₂O. Extrapolation of the data-points to zero flow rate zero suggests a realistic non-zero closure pressure, increasing with cuff pressure.

UK) represented a relatively short pressure zone. A sequence of two of these Tricomed-cuffs represented a relatively long zone. The third pressure zone was a 55 mm wide single cuff (Critikon 5, Johnson & Johnson Medical Inc., Arlington, USA), thus creating a second relatively long zone. The cuffs were inflated to pressures varying from 60 to 160 cm H₂O in steps of 10 cm H₂O. We assessed the closure properties of the urethral model by applying increasing bladder pressure values and simultaneously recording the flow rate at three cuff pressures (i.e. 60, 100 and 140 cm H₂O) using the Critikon-cuff.

Leak Point Pressure In order to measure LPP, we connected one side of the model to a water column representing the bladder. The water level in this column was kept constant using a floating device. At each cuff pressure we increased the water level in steps of 1 cm H₂O from 0 cm H₂O up to the pressure at which the model showed leakage. This leakage was, conform common clinical practice, visually detected. The corresponding water level was noted as LPP.

Urethral Pressure Profilometry We measured UPP of the model urethra using the perfusion method²³. We used a 5F catheter with an end-hole³ commonly used in our clinic. The perfusion fluid used was demineralised water. The catheter was withdrawn through the model by a retractor, driven by a urodynamic measurement unit (Menuet, Dantec Dynamics, Bristol, UK), at four different withdrawal rates (0.5, 1, 2 and 4 mm/s). We maintained a constant perfusion rate through the catheter with an infusion pump (B. Braun Melsungen AG, Melsungen, Germany) and applied 5 different perfusion rates (0.5, 1, 2, 5 and 10 ml/min). At a t-connector between infusion pump and catheter we recorded the pressure needed to maintain a constant perfusion rate using a disposable pressure transducer. The measured pressure was recorded on a computer using an A/D-converter (BNC-2110, National Instruments, Woerden, The Netherlands) in combination with a self-written Labview-program (National Instruments, Woerden, The Netherlands). For each of the three types of pressure zone we recorded one pressure profile at each combination of cuff pressure, perfusion rate and withdrawal rate. Each profile was corrected for pressure loss caused by the resistance of the catheter. At each of the 5 different perfusion rates this pressure loss was measured with the catheter outside the model²⁴. MUCP was calculated from the corrected pressure profile as the maximum recorded pressure using self-written Matlab[®]-programs. During the UPP measurements no column of water was connected to the model and therefore the bladder pressure was set to zero.

Statistical analysis We tested the dependence of LPP on type of pressure zone using Analysis of Variance (ANOVA). Similarly the dependence of MUCP on type of pressure zone, perfusion rate and withdrawal rate of the catheter was tested. For each combination of pressure zone, perfusion rate and withdrawal rate we tested the relation between MUCP and LPP using Pearson's correlation coefficient and performed linear regression on MUCP as a function of LPP. We compared the slope of each linear function statistically to the ideal slope of 1 using a Student's t-test.

Results

Pressure-flow measurements for the assessment of the closure properties of the model are presented in figure 6.2. The flow rate was found to increase with increasing bladder pressure and the pressure-flow curve was found to be at higher pressure-values for higher cuff pressure. Extrapolation of the curves towards zero flow rate clearly indicates non-zero closure pressure of the model.

LPP increased with increasing cuff pressure in the three cuff types (see figure 6.3). The measured LPP-values were not statistically dependent (ANOVA, $p = 0.797$) on the type of pressure zone. The LPP-value, however, did not equal the applied cuff pressure. An initial pressure was necessary for the cuff to contact the urethral model. At increasing cuff pressure this phase was followed by adaptation of the cuff to the urethral model in order to achieve 'full contact'. After this point had been reached LPP was found to linearly increase with increasing cuff pressure with a slope of one²⁵.

Examples of UPP-recordings in the urethral model are shown in figure 6.4. These profiles were recorded at two different perfusion rates (a), two different withdrawal rates (b) and three different pressure zones (c). MUCP was higher at higher perfusion rate and lower

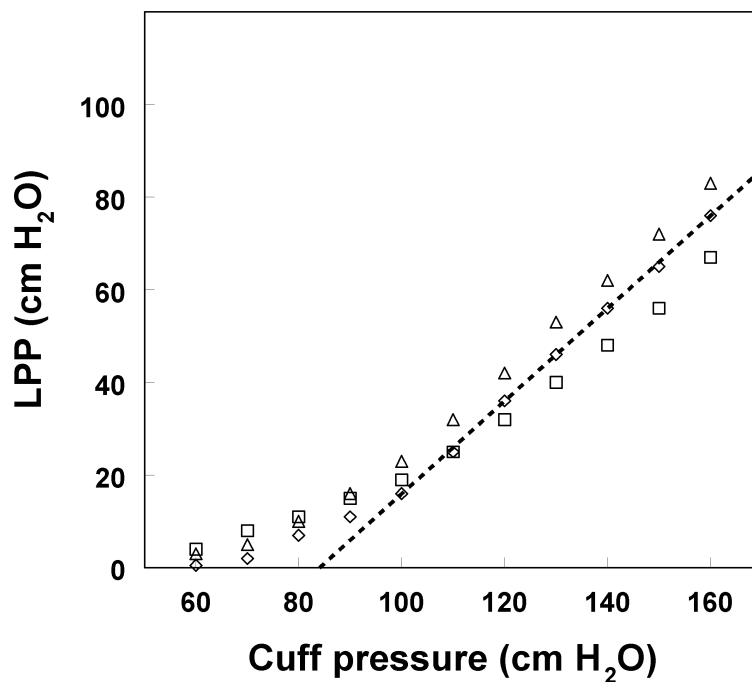


Figure 6.3: LPP as a function of the applied cuff pressure for the different cuff-types (indicated as: ◇ = single Tricomed-cuff, □ = double Tricomed-cuff and △ = Critikon-cuff). The dotted line represents the linear function fitted to LPP in the single Tricomed-cuff (at cuff pressures between 100 and 160 cm H₂O) with a slope of one.

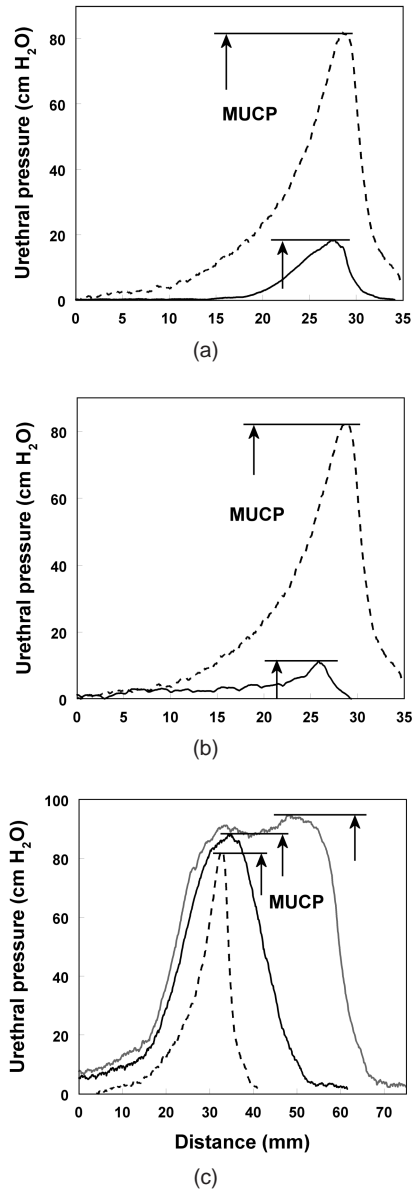


Figure 6.4: Examples of UPP-recordings at a cuff pressure of 150 cm H₂O. The recordings were done with: a) a constant withdrawal rate (0.5 mm/s) in combination with two different perfusion rates (— = 0.5 ml/min and - - - = 10 ml/min) and b) a constant perfusion rate (10 ml/min) in combination with two different withdrawal rates (- - - = 0.5 mm/s and — = 2 mm/s) using the single Tricomed-cuff. In c) the recordings were done with a constant withdrawal rate (0.5 mm/s) and a constant perfusion rate (10 ml/min) using the three different cuff-types (- - - = single Tricomed, — = Critikon 5 and — = double Tricomed). The horizontal axis represents distance measured from the proximal end of the model urethra.

at higher withdrawal rate. The types of pressure zone had different effective lengths of pressure-plateaus. MUCP depended significantly on the type of pressure zone, perfusion rate, withdrawal rate (ANOVA, $p < .01$) and on the interaction between pressure zone and withdrawal rate (ANOVA, $p < .05$).

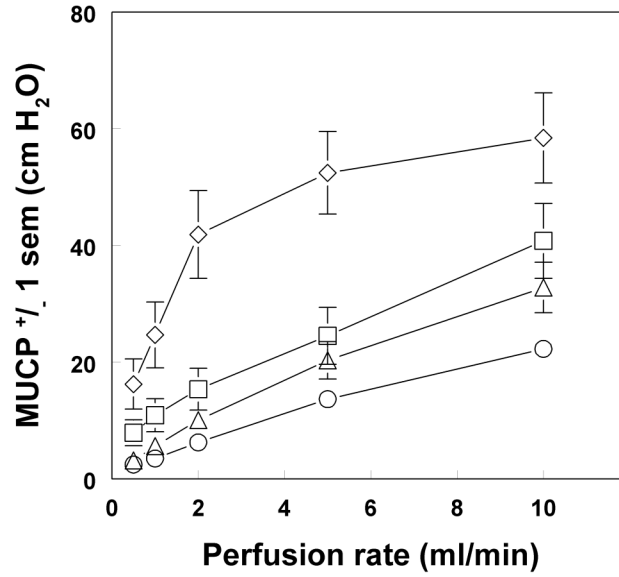
Figure 6.5 shows MUCP: (a) as function of perfusion rate at four different withdrawal rates and (b) as function of withdrawal rate at five different perfusion rates; all data were measured using the Critikon-cuff at maximum cuff pressure (160 cm H₂O). With increasing perfusion rate MUCP increased and with increasing withdrawal rate it decreased. This behavior was also observed using the two other types of pressure zone and at lower cuff-pressures.

Figure 6.6 shows an example of a linear function fitted to MUCP as a function of LPP. Pearson's correlation coefficient of the linear fits ranged from 0.94 to 1. For most combinations of perfusion and withdrawal rate the slope of the linear functions was significantly different from 1 ($p < 0.05$). The combinations of perfusion and withdrawal rate for which the slope was not significantly different from 1 for the single Tricomed cuff were: 5 ml/min & 0.5 mm/s ($p = 0.115$), 10 ml/min & 0.5 mm/s ($p = 0.212$) and 10 ml/min & 1 mm/s ($p = 0.164$). For the double Tricomed cuff: 0.5 ml/min & 0.5 mm/s ($p = 0.083$) and 1 ml/min & 1 mm/s ($p = 0.446$). And for the Critikon cuff: 10 ml/min & 0.5 mm/s ($p = 0.081$).

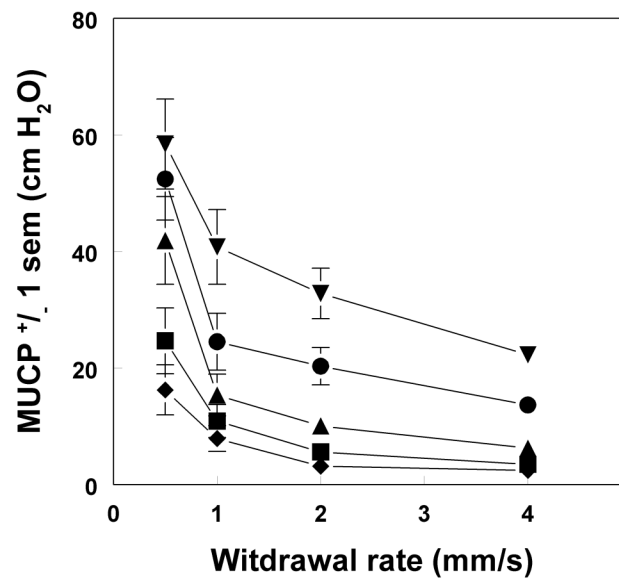
Discussion

The increase in flow rate with bladder pressure and extrapolation of the pressure-flow curves to a zero flow rate suggests a realistic non-zero closure pressure of the urethral model, which increases with increasing cuff pressure. Therefore our urethral model can be described as a distensible model²⁶. In our model LPP was not equal to the applied cuff pressure, but increased linearly with the cuff pressure above a certain threshold pressure. This threshold was probably due to flexible properties of the system, e.g. compressibility of the PVA and extensibility of the blood pressure cuffs. When the cuff is pressurized part of the pressure is balanced by tension in its wall, resulting in a lower pressure exerted upon the wall of the model urethra. Also the model itself may exert a counter pressure due to its compressibility. In spite of this loss of pressure due to the flexible properties of the system LPP did increase linearly above the threshold, so that it may be concluded that LPP adequately reflected the urethral resistance. This was independent of the type of pressure zone.

Urethral pressure recordings in the urethral model (see figure 6.4) showed much similarity with recordings done in patients. MUCP, however, depended significantly on perfusion rate, withdrawal rate and pressure zone. Increasing the perfusion rate resulted in an increase of MUCP and increasing the withdrawal rate resulted in a decrease of MUCP. MUCP and LPP correlated very well in each set of cuff pressures. However, the slope of the linear regression was only in a limited number of cuff pressure sets comparable to 1. MUCP therefore only accurately corresponded with LPP at a limited number of combinations of perfusion and withdrawal rate. Either the perfusion rate had to be high (10 ml/min) or the withdrawal rate had to be low (0.5 mm/s). The different perfusion rates used in the literature⁸⁻¹² could account for the meager correlation between MUCP and LPP¹³⁻¹⁵. The perfusion and withdrawal rate that we found are larger and smaller, re-



(a)



(b)

Figure 6.5: (a) MUCP as a function of the perfusion rate for four different withdrawal rates (indicated as: $\diamond = 0.5$ mm/s, $\square = 1$ mm/s, $\triangle = 2$ mm/s and $\circ = 4$ mm/s). MUCP was recorded using a Critikon cuff at a cuff pressure of 160 cm H₂O. (b) MUCP as a function of withdrawal rate for five different perfusion rates (indicated as: $\diamond = 0.5$ ml/min, $\blacksquare = 1$ ml/min, $\blacktriangle = 2$ ml/min, $\bullet = 5$ ml/min and $\blacktriangledown = 10$ ml/min).

spectively, than the rates found by Asmussen²⁷. This difference may have been caused by differences in model urethras used. The nature of the relation between MUCP and perfusion and withdrawal rate, however, was practically the same.

The observed dependence of MUCP on perfusion and withdrawal rate can be explained from the basic principle of UPP. To measure pressure in the urethra a pressure-equilibrium needs to be established at the tip of the catheter that reflects this pressure. However, it takes time (i.e. response time of the system) to reach this pressure-equilibrium, the perfusion fluid has to open the urethral lumen at the tip of the catheter to the level where wall stress balances pressure exerted by the fluid. When the time-span in which the catheter passes the high-pressure zone is smaller than the time it takes to reach the pressure-equilibrium the measured MUCP underestimates urethral pressure. The perfusion rate of the catheter and the volume of the urethra determine the response time; the withdrawal rate and the length of the high-pressure zone determine the time-span of passage. Consequently for a realistic pressure profile the combination of perfusion and withdrawal rate should result in a response time smaller than or equal to the time-span in which the catheter passes the high-pressure zone.

The increase in MUCP with increasing perfusion rate contrasts with the absence of, or only slight dependence on, perfusion rates between 2 and 10 ml/min found by Abrams²⁸ in patients. They did find a dependence at rates < 2 ml/min. Martin and Griffiths²⁹ ascribed the dependence at <2 ml/min to imperfect sealing of the catheter by their model, so that at low perfusion rates fluid was able to escape through small leaks at pressures lower than that exerted by the applied obstruction. This may also have been the case in our urethral model, as MUCP, extrapolated from the data in figure 6.2, is higher than the corresponding LPP in figure 6.3. It could be said that a 'measure' for leakage in our model is the 'leak rate' being smaller than 2 ml/min. Probably this leakage occurred at all perfusion rates, but with increasing perfusion rate the pressure loss became relatively less important.

Our PVA model urethra is used as a static approximation of the urethra in vivo. The viscoelastic properties of the model urethra have been tuned to those of the male pig urethra in vitro²². One of the main differences between the model and the urethra in vivo is that the model urethra cannot contract, as muscular components have not been included. The dynamic viscoelastic properties caused by muscle contraction in the urethra in vivo could lead to different pressure values. This could contribute to the meager correlation between MUCP and LPP found in patients¹³⁻¹⁵. Additionally, when applying the current model results to clinical use of UPP it should be considered that the optimal combination of perfusion and withdrawal rate in the model urethra might not give the most accurate results in the human situation. This could possibly be caused by a difference in urethral calibre between the model urethra and the human urethra. Future measurements using adapted urethral models with different calibres could reflect the natural variation in human urethral calibre. Furthermore, our model is about three times as long as the female urethra (± 4 cm in length). However, we do not expect this difference in length to affect the pressure recordings, since LPP at zero cuff pressure was approximately zero, see figure 6.3. Despite these drawbacks of the model we think our main conclusions are valid for clinical UPP and LPP measurements: MUCP increased with urethral resistance but strongly depends on the perfusion and withdrawal rate of the catheter as well as the type of pressure zone. In a clinical setting, therefore, perfusion and withdrawal rate need to

be carefully chosen and standardized. LPP, on the other hand, increases linearly with urethral resistance and did not depend on the type of pressure zone.

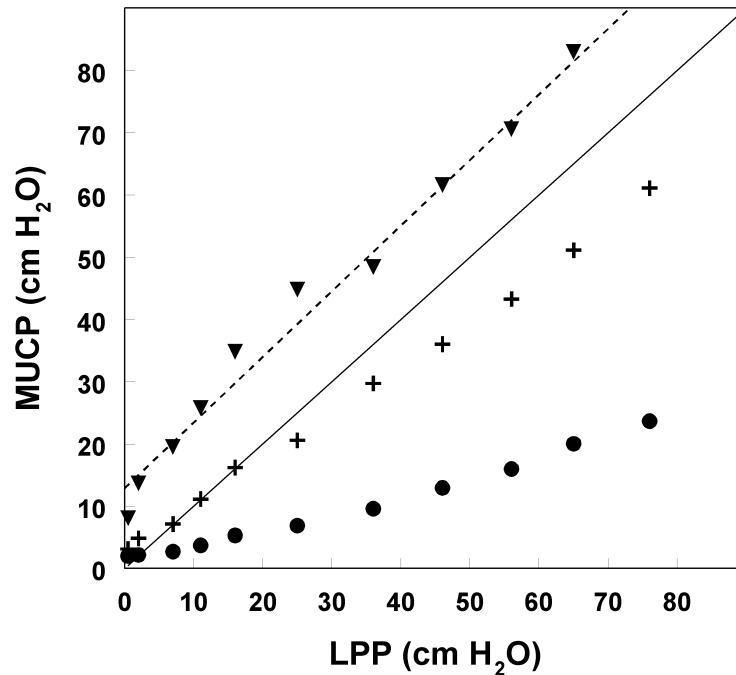


Figure 6.6: MUCP as a function of LPP measured in the single Tricomed cuff at a withdrawal rate of 0.5 mm/s and three different perfusion rates (● = 0.5 ml/min, + = 2 ml/min and ▼ = 10 ml/min). The dotted line represents a linear function, fitted to MUCP values measured with a perfusion rate of 10 ml/min, with a slope not significantly different from 1. The solid line represents MUCP equal to LPP.

Literature

1. P. Abrams, L. Cardozo, M. Fall, D. Griffiths, P. Rosier, U. Ulmsten, P. van Kerrebroeck, A. Victor, and A. Wein. The standardisation of terminology of lower urinary tract function: report from the standardisation sub-committee of the international continence society. *Neurourol Urodyn*, 21(2):167–78, 2002.
2. R. Bruskewitz and S. Raz. Urethral pressure profile using microtip catheter in females. *Urology*, 14(3):303–7, 1979.
3. D.J. Griffiths. The pressure within a collapsed tube, with special reference to urethral pressure. *Phys. Med. Biol.*, 30(9):951–963, 1985.
4. R.S. Anderson, A.M. Shepherd, and R.C.L. Feneley. Microtransducer urethral pro-

- file methodology: variations caused by transducer orientation. *Journal of Urology*, 130:727–731, 1983.
5. W. Schaefer. Some biomechanical aspects of continence function. *Scand J Urol Nephrol Suppl*, (207):44–60; discussion 106–25, 2001.
 6. P. Abrams, L. Cardozo, S. Khoury, and A. Wein, editors. *Incontinence: Basics & Evaluation, Chapter 11*, volume 1. Health Publication Ltd, 2005.
 7. A.M. Weber. Is urethral pressure profilometry a useful diagnostic test for stress urinary incontinence? *Obstetrical and Gynecological Survey*, 56(11):720–735, 2001.
 8. M. Shower, M. Brown, and J.R. Sutherst. Comparative examination of female urethral pressure profiles measured by co2 and h2o infusion techniques. *Br J Urol*, 55(3):326–31, 1983.
 9. E. Hanzal, E. Berger, and H. Koelbl. Reliability of the urethral closure pressure profile during stress in the diagnosis of genuine stress incontinence. *Br J Urol*, 68(4):369–71, 1991.
 10. P. Meunier and P. Mollard. Urethral pressure profile in children: a comparison between perfused catheters and micro-transducers, and a study of the usefulness of urethral pressure profile measurements in children. *J Urol*, 120(2):207–10, 1978.
 11. D. De Haas, P.J. Steinberg, and P.J. Klopper. Qualitative analysis of the four-channel, high-resolution urethral pressure profile of the female dog. *J Urol*, 142(3):855–9, 1989.
 12. B.M. Carnaille, J.M. Rigot, J.P. Bailleul, J.L. Quievreux, J.L. Wemeau, and C.A. Proye. Urodynamics in patients with pheochromocytoma: a peri-operative study of 10 cases. *World J Surg*, 16(4):676–9, 1992.
 13. M.T. McLennan, C.F. Melick, and A.E. Bent. Leak-point pressure: clinical application of values at two different volumes. *Int Urogynecol J Pelvic Floor Dysfunct*, 11(3):136–41, 2000.
 14. Jr. Feldner, P.C., L.R. Bezerra, R.A. de Castro, M.G. Sartori, E.C. Baracat, G.R. de Lima, and M.J. Girao. Correlation between valsalva leak point pressure and maximal urethral closure pressure in women with stress urinary incontinence. *Int Urogynecol J Pelvic Floor Dysfunct*, 15(3):194–7, 2004.
 15. C.W. Nager, J.A. Schulz, S.L. Stanton, and A. Monga. Correlation of urethral closure pressure, leak-point pressure and incontinence severity measures. *Int Urogynecol J Pelvic Floor Dysfunct*, 12(6):395–400, 2001.
 16. K. Baessler, K. Miska, R. Draths, and B. Schuessler. Effects of voluntary pelvic floor contraction and relaxation on the urethral closure pressure. *Int Urogynecol J Pelvic Floor Dysfunct*, 16(3):187–90; discussion 190–1, 2005.
 17. J.P. Theofrastous, G.W. Cundiff, R.L. Harris, and R.C. Bump. The effect of vesical volume on valsalva leak-point pressures in women with genuine stress urinary incontinence. *Obstet Gynecol*, 87(5 Pt 1):711–4, 1996.
 18. G.J. Faerber and A.R. Vashi. Variations in valsalva leak point pressure with increasing vesical volume. *J Urol*, 159(6):1909–11, 1998.
 19. R.M. Decter and L. Harpster. Pitfalls in determination of leak point pressure. *J Urol*, 148(2 Pt 2):588–91, 1992.
 20. J.K. Nguyen, G.C. Gunn, and N.N. Bhatia. The effect of patient position on leak-point pressure measurements in women with genuine stress incontinence. *Int Urog-*

- ynecol J Pelvic Floor Dysfunct*, 13(1):9–14, 2002.
21. T. Idzenga, J.J.M. Pel, R. A. Baldewsing, and R. van Mastrigt. Perineal noise recording as a non-invasive diagnostic method of urinary bladder outlet obstruction: a study in polyvinyl alcohol and silicone model urethras. *Neurourology and Urodynamics*, 24(4):381–8, 2005.
 22. T. Idzenga, J.J.M. Pel, and R. van Mastrigt. A biophysical model of the male urethra: Comparing viscoelastic properties of polyvinyl alcohol urethras to male pig urethras. *Neurourology and Urodynamics*, 25(5):451–460, 2006.
 23. M. Brown and J.E.A. Wickham. The urethral pressure profile. *British Journal of Urology*, 41(2):211–217, 1969.
 24. P. Abrams, J.G. Blaivas, S.L. Stanton, and J.T. Andersen. The standardisation of terminology of lower urinary tract function. *Scand J Urol Nephrol Suppl*, 114:5–19, 1988.
 25. T. Idzenga, J.J.M. Pel, and R. van Mastrigt. Leak point pressure or urethral pressure profilometry? urodynamic evaluation of continence tested in a model urethra. In *International Continence Society 35th Annual meeting*, Montreal, Canada, 2005.
 26. D.J. Griffiths. *Urodynamics. The mechanics and hydrodynamics of the lower urinary tract*, volume 4 of *Medical Physics Handbooks*. Hilger, Bristol, 1980.
 27. M. Asmussen. Intraurethral pressure recording. a comparison between tip-transducer catheters and open-end catheters with constant flow. *Scand J Urol Nephrol*, 10(1):1–6, 1976.
 28. P.H. Abrams, S. Martin, and D.J. Griffiths. The measurement and interpretation of urethral pressures obtained by the method of brown and wickham. *Br J Urol*, 50(1):33–8, 1978.
 29. S. Martin and D.J. Griffiths. Model of the female urethra: Part 1-static measurements of pressure and distensibility. *Med Biol Eng*, 14(5):512–8, 1976.

Chapter 7

Abstract

On average in ageing males the prostate enlarges (Benign Prostatic Enlargement or BPE) and may cause Bladder Outlet Obstruction (BOO). The internationally standardised method for diagnosing BOO is based on measurements of urinary flow rate and bladder pressure, using a catheter inserted into the bladder via the urethra. This method is invasive, time-consuming and uncomfortable for the patient. We are developing a novel diagnostic method based on perineal recording of noise during urinary flow. Although it is known that (some aspects of) the recorded noise are (among others) related to the degree of obstruction, an exact and unique relation allowing derivation of the degree of obstruction from the noise recording is not known. In a biophysical model of the urethra we found that the weighted average frequency, the standard deviation and the skewness of the power spectrum are monotonic related to the degree of obstruction. The standard deviation was found to be the best significant predictor of BOO (89% correct). Based on this model study, we are confident that a simple non-invasive acoustic method for diagnosing BOO caused by BPE can be developed, which would lower the threshold for urodynamic testing of patients with lower urinary tract symptoms.

Adapted from: T. Idzenga, J.J.M. Pel and R. van Mastrigt, "*Towards an acoustic non-invasive diagnosis of urinary bladder outlet obstruction*", IEEE Transactions on Biomedical Engineering, *accepted for publication*, 2007.

Chapter 7

Towards an acoustic non-invasive diagnosis of urinary bladder outlet obstruction

Introduction

Lower Urinary Tract Symptoms (LUTS) in ageing males, e.g. a weak stream, dribbling or frequent nightly voiding, mostly result from an obstructed urethra caused by an enlarged prostate (Benign Prostatic Enlargement or BPE) or a weakly contracting bladder. At present the authoritative International Continence Society (ICS) recommends a provisional method for differentiating between these causes by diagnosing Bladder Outlet Obstruction (BOO). This method is based on the maximum urinary flow rate and the associated bladder (detrusor) pressure, graphically represented in a pressure-flow plot¹. The most frequently used method for measuring the detrusor pressure is inserting a catheter into the bladder via the urethra. This method is invasive, time-consuming and uncomfortable for the patient. Therefore, not all patients with LUTS are urodynamically tested. This may lead to erroneous diagnoses and failing treatment. Furthermore, the transurethral catheters used induce the risk of urinary tract infection and urethral trauma^{2,3}. Presently, more patient-friendly methods are being developed and validated to diagnose BOO in patients with LUTS⁴⁻¹⁰. Most of these methods are based on non-invasive assessment of pressure and flow signals during manipulated/interrupted voiding or on long-term changes caused by BOO, such as changes in bladder-wall thickness^{8,9}. Alternatively, a simple non-invasive diagnosis might be based on recording of sound, produced by turbulent urinary flow caused by prostatic obstruction of the urethra. It would enable the patient to void freely without interruptions and it could be specifically directed towards diagnosing BOO.

It is known that an object in a fluid flow with a high enough Reynolds number induces turbulence downstream. An obstruction in a tube causes a jet downstream of the narrowing where the streamlines detach from the tube wall. This detachment creates a shear

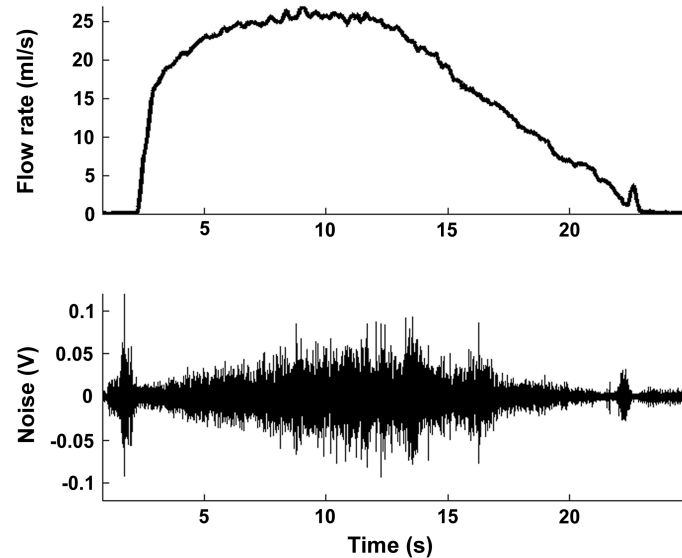


Figure 7.1: An example of simultaneously measured urine flow rate (top panel) and perineal sound (lowest panel). The sound was recorded using a microphone pressed against the perineum. The peaks in the sound recording before voiding starts and at the end of voiding are caused by contraction of pelvic floor muscles.

layer between the high-velocity jet and the slower moving fluid closer to the wall, forming a recirculation zone with backward flow. Further downstream the streamlines reattach to the tube wall, at the so-called reattachment point. At high enough Reynolds numbers instabilities in the shear layer extract energy from the mean flow and cause the jet to break down into a turbulent flow resulting in pressure variations at the tube wall^{11,12}. In cardiology these pressure variations have been studied in patients^{13–16} and in models^{11,17–20} to relate spectral analysis to the degree of arterial stenosis. In the mid seventies the recording of pressure variations was introduced in the field of urology, since in men an enlarged prostate may obstruct the bladder outlet. It was hypothesized that recordings with a microphone at the perineum (between scrotum and anus) were related to the degree of prostatic obstruction²¹. Furthermore, it was hypothesized that the degree of obstruction could be derived from (a combination of) aspects of the recorded sound^{22,23}. An example of a perineal sound recording is shown in figure 7.1.

In the earlier studies^{11,17–20,22} in models of arteries and urethras consisting of latex^{18,20}, tygon^{17,19}, silicone²² or other flexible¹¹ tubing it was shown that the maximum amplitude, and some other aspects of the frequency spectrum of the sound depended on the degree of obstruction. These models, however, are rather stiff compared to the more flexible and distensible blood vessel or urethra. No exact relationship or method to calculate the degree of obstruction from the sound recording was published. In a previous study²⁴ we

found that the average amplitude of the sound-signal and the weighted average frequency of the recorded power spectrum significantly depended on the degree of obstruction, the position of the microphone as well as the viscoelastic properties of the model urethra. To try to establish a unique relation between (combinations of) aspects of the sound and the degree of obstruction we constructed a flexible and extensible biophysical model^{24,26}. We imposed different degrees of obstruction by inflating a blood pressure cuff around the model and recorded sound at different positions downstream of the obstruction.

Materials & Methods

We constructed the biophysical model of the urethra from a 10% aqueous solution of PolyVinyl Alcohol (PVA-cryogel, Chu, Kingston, USA)²⁷. This cryogel was heated in boiling water for 30 min. and poured in a cylindrical mould (450 mm in length, 16 mm in diameter). A copper strip with Y-shaped cross section (legs of 4 mm wide) was placed along the centre of the mould to create a channel allowing flow through the model. Exposure of the cryogel to air was minimized to prevent evaporation of water. Some free space was maintained at the top of the mould to allow air bubbles to escape and to allow expansion of the cryogel during freezing. After 6 hours of rest at room temperature (21°C), the mould was stored in a freezer at -20°C. After 14 hours in the freezer the mould was stored at room temperature for 10 hours. That completed one freeze-thaw cycle that was repeated three times. This resulted in a model urethra with viscoelastic properties comparable to the male pig urethra²⁵ and urethral pressure profiles compa-

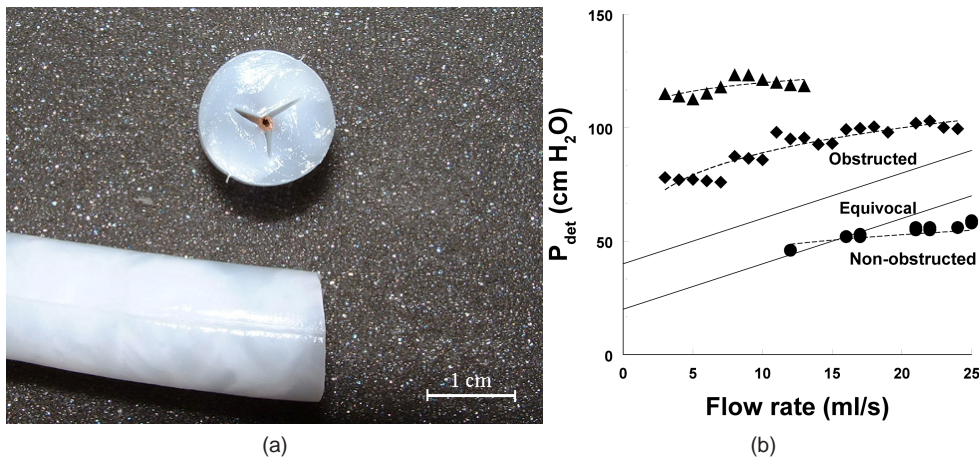


Figure 7.2: a) Cross-section and side view of a PVA model urethra with a Y-shaped channel to allow flow through the model. b) Detrusor pressure plotted versus the resulting flow rate in the PVA model urethra at three different cuff-pressures (\bullet : $P_{cuff} = 0$ cm H₂O, \blacklozenge : $P_{cuff} = 80$ cm H₂O and \blacktriangle : $P_{cuff} = 140$ cm H₂O). The two drawn lines delineate the unobstructed, equivocal and obstructed areas used in the diagnosis of patients.

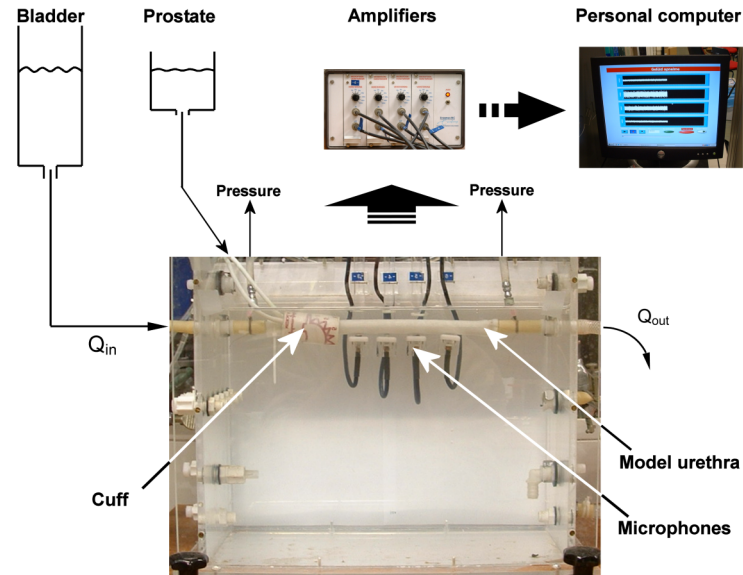


Figure 7.3: The measurement setup for studying the relation between recorded sound and degree of prostatic obstruction. Changing the combination of “bladder pressure” and “prostate pressure” varied the degree of obstruction. Pressure is measured up- and downstream of the obstruction.

rable to the male urethra²⁶. Figure 7.2 shows a cross-section of the model urethra (a) and pressure-flow data in model urethra at different cuff pressures (b). The pressure-flow values measured in the model urethra were comparable to those measured in patients as illustrated by the inserted borderlines for obstruction in patients. The model urethra was placed in a container filled with demineralised water to prevent evaporation. One side of it was connected to a water column and the other side to an outflow tube (see figure 7.3). A blood pressure cuff was placed around the model urethra and connected to a second water column. This blood pressure cuff forms a distensible obstruction of the model urethra, similar to an elastic prostate. The water in the second column regulates the distensibility of the obstruction. The level in the first water column (bladder pressure) was varied between 60 and 180 cm and in the second column (cuff) between 20 and 180 cm (both in steps of 20 cm) resulting in 63 combinations. Only in 35 combinations of the two column levels a flow rate higher than 2 ml/s was realized. The degree of obstruction was quantified by the bladder outlet obstruction index (BOOI)²⁸:

$$\text{BOOI} = P_{\text{det}} - 2 \cdot Q_{\text{max}} \quad (7.1)$$

with P_{det} (in cm H₂O) being the detrusor pressure at maximum urinary flow rate, modeled by the pressure-drop over the model urethra, and Q_{max} (in ml/s) being the maximum

urinary flow rate, modeled by the flow rate through the model urethra. According to the international golden standard¹ an unobstructed urethra is defined by BOOI < 20 and an obstructed urethra by BOOI > 40. For 20 < BOOI < 40 the pressure-flow study is equivocal. As equation (1) is dimensionally inconsistent the index BOOI only has clinical value if P_{det} and Q_{max} are expressed in the indicated units. With the pressure drop over the obstruction taken as the detrusor pressure the 35 combinations of column levels resulted in a BOOI distribution between -17 and +118 with a mean of 51 and a standard deviation of 32. At each BOOI value we recorded sound in a randomized fashion at twelve distances (i.e. 1 to 12 cm) downstream of the obstruction using 4 identical piëzoceramic microphones (Electret, a flat frequency response between 20 and 18000 Hz) sealed from the water using polyurethane condoms (Durex Avanti, SSL International, Manchester, UK). We made four different measurement sets each consisting of four microphone positions, totaling to 16 positions (i.e. 1, 2, 3,..., 12 cm downstream of the obstruction and repetitive measurements at 1, 2, 4 and 9 cm). At each set of 4 positions we applied all 35 combinations of water levels in the two columns and recorded sound from the four microphones simultaneously. After each measurement set all microphones were replaced to the next set of positions and the measurement series was repeated. No microphone remained at the same position between sets. sound recordings were repeated five times at each microphone position and had a duration of ~54 seconds. This resulted in 2800 sound recordings at 35 different degrees of obstruction and 16 positions (including the repetitive positions) downstream of the obstruction. The sound signals were amplified and band-pass filtered between 50 and 5000 Hz using amplifiers with integrated 2-pole band-pass filters, constructed at the department of Experimental and Medical Instrumentation, Erasmus MC, Rotterdam, The Netherlands. The filtered signals were sampled at a rate of 10 kHz and stored in a PC using a PCI-6221 (National Instruments Corporation, Austin, Texas, USA) AD converter. The stored signals were analysed using self-written programs in Matlab® (The Mathworks, Inc., Natick, MA, USA). From each sound recording we calculated the average amplitude (A) and the power spectrum, using Fast Fourier Transform. We derived three parameters from the power spectrum $P(f)$: the weighted average frequency²² (f_c , equation 2), the standard deviation (σ , equation 3) and the skewness (γ_1 , equation 4)²⁹:

$$f_c = \frac{\int_{f_0}^{f_1} f \cdot P(f) \cdot df}{\int_{f_0}^{f_1} P(f) \cdot df} \quad (7.2)$$

$$\sigma = \sqrt{\mu_2} = \sqrt{\frac{\int_{f_0}^{f_1} (f - f_c)^2 \cdot P(f) \cdot df}{\int_{f_0}^{f_1} P(f) \cdot df}} \quad (7.3)$$

$$\gamma_1 = \frac{\mu_3}{\mu_2^{3/2}} = \frac{\int_{f_0}^{f_1} (f - f_c)^3 \cdot P(f) \cdot df}{\int_{f_0}^{f_1} P(f) \cdot df} \cdot \left[\frac{\int_{f_0}^{f_1} (f - f_c)^2 \cdot P(f) \cdot df}{\int_{f_0}^{f_1} P(f) \cdot df} \right]^{-3/2} \quad (7.4)$$

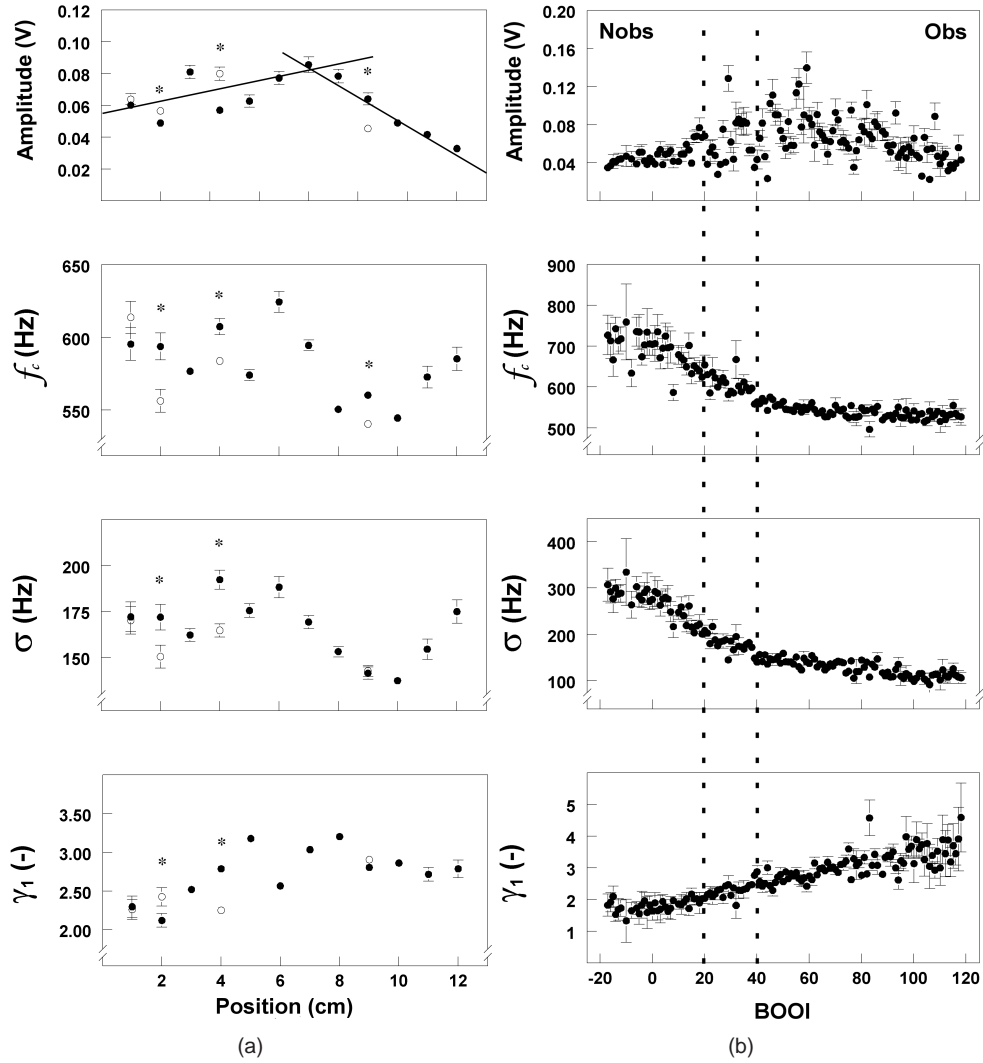


Figure 7.4: a) Four parameters (average amplitude of the sound and the weighted average frequency (f_c), standard deviation (σ) and skewness (γ_1) of its power spectrum) derived from the sound recording are plotted (mean \pm standard error of the mean) as a function of a) the microphone position downstream of the obstruction and b) the degree of bladder outlet obstruction (BOOI). At each position the parameters were averaged over all recordings at that position. The repeated measurements are shown as an open circle. Pairs of repeated measurements that were significantly different (Mann-Whitney, $p < .05$) are marked with an asterisk. The increase and decrease of amplitude with increasing distance below and above 7 cm are indicated by the two straight lines (Linear Regression, $p < .001$). At each value of BOOI the mean and standard error of the mean of 5 recordings at 12 distances downstream of the obstruction are shown. The critical BOOI-values are indicated by the dotted lines, unobstructed (Nobs) is defined by BOOI < 20 and obstructed (Obs) is defined by BOOI > 40¹.

where μ_i is the i th central moment of the power spectrum $P(f)$. These three spectral parameters depend on the part of the power spectrum that is analysed, defined by the lower (f_0) and upper (f_1) boundary frequency. We have set f_1 to 2500 Hz, i.e. half the Nyquist-frequency. To find the part of the power spectrum that best predicted the degree of obstruction we varied f_0 between 50 and 1000 Hz in steps of 50 Hz. At each f_0 we used logistic regression to evaluate the predictive value for each of the three spectral parameters separately. Using the Bootstrap method³⁰ we constructed 50 new populations from the original population and established the 95% confidence interval of the predictive values.

Results & Discussion

All four parameters (A , f_c , σ and γ_1) calculated from the sound recordings were significantly related to the microphone position and the degree of obstruction (ANOVA, $p < .001$). For each parameter some pair(s) of repeated measurements done after replacing the microphones at 1, 2, 4 and 9 cm were significantly different (Mann-Whitney, $p < .05$, see figure 7.4a). These differences between the repeated measurements may be ascribed to variation in contact between microphone and model wall as a result of replacement of the microphones. If this is the case, it is important to measure the contact between microphone and perineum and standardize it for clinical use.

Time-domain analysis

Although significant, the correlation between the average amplitude and the microphone position was very weak (Spearman's correlation coefficients, see table 7.1). The average amplitude did show an increase with increasing distance between 1 and 7 cm (Linear Regression, $p < .001$) followed by a decrease between 7 and 12 cm (Linear Regression, $p < .001$, see figure 7.4a). Several authors also found such a relation between the root-mean-square of the pressure variations^{11,17,20} or spectral characteristics^{18-20,22} and the distance between microphone and obstruction. The low amplitude directly downstream of the obstruction can be explained from the low pressure in the recirculation zone³¹. The increase of the average amplitude to a maximum could be explained from the reattachment of the streamlines downstream of the obstruction. It has been shown that the position of maximum wall pressure variation is located just upstream of the so-called reattachment point^{17,20}. Further downstream the conversion of turbulent flow into laminar flow accounts for the decrease in average amplitude^{11,12}.

Averaged over all microphone positions the amplitude first increased with increasing BOOI and then decreased (see figure 7.4b, top panel). This was found at the separate microphone positions as well (see figure 7.5a, top panel, for two examples). At low values of BOOI (generally a high flow rate) the low average amplitude is presumably caused by the low degree of turbulence due to the lack of a shear layer. With increasing BOOI a shear layer develops and turbulence increases with the increasing amount of kinetic energy in the mean flow. At high values of BOOI (generally a low flow rate) the low average amplitude is presumably caused by the decreasing amount of kinetic energy in the mean flow. The amplitude increases with flow rate at the different constant cuff pressures (see

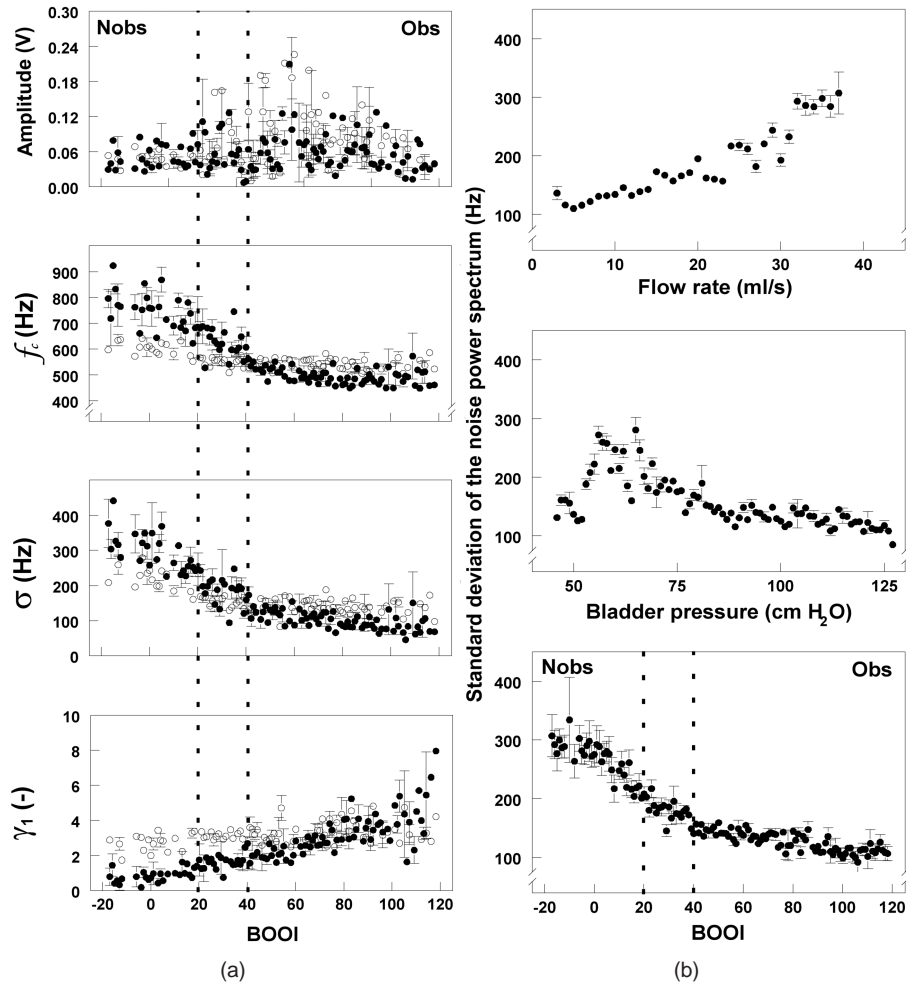


Figure 7.5: a) Four parameters (average amplitude of the sound and the weighted average frequency (f_c), standard deviation (σ) and skewness (γ_1) of its power spectrum) derived from the sound recording are plotted (mean \pm standard error of the mean) as a function of the degree of bladder outlet obstruction (BOOI) at two microphone positions (●: distance = 2 cm, ○: distance = 8 cm). b) Standard deviation of the sound frequency spectrum plotted (mean \pm standard error of the mean) as a function of the flow rate (Q_{max} , ml/s), the bladder pressure (P_{det} , cm H₂O) and a combination of these two: BOOI. The standard deviation is uniquely related to the flow rate, but not to the bladder pressure. It is also uniquely related to BOOI.

Table 7.1: Statistical test-results of the four parameters derived from the recorded sound. The first two columns present the Spearman's coefficient for the correlation between the four parameters and the microphone position and the degree of obstruction (BOOI). The next two columns present the linear regression coefficients of the four parameters as a function of Position and BOOI. All the coefficients were significant ($p < .001$), except the two marked with an asterisk ($p < .05$). The last two columns present the values (Mean \pm Standard error of the mean) of the four parameters in unobstructed (BOOI < 20) and obstructed (BOOI > 40) models. All four parameters were significantly different between obstructed and unobstructed (Student's t-test, $p < .001$).

	Spearman's correlation coefficient		Linear regression coefficient		Unobstructed (n = 508)	Obstructed (n = 1704)
	Position	BOOI	Position	BOOI		
A (mV)	-.131	.089	-.120	.091	.051 ($\pm .001$)	.067 ($\pm .001$)
f_c (Hz)	-.065*	.571	-.126	.568	682 (± 5)	541 (± 1)
σ (Hz)	-.042*	.651	-.092	.653	255 (± 4)	132 (± 1)
γ_1 (-)	-.216	.433	-.189	.466	1.87 ($\pm .04$)	3.02 ($\pm .03$)

figure 7.5a, top panel). At higher cuff pressures this increase is steeper than at lower cuff pressures. This is also presumably caused by a low degree of turbulence at low cuff pressures, or small degree of obstruction. The sound recording in a volunteer (see figure 7.1) also shows an increase in amplitude with increasing flow rate. The relation between average amplitude and degree of obstruction is not monotonic (see figure 7.4a); therefore the average amplitude is not suitable for use as a measure for the degree of obstruction.

Frequency-domain analysis

The other three parameters (f_c , σ and γ_1) were calculated from the power spectrum of the recorded sound. These three 'spectral' parameters were calculated between two boundary frequencies f_0 and f_1 with f_1 set at 2500 Hz. For each parameter we found the maximum predictive value at a different f_0 , i.e. 400 Hz for f_c , 200 Hz for σ and 600 Hz for γ_1 . The parameters were significantly, but weakly, correlated to the microphone position and strongly to BOOI (Spearman's correlation coefficients, see table 7.1); they depended monotonically on BOOI (see figure 7.4a). We also found that the linear regression coefficient for BOOI was in absolute sense much higher than that for the microphone position (see table 7.1). At different microphone locations the three parameters derived from the power spectrum were uniquely related to BOOI, but the steepness of this relation varied (see figure 7.5a). In our model urethra we varied the microphone position through a large range. In clinical measurements the possible microphone positions are limited to the perineum. Therefore variation in the four parameters, caused by variation in the microphone position, is expected to be smaller in patients than in our model urethra.

Each parameter derived from the recorded sound might depend on: the bladder pressure, the flow rate and the cuff pressure. In the model urethra these three variables are related, any of the three can be calculated from the other two. Therefore each parameter can be described as a function of two independent variables, e.g. bladder pressure and flow rate.

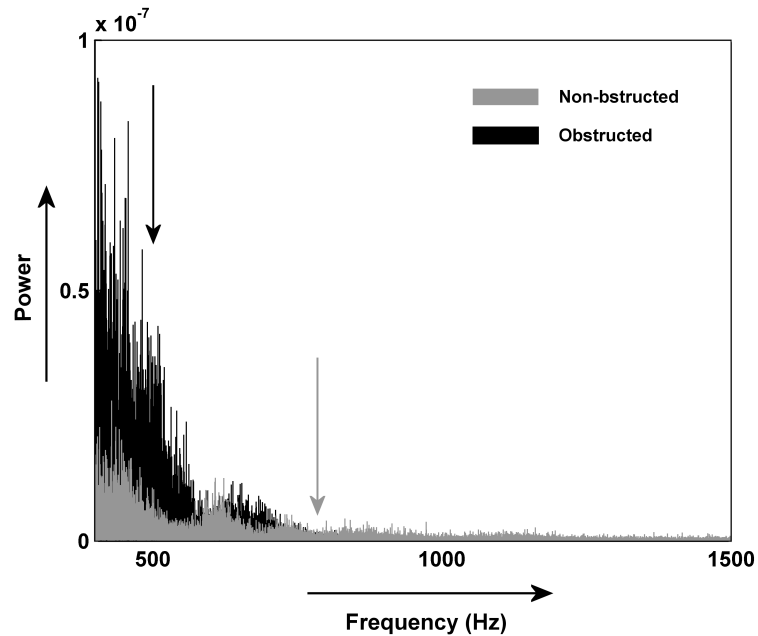


Figure 7.6: Example of two power spectra and their weighted average frequencies (indicated by arrows) in an obstructed model urethra (BOOI = 105, f_c = 499 Hz, black) and in a non-obstructed model urethra (BOOI = 16, f_c = 775 Hz, grey).

In the example in figure 7.5b, the standard deviation of the power spectrum appears to be uniquely related to the flow rate (which is not a unique measure of BOO), but not to the bladder pressure. The lowest panel of figure 7.5b shows the resulting dependence on the Bladder Outlet Obstruction Index BOOI, which is a combination of these two variables and a unique measure for BOO.

For all three parameters the mean was found to be significantly different between obstructed and unobstructed recordings (Student's t-test, $p < .001$, see table 7.1). A decrease in f_c means a shift of the centre of gravity of the power spectrum to lower frequencies. This shift indicates that turbulence in the urinary flow as a result of an increasing degree of obstruction added relatively more power to the lower frequency part of the spectrum. The decrease in standard deviation σ of the power spectrum means that the power is more concentrated around the weighted average frequency. In figure 7.6 an example is presented of power spectra in two extreme flow cases, severely obstructed and non-obstructed. Using logistic regression, we assessed the significance of each parameter as a predictor of the outcome parameter BOOI and found that only the standard deviation σ was a significant predictor. With f_0 and f_1 set at 200 and 2500 Hz, respectively, the standard deviation of the power spectrum predicted 89% of the measurements correctly. The 95% confidence interval for the predictive value, as derived from 50 newly constructed populations using the Bootstrap method, was 88-90%. The Receiver Opera-

for Characteristic (ROC) curve for perineal sound recording as a non-invasive method for diagnosing BOO had an area under the curve of 0.934.

The results found in this study are based on experimental values in a biophysical model of the urethra. In earlier studies we showed that the produced sound depended on the viscoelastic properties²⁴ and that the viscoelastic properties of this model are comparable to those of the human male urethra²⁵. Furthermore, the pressure-flow data in figure 7.2 show that our model urethra displays the hydrodynamic behaviour of a distensible tube with an elastic obstruction. A loop as measured in patients is caused by continuous changes in urethral resistance and bladder contractility, which the model does not support. However, our model urethra could simulate the first part of the micturition. The sound recorded in this model urethra is induced by turbulence of the stream as a result of an obstruction. In humans anatomical aspects of the obstruction and the lower urinary tract may vary between individuals and possibly affect the sound recording. Furthermore the contact between the microphone and the perineum is of importance and needs to be measured and standardized for clinical use. Therefore, further testing of perineal sound recording in male volunteers and patients is needed to establish the diagnostic value of this method.

Conclusion

Our findings confirm earlier reports^{11,17–20,22,24} that sound, recorded at the wall downstream of an obstruction in a tube, is related to the degree of obstruction. Some earlier attempts have been made to relate parameters calculated from these pressure-variations to the degree of obstruction^{17,18,20,22}. However, in these attempts knowledge of other parameters like the jet-velocity, the diameter of the obstruction or the percentage of area reduction in the obstruction was needed. Our findings show that the degree of obstruction can be derived from a sound recording at the wall of our realistic model of the urethra. The standard deviation of the power spectrum (between 200 and 2500 Hz) classified the model urethra as obstructed or unobstructed conform the guidelines of the International Continence Society¹ with a success rate of 89% (95% confidence interval: 88-90%). Therefore, perineal sound recording could possibly be used as a non-invasive method for clinically diagnosing Bladder Outlet Obstruction caused by Benign Prostatic Enlargement. The diagnostic value of perineal sound recording *in vivo* will be determined by further clinical testing.

Literature

1. D.J. Griffiths, K. Höfner, R. van Mastrigt, H.J. Rollema, A. Spångberg, and D.M. Gleason. Standardization of terminology of lower urinary tract: pressure-flow studies of voiding, urethral resistance and urethral obstruction. *Neurourology and Urodynamics*, 16:1–18, 1997.
2. H.C. Klingler, S. Madersbacher, B. Djavan, G. Schatzl, M. Marberger, and C.P. Schmidbauer. Morbidity of the evaluation of the lower urinary tract with transurethral multichannel pressure-flow studies. *Journal of Urology*, 159(1):191–194, 1998.

3. D. Porru, G. Madeddu, G. Campus, I. Montisci, R.M. Scarpa, and E. Usai. Evaluation of morbidity of multi-channel pressure-flow studies. *Neurourology and Urodynamics*, 18(6):647–652, 1999.
4. J.J.M. Pel and R. van Mastrigt. The variable outflow resistance catheter: a new method to measure bladder pressure noninvasively. *Journal of Urology*, 165:647–652, 2001.
5. D.J. Griffiths, D. Rix, M. MacDonald, M.J. Drinnan, R.S. Pickard, and P.D. Ramsden. Noninvasive measurement of bladder pressure by controlled inflation of a penile cuff. *Journal of Urology*, 167:1344–1347, 2002.
6. Y.Y. Ding, H. Ozawa, T. Yokoyama, Y. Nasu, M.B. Chancellor, and H. Kumon. Reliability of color doppler ultrasound urodynamics in the evaluation of bladder outlet obstruction. *Urology*, 56:967–971, 2000.
7. M.P. Sullivan and V.S. Yalla. Penile urethral compression-release maneuver as a non-invasive screening test for diagnosing prostatic obstruction. *Neurourology and Urodynamics*, 19:657–669, 2000.
8. C. Manieri, S.S. Carter, G. Romano, A. Trucchi, M. Valenti, and A. Tubaro. The diagnosis of bladder outlet obstruction in men by ultrasound measurement of bladder wall thickness. *J Urol*, 159(3):761–5, 1998.
9. M. Oelke, K. Höfner, U. Jonas, D. Ubbink, J. de la Rosette, and H. Wijkstra. Ultrasound measurement of detrusor wall thickness in healthy adults. *Neurourol Urodyn*, 25(4):308–17; discussion 318, 2006.
10. A. Tubaro, S. Carter, A. Hind, C. Vicentini, and L. Miano. A prospective study of the safety and efficacy of suprapubic transvesical prostatectomy in patients with benign prostatic hyperplasia. *J Urol*, 166(1):172–6, 2001.
11. J.J. Fredberg. Origin and character of vascular murmurs: Model studies. *Journal of Acoustic Society of America*, 61(4):1077–1085, 1977.
12. J.J. Fredberg. Pseudo-sound generation at atherosclerotic constrictions in arteries. *Bull Math Biol*, 36(2):143–55, 1974.
13. J.P. Kistler, R.S. Lees, J. Friedman, M. Pressin, J.P. Mohr, G. Roberson, and R.G. Ojemann. The bruit of carotid stenosis versus radiated basal heart murmurs. *Circulation*, 57(5):975–981, 1978.
14. J.P. Kistler, R.S. Lees, A. Miller, R.M. Crowell, and G. Roberson. Correlation of spectral phonoangiography and carotid angiography with gross pathology in carotid stenosis. *New England Journal of Medicine*, 305(8):417–419, 1981.
15. R.S. Lees and C. Forbes Dewey Jr. Phonoangiography: A new diagnostic method for studying arterial disease. *Proceedings of the National Academy of Sciences*, 67(2):935–942, 1970.
16. G.W. Duncan, G.O. James, C. Forbes Dewey Jr, G.S. Myers, and R.S. Lees. Evaluation of carotid stenosis by phonoangiography. *New England Journal of Medicine*, 27(Nov):1124–1128, 1975.
17. S.A. Abdallah and N.H.C. Hwang. Arterial stenosis murmurs: An analysis of flow and pressure fields. *Journal of Acoustic Society of America*, 83(1):318–334, 1998.
18. S.A. Jones and A. Fronek. Analysis of break frequency downstream of a constriction in a cylindrical tube. *Journal of Biomechanics*, 20(3):319–327, 1987.
19. P.C. Lu, C.N. Hui, and N.H.C. Hwang. A model investigation of the velocity and pressure spectra in vascular murmurs. *Journal of Biomechanics*, 16(11):923–931,

- 1983.
20. R.J. Tobin and I.D. Chang. Wall pressure spectra scaling downstream of stenoses in steady tube flow. *Journal of Biomechanics*, 9:633–640, 1976.
 21. W.E. Bradley, B.P. Brockway, and G.W. Timm. Auscultation of urinary flow. *Journal of Urology*, 118:73–75, 1977.
 22. H. Teriö. Acoustic method for assessment of urethral obstruction: a model study. *Medical and Biological Engineering and Computing*, 29:450–456, 1991.
 23. A.J. van Koeveeringe and R. van Mastrigt. A relation between the sound produced by urethral turbulence in patients and objectively assessed subvesical obstruction. *Neurourology and Urodynamics*, 10:442–443, 1991.
 24. T. Idzenga, J.J.M. Pel, R.A. Baldewsing, and R. van Mastrigt. Perineal noise recording as a non-invasive diagnostic method of urinary bladder outlet obstruction: a study in polyvinyl alcohol and silicone model urethras. *Neurourology and Urodynamics*, 24(4):381–8, 2005.
 25. T. Idzenga, J.J.M. Pel, and R. van Mastrigt. A biophysical model of the male urethra: Comparing viscoelastic properties of polyvinyl alcohol urethras to male pig urethras. *Neurourology and Urodynamics*, 25(5):451–460, 2006.
 26. T. Idzenga, J.J.M. Pel, and R. van Mastrigt. Fluid perfused urethral pressure profilometry and valsalva leak point pressure: a comparative study in a biophysical model of the urethra. *World J Urol*, 25(4):423–9, 2007.
 27. K.C. Chu and B.K. Rutt. Polyvinyl alcohol cryogel: an ideal phantom material for mr studies of flow and elasticity. *MRM*, 37:314–319, 1997.
 28. P. Abrams. Bladder outlet obstruction index, bladder contractility index and bladder voiding efficiency: three simple indices to define bladder voiding function. *BJU International*, 84:14–15, 1999.
 29. W.H. Beyer, editor. *Handbook of tables for probability and statistics*. The Chemical Rubber Co., Ohio, second edition edition, 1968.
 30. B. Efron. Bootstrap methods: another look at the jackknife. *Annals of Statistics*, 7:1–26, 1979.
 31. J.J.M. Pel and R. van Mastrigt. Development of a cfd urethral model to study flow-generated vortices under different conditions of prostatic obstruction. *Physiological Measurement*, 28(Accepted for publication):13–24, 2006.

Chapter 8

Abstract

Objectives: In a population of 16 healthy male volunteers we studied the variability and repeatability of perineal sound recording as a non-invasive method for diagnosing bladder outlet obstruction. **Materials & methods:** The volunteers had a flat age-distribution (22-62 years), a median IPSS-score of 1 (range: 0-18) and voided at least ten times. From each perineal sound recording the frequency spectrum was calculated and characterized by its weighted average frequency, standard deviation and skewness. We assessed the variability of these parameters using the Kruskal-Wallis test, differences between volunteers using Dunn's test and the repeatability by the normalised standard deviation of the differences between pairs of recordings in each volunteer. **Results:** For each parameter the variability within volunteers was significantly smaller than the variability between volunteers (Kruskal-Wallis, $p < .05$). For each parameter more than one volunteer was significantly different from three or more volunteers (Dunn's test, $p < .05$). The repeatability of each parameter was comparable to that of the maximum flow rate. **Conclusion:** Perineal sound recording gives repeatable results, which are significantly different between volunteers. In combination with the earlier published results from model-experiments the present results increase the probability that perineal sound recording can be used as a very simple and cheap method to non-invasively diagnose BOO. Clinical testing of this method is therefore strongly indicated.

Adapted from: T. Idzenga, J.J.M. Pel and R. van Mastrigt, "Variability and repeatability of perineal noise recording in a population of healthy male volunteers", *Neurourology and Urodynamics*, Accepted for publication, 2008.

Chapter 8

Variability and repeatability of perineal sound recording in a population of healthy male volunteers

Introduction

Elderly men generally develop Lower Urinary Tract Symptoms (LUTS), such as a low flow rate, frequent (nocturnal) voiding and incomplete emptying of the bladder. Possible causes for these symptoms are a weakly contracting bladder muscle or an enlarged prostate obstructing the bladder outlet (Bladder Outlet Obstruction or BOO). At the age of sixty approximately 60 percent of men have biological symptoms of an enlarged prostate¹. To differentiate between the two possible causes the most frequently used urodynamic test is a pressure-flow study². The transurethral catheters used for such a study, however, induce the risk of urinary tract infection and urethral trauma^{3,4}. Recently, non-invasive (and more patient friendly) measurement techniques to diagnose BOO have been developed and tested to avoid these risks: the Doppler flowmetry method⁵, the condom-catheter method⁶, the cuff method⁷ and measurement of changes in bladder wall thickness⁸. These techniques were found to be applicable in patients, but require manipulation of the urinary flow or a great deal of expertise from the observer. A cheap and simple alternative method for diagnosing BOO is non-invasive recording of sound at the perineum during voiding. The development of this technique started in the mid-sixties with a voiding audiograph⁹ and it has been applied in two clinical urophonographic studies^{10,11}. The general conclusion from these two studies was that pressure variations at the urethral wall could be measured in the form of audible sound, both in a model as well as in patients. However, optimization of the transducer and recording equipment was needed for urophonographic assessment of urethral obstruction in patients. Furthermore, it was not known how the degree of obstruction could be derived

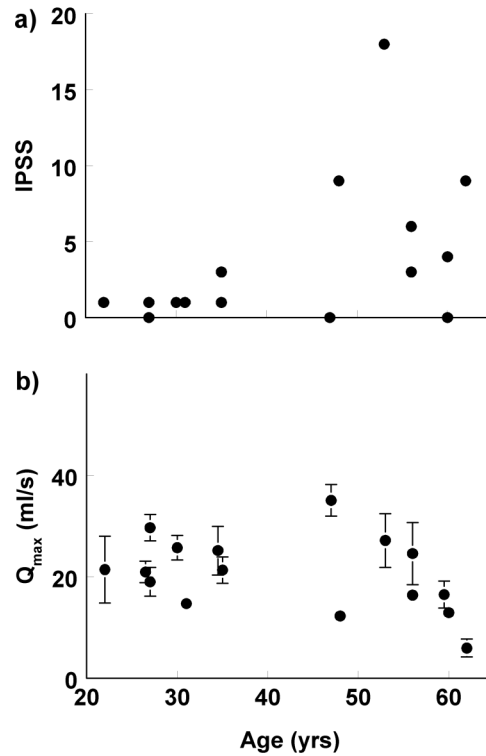


Figure 8.1: Characteristics of the population of 16 healthy male volunteers. The International Prostate Symptom Score (a) and maximum urinary flow rate (mean ± 1 sd) (b) are plotted as a function of the age of the volunteers. One volunteer (age 48 years) had a standard deviation of the maximum flow rate that was within the plotting area of the marker. Two volunteers were of the same age and had identical IPSS values. For display purposes the values of Q_{max} for volunteers of the same age are slightly separated.

from such a sound recording. In an earlier study we have shown in a biophysical model of the male urethra¹² that three parameters, derived from the frequency spectrum of the recorded sound (i.e. the weighted average frequency, the standard deviation and the skewness of the frequency spectrum), were uniquely related to the degree of obstruction¹³. Following this finding we developed a measurement setup for perineal sound recording in patients with LUTS. In the current study we applied this equipment to 16 healthy male volunteers and tested the variability of perineal sound recording within and between the volunteers and the repeatability within each volunteer, which was compared to that of the maximum urinary flow rate.

Materials & Methods

We recruited 16 healthy male volunteers to void at least ten times at normal desire. They voided in a standing position with a microphone pressed against the perineum directly behind the scrotum. At recruitment, the volunteers filled out an IPSS-form as a measure of their urological condition. Before voiding the volunteer was fitted out with a modified jockstrap. The front surface of the protective cup was removed, leaving the bottom part of the cup. The microphone, consisting of a modified dual head stethoscope (MDF Instruments Europe, Copenhagen, Denmark) with the ear piece replaced by a piézoceramic transducer, was placed in a slit in this bottom part (see figure 8.2). Using a weight transducer we measured the voided volume. By differentiating this voided volume with respect to time in 1s time-windows we calculated the flow rate. In each window a straight line was fitted through the voided volume signal using the least squares method. The flow rate was calculated as the slope of this straight line. Subsequently the window was shifted 0.025 s and the calculation was repeated. This procedure has a smoothing effect on the flow rate curve, but does not affect the value of the measured flow rate drastically. The sound signal was amplified and band-pass filtered between 50 and 5000 Hz using an amplifier with an integrated 2-pole band-pass filter, constructed at the department of Experimental and Medical Instrumentation, Erasmus MC, Rotterdam, The Netherlands. The voided volume and the sound signal were sampled at a rate of 10 kHz and stored in a PC using a PCI-6024E (National Instruments Corporation, Austin, Texas, USA) AD converter and analyzed using self-written programs in Matlab[®] (The Mathworks, Inc., Natick, MA, USA).

Signal analysis From each sound recording we selected the part for which the flow rate was higher than 50 percent of the maximum (see figure 8.3a left and right). For this section we calculated the frequency spectrum as a function of time. In a time-window of ~ 0.8 seconds (8192 samples) we calculated the frequency spectrum between 100 and 1000 Hz using Fast Fourier Transform. The time-window was then shifted ~ 0.2 seconds (2048 samples) and calculation of the frequency spectrum was repeated. This procedure was repeated until the end of the recorded time signal was reached. In each time-window the frequency spectrum was characterized by three parameters: i.e. the weighted average frequency (each frequency was weighted by its contribution to the frequency spectrum and these weighted frequencies were averaged), the standard deviation of the spectrum around this weighted average frequency and the skewness of the spectrum¹³. From each recording we calculated the median value of each parameter. Furthermore, we assessed for each perineal sound recording the maximum flow rate (Q_{\max}) from the flow signal. For each parameter outliers were identified from a box-whisker plot of that parameter as values higher (lower) than the 75th (25th) percentile plus (minus) 1.5 times the interquartile range. The original recordings identified as outliers were inspected and assessed as a correct or incorrect recording.

Statistical analysis For each parameter we assessed the inter-volunteer variability using the non-parametric Kruskal-Wallis test, no corrections were made for tied ranks. Differences between the volunteers were tested using the Dunn's test¹⁴, i.e. a non-

parametric equivalent of the Bonferroni multiple t-test. We calculated the correlation between parameters using the non-parametric Spearman's correlation coefficient. To derive a measure of repeatability we have drawn random pairs of recordings from each volunteer data set, with replacement. None of the pairs were identical. The three parameters and the maximum flow rate were measured on different scales. Therefore, for comparison with the repeatability of the maximum flow rate we calculated a slightly modified version of the normalized repeatability statistic used by van van Mastrigt and Huang Foen Chung¹⁵. For each pair of recordings we calculated the difference and the mean of the values of the three parameters and the maximum flow rates. The normalized statistic was calculated as the standard deviation of the differences, divided by the range of the means. We compared the thus normalized repeatability of the three parameters to that of the maximum flow rate using the non-parametric Wilcoxon's signed rank test.

Results

The median age (min-max) of the volunteers was 41 (22-62) years and the IPSS-value ranged from 0 to 18 with a median of 1, see figure 8.1. The total number of perineal sound recordings was 237 of which 38 (16%) had parameter values identified as outliers. After inspection of the original signals 20 (53%) of these were found to be incorrect recordings and excluded from analysis. An example of a correct and an incorrect perineal sound recording and their frequency spectra are presented in figure 8.3a and 8.3b, respectively. The IPSS-value was moderately correlated poorly with the age of the volunteers (Spearman's $\rho = .529$, $p < .05$). 13 out of the 16 (81%) volunteers had an IPSS-score of 0-7 and 3 (19%) volunteers had an IPSS-score of 8-19. The maximum flow rate also correlated weakly with the age of the volunteers (Spearman's $\rho = -.389$, $p < .001$). The correlations (Spearman's ρ) between the three parameters and IPSS and age were (if significant) in the order of 0.1. The weighted average frequency had a good correlation with the standard deviation (Spearman's $\rho = .720$, $p < .05$) and with the skewness (Spearman's $\rho = -.699$, $p < .05$). The standard deviation had a poor correlation with the skewness (Spearman's $\rho = -.299$, $p < .05$).

For each parameter the variability within volunteers was significantly smaller than the variability between volunteers (Kruskal-Wallis, $p < .001$). Therefore, for each parameter at least one volunteer had results that were significantly different from the other volunteers. The three parameters are plotted as box-whisker plots in figure 8.4 with the volunteers sorted by their mean maximum flow rate (ranging from 6 to 35 ml/s). The volunteers that were significantly different from three or more other volunteers (Dunn's test, $p < .05$) are indicated with an asterisk in figure 8.4. Four volunteers were significantly different in more than one parameter.

The repeatability measures for the three parameters, derived from the sound frequency spectrum, and that of the maximum flow rate are presented in table 8.1. The repeatability measures of the three parameters were not significantly different from that of the maximum flow rate (Wilcoxon's signed rank test, p-values are noted in table 8.1).

Table 8.1: Median repeatability (interquartile range) for the three parameters, derived from the sound frequency spectrum, and the maximum flow rate. In the right column the results (p -values) of the non-parametric Wilcoxon's signed rank tests are shown for the comparisons between each parameter derived from the frequency spectrum and the maximum flow rate.

Parameter	Repeatability	p -value
Maximum flow rate	0.72 (0.19)	
Weighted average frequency	0.74 (0.30)	$p = .438$
Standard deviation	0.73 (0.17)	$p = .163$
Skewness	0.70 (0.35)	$p = .756$

Discussion

In 16 volunteers with a flat age distribution between 22 and 62 years we recorded perineal sound during voiding. The correlation coefficients between IPSS and age of the volunteers and between the maximum flow rate and age were, as expected, significantly positive and negative respectively. This shows that our sample of volunteers is a small, but suitable cross-section of a non-referred population.

38 of the 237 sound recordings resulted in parameter values identified as outliers. Upon inspection approximately half of these outliers were found to result from incorrect sound recordings and subsequently they were excluded from analysis. A possible cause for these incorrect recordings is variation in the contact between the microphone and the



Figure 8.2: Modified jockstrap to fix the microphone at the perineum during voiding.

skin. With a bad contact there is little or no transmission of pressure variations from the urethral wall to the microphone, which then records mainly external noise. The equipment for recording the urinary flow rate may have caused an additional disturbance. Each volunteer was asked to void in a cylinder that was placed on a weight transducer. Urine droplets falling on the fluid surface in the cylinder sometimes generated a splattering noise. We attempted to avoid the effect of the urine droplets by asking each volunteer to aim at the wall of the cylinder, but this was difficult to maintain at low flow rates (< 5 ml/s). Therefore we only analysed the part of the sound recording with a flow rate above 50% of the maximum flow rate. For future perineal sound recordings in patients with a flow rate smaller than 5 ml/s the method of recording needs to be improved. To do this, a first possibility is to reduce the influence of the background noise. This can either be done by shielding the microphone or by minimizing the background noise itself, for example by preventing the splattering of urine droplets by adapting the flow meter receptacle. A second possibility is optimization of the contact between microphone and tissue to ensure optimal transmission of the pressure variations from the urethral wall to the microphone. The sound recordings in this study are similar to the examples presented by Koiso¹¹ and Teriö¹⁶. The values for the weighted average frequency given by Teriö for the one volunteer in his study (112 and 129 Hz) are comparable to the values we found in our volunteer population (125-240 Hz). However, the values given for the patients (170-454 Hz) appear to be higher than those in our volunteers. Even though these values are calculated from a slightly different part of the sound frequency spectrum this hints at a possible way to discriminate healthy volunteers from patients. Furthermore, we found in our study that for the three parameters derived from the sound frequency spectrum the intra-volunteer variability was significantly smaller than the inter-volunteer variability (Kruskal-Wallis, $p < .05$). Multiple volunteers were significantly different from two or more other volunteers in each parameter. This means that in our population volunteers could be distinguished on the basis of one of these parameters. The variation in recorded sound between the volunteers most likely results from physiological variation, e.g. differences in structure of the lower urinary tract. The good correlations (Spearman's rho ~ 0.7) between the three parameters indicate that when a volunteer is on the top end of one scale he will much likely also be on the top or bottom end of another scale. For one volunteer it was shown that he was significantly (Dunn's test, $p < .05$, see figure 8.4) on the described ends of the scales. This was as expected from the earlier published model experiments¹⁷. In these experiments the weighted average frequency and the standard deviation were negatively related to increasing degree of obstruction and the skewness was positively related.

The repeatability of the three sound parameters in our study (see table 8.1) was comparable to that of the repeatability of the maximum flow rate measured in the same population. The repeatability of the standard deviation appeared to be closest to that of the maximum flow rate. Correction of the maximum flow rate for the voided volume gave identical results. The method used to calculate these values was similar to the method used by van Mastrigt and Huang Foen Chung¹⁵. However, we modified the methodology by calculating the repeatability in each volunteer separately to exclude the mean differences between volunteers (as opposed to van Mastrigt and Huang Foen Chung). A consequence of this modification is that the values, calculated in our study, are not comparable to the values found in their study. Correction of the maximum flow rate for the voided volume gave identical results.

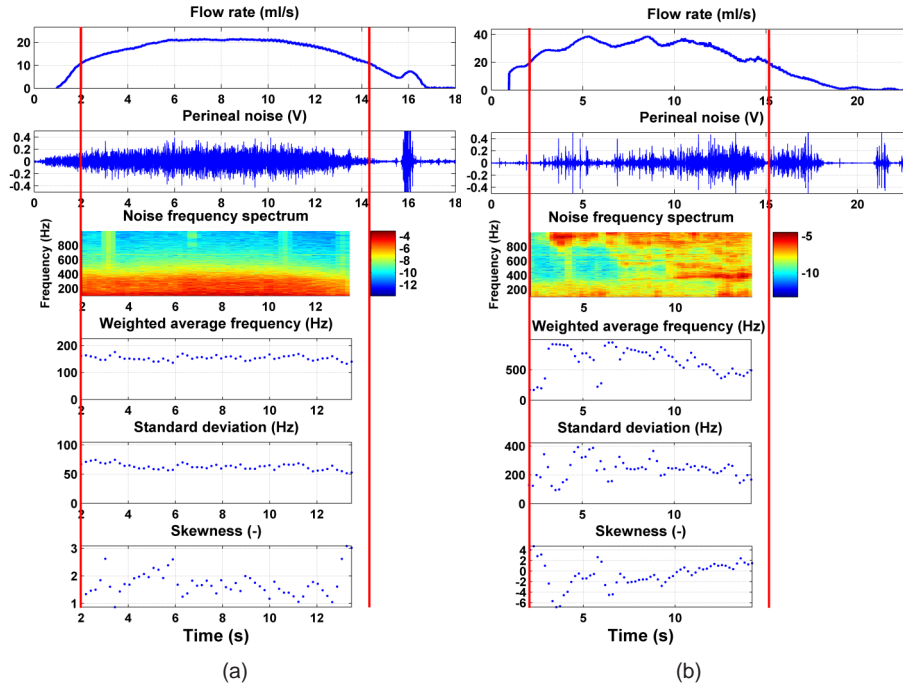


Figure 8.3: Example of a good (left) and bad (right) perineal sound recording. In the example the flow rate (a), perineal sound (b) and the frequency spectrum of the perineal sound (c) are plotted as a function of time. For each frequency (on the vertical axis) in the sound frequency spectrum red represents a high power and blue represents a low power. In the bottom three panels of each example the weighted average frequency (d), the standard deviation (e) and the skewness (f), derived from the sound frequency spectrum, are presented as a function of time.

Conclusion

In this study of perineal sound recording in 16 healthy male volunteers we found that the inter-volunteer variability of the three parameters, derived from the sound frequency spectrum, was significantly smaller than the intra-volunteer variability. We also found that the repeatability of the three parameters was comparable to that of the maximum urinary flow rate. Based on these findings we conclude that perineal sound recording gives repeatable results and that these results are significantly different between volunteers. In combination with the earlier published results from model-experiments the present results increase the probability that perineal sound recording can be used as a very simple and cheap method to non-invasively diagnose BOO. Clinical testing of this method is therefore strongly indicated.

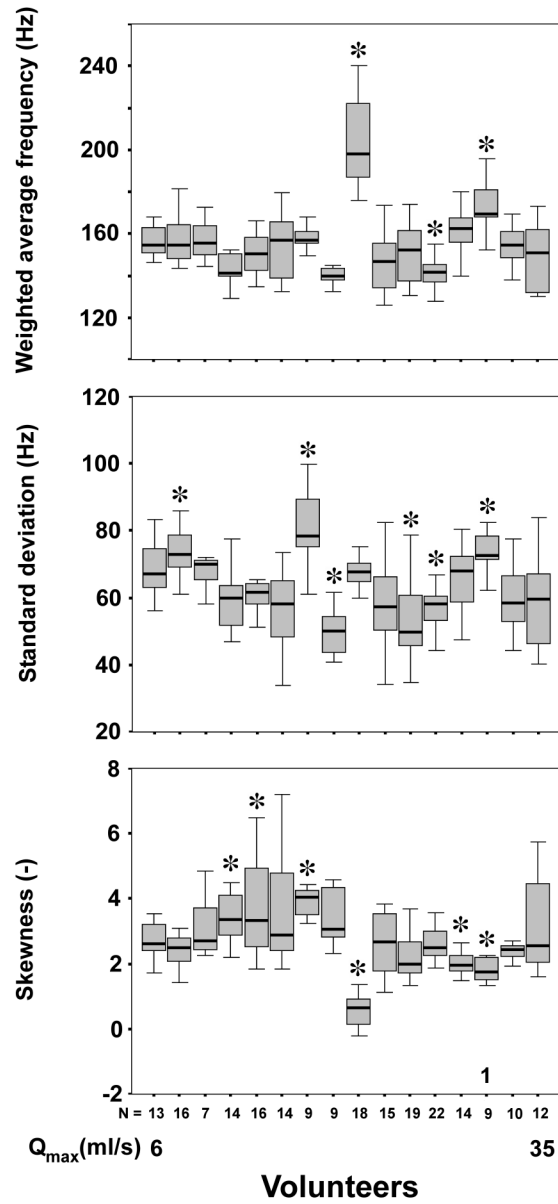


Figure 8.4: Box-whisker plot of the three parameters, derived from the sound frequency spectra of each volunteer. The box represents the median value and the 25th and 75th percentile and the whiskers represent the highest and lowest value. Volunteers that were significantly different from three or more other volunteers (Dunn's test, $p < .05$) are marked with an asterisk. The number 1 identifies a volunteer that was significantly on the top end of the weighted average frequency and the standard deviation scale and on the bottom end of the skewness scale.

Literature

1. P.T. Scardino and J. Kelman. *Prostate book, the complete guide to overcoming prostate cancer, prostatitis and BPH*. Penguin Group, New York, 2006.
2. D.J. Griffiths, K. Höfner, R. van Mastrigt, H.J. Rollema, A. Spångberg, and D.M. Gleason. Standardization of terminology of lower urinary tract: pressure-flow studies of voiding, urethral resistance and urethral obstruction. *Neurourology and Urodynamics*, 16:1–18, 1997.
3. H.C. Klingler, S. Madersbacher, B. Djavan, G. Schatzl, M. Marberger, and C.P. Schmidbauer. Morbidity of the evaluation of the lower urinary tract with transurethral multichannel pressure-flow studies. *Journal of Urology*, 159(1):191–194, 1998.
4. D. Porru, G. Madeddu, G. Campus, I. Montisci, R.M. Scarpa, and E. Usai. Evaluation of morbidity of multi-channel pressure-flow studies. *Neurourology and Urodynamics*, 18(6):647–652, 1999.
5. Y.Y. Ding, H. Ozawa, T. Yokoyama, Y. Nasu, M.B. Chancellor, and H. Kumon. Reliability of color doppler ultrasound urodynamics in the evaluation of bladder outlet obstruction. *Urology*, 56:967–971, 2000.
6. J.J.M. Pel and R. van Mastrigt. The variable outflow resistance catheter: a new method to measure bladder pressure noninvasively. *Journal of Urology*, 165:647–652, 2001.
7. D.J. Griffiths, D. Rix, M. MacDonald, M.J. Drinnan, R.S. Pickard, and P.D. Ramsden. Noninvasive measurement of bladder pressure by controlled inflation of a penile cuff. *Journal of Urology*, 167:1344–1347, 2002.
8. C. Manieri, S.S. Carter, G. Romano, A. Trucchi, M. Valenti, and A. Tubaro. The diagnosis of bladder outlet obstruction in men by ultrasound measurement of bladder wall thickness. *J Urol*, 159(3):761–5, 1998.
9. W.A. Keitzer and G.C. Huffman. The voiding audiograph: a new voiding test. *Journal of Urology*, 95:404–410, 1966.
10. A.J. van Koeveeringe and R. van Mastrigt. A relation between the sound produced by urethral turbulence in patients and objectively assessed subvesical obstruction. *Neurourology and Urodynamics*, 10:442–443, 1991.
11. K. Koiso, R. Nemoto, and M. Ohtani. Urographic studies of benign prostatic hyper trophy. *Journal of Urology*, 145:1071–1077, 1991.
12. T. Idzenga, J.J.M. Pel, and R. van Mastrigt. A biophysical model of the male urethra: Comparing viscoelastic properties of polyvinyl alcohol urethras to male pig urethras. *Neurourology and Urodynamics*, 25(5):451–460, 2006.
13. T. Idzenga, J.J.M. Pel, and R. van Mastrigt. Perineal noise recording related to bladder outlet obstruction? *Neurourology and Urodynamics*, 26(5):623–624, 2007.
14. S.A. Glantz. *Primer of biostatistics*. McGraw-Hill, 5th edition edition, 2002.
15. R. van Mastrigt and J.W. Huang Foen Chung. Comparison of repeatability of non-invasive and invasive urodynamics. *Neurorol Urodyn*, 23(4):317–21, 2004.
16. H. Teriö. Acoustic method for assessment of urethral obstruction: a model study. *Medical and Biological Engineering and Computing*, 29:450–456, 1991.
17. T. Idzenga, J.J.M. Pel, and R. van Mastrigt. Towards an acoustic non-invasive diagnosis of urinary bladder outlet obstruction. *IEEE Transactions on Biomedical Engineering*, Accepted for publication, 2007.

General discussion

Chapter 9

General discussion

Generally, elderly men are prone to developing Lower Urinary Tract Symptoms (LUTS), such as a low flow rate, frequent (nocturnal) voiding and incomplete emptying of the bladder. The two most probable causes for these symptoms are a weakly contracting bladder muscle or an enlarged prostate obstructing the bladder outlet (Bladder Outlet Obstruction or BOO). In most cases, BOO is what causes voiding problems which is, in turn, frequently caused by Benign Prostatic Enlargement (BPE). Prostatic enlargement is very common in the elderly male population. The currently recommended urodynamic method to diagnose BOO is an invasive, time-consuming, and expensive pressure-flow study¹, which can be rather uncomfortable for the patient. In a pressure-flow study a catheter is inserted into the bladder via the urethra. This catheter then measures the bladder pressure upon voiding. Simultaneously, the abdominal pressure is measured by a catheter which is inserted into the rectum. The urinary flow rate is measured using an external flow meter. The combination of maximum flow rate and the detrusor pressure (i.e. bladder minus abdominal pressure) at this maximum flow rate is taken as a measure for the degree of obstruction. For example, a high detrusor pressure generating a low flow rate suggests an obstruction between the bladder and the meatus. This method of diagnosing has several drawbacks. For example, the catheter inserted via the urethra may induce urethral trauma^{2,3} or lead to infections. Several alternative non-invasive urodynamic methods have therefore been developed: the condom-catheter method⁴, the penile-cuff method⁵, penile compression-release technique⁶, Doppler flowmetry⁷ and measurement of changes in Bladder Wall Thickness (BWT)⁸. Another possible method to diagnose BOO is based on sound which is recorded at the urethral wall downstream of the obstruction using a simple hand-held microphone^{17,18}. In this thesis I will study this diagnosing method as it was shown earlier that sound could be recorded at the perineum during voiding and it was hypothesized that the recorded sound was related to the degree of obstruction¹⁹. However, the relation between this sound and the degree of obstruction was yet unknown. It was also unclear how the degree of obstruction could be derived from a perineal sound recording. In this thesis I addressed three research questions. I investigated whether the recorded sound is related to the degree of obstruction in a model urethra. And since they were related, I defined the relationship between the two. I also explored the possibility of perineal sound recording being applied in a clinical setting as a

non-invasive method to diagnose bladder outlet obstruction in patients with lower urinary tract symptoms.

To address the first research question I developed three model urethras with different viscoelastic properties and applied three degrees of obstruction to these models. sound was recorded at three microphone positions downstream of the obstruction. It became clear that, in this experimental setting, the average amplitude of the sound and the essential frequency of its power spectrum were significantly (ANOVA, $p < .001$) related to (among others) the degree of obstruction⁹. It can therefore be concluded that the sound recorded downstream of an obstruction in the model urethra is significantly related to the degree of obstruction. However, the recorded sound also significantly depended on the position of the microphone and the viscoelastic properties of the model urethra. In humans there is a variation in the anatomical viscoelastic properties of the urethra and surrounding tissues, and how these variations influence the recorded sound downstream of the obstruction is not known. When diagnosing patients, one could possibly correct for variations in the microphone position by standardizing the location of measurement, but unfortunately it is not possible to correct for variations in viscoelastic properties. So in order to be able to study the relation between the recorded sound and the degree of obstruction in detail, I developed a model urethra with viscoelastic properties that are comparable to those of the male pig urethra¹⁰. This I accomplished by comparing the viscoelastic properties of multiple model urethras to those of the male pig urethra. The matching model I then used as a model of the human male urethra. A drawback of this method is that the relation between the recorded sound and the degree of obstruction is studied for only one set of viscoelastic properties. Furthermore, it is not yet known how exactly variation in these viscoelastic properties influence the recorded noise.

As an application of the knowledge on constructing model urethras I developed a model urethra which served as a bench model for a neo-urethra in asymptomatic boys with an impaired flow rate after the correction of hypospadias (a birth defect that involves an abnormally placed urinary opening¹⁵). The hypothesis was that the impaired flow rate was possibly caused by an increased stiffness of the neo-urethral wall. I constructed two model urethras with exactly the same stiffness with one of these two model urethras containing a section, which was significantly stiffened (the neo-urethra). I applied different bladder pressures on both models and found that at each bladder pressure the flow rate in the neo-urethral model was significantly lower than in the 'healthy' model urethra. The length of the neo-urethral section had little or no effect on the flow rate. Extrapolated to patients after a hypospadias correction, this means that an impaired flow rate could be caused by low compliance of the newly constructed urethra due to a local aberration of the surrounding tissue. Thus, when an impaired urinary flow rate is observed in asymptomatic boys after a hypospadias correction, low compliance of the newly constructed urethra has to be considered which in itself warrants a watchful waiting policy.

To show that the selected model urethra with viscoelastic properties comparable to the male urethra possesses hydrodynamic behavior comparable to the human urethra, I recorded pressure profiles in the model urethra. These pressure profiles are recorded by withdrawing a catheter through the urethra and measuring the pressure that was necessary to maintain a continuous fluid flow through the catheter. I compared these pressure profiles to those measured in actual patients and also assessed the correlation between the Maximum Urethral Closure Pressure (MUCP, maximum difference between urethral

and bladder pressure²⁰) and the Valsalva Leak Point Pressure (LPP)²⁰) and the Valsalva Leak Point Pressure (LPP)¹⁴. LPP refers to the event of bladder pressure is being increased when the abdominal pressure increases, like in a Valsalva manoeuvre or when one coughs. When leakage is visually observed, the bladder pressure is noted as LPP²⁰. Literature shows this correlation was found to be weak at best^{11–13}, even though both techniques aim at estimating the same parameter, i.e. the maximum bladder pressure the bladder outlet can withstand. I recorded the urethral pressure profile using an open-end catheter and varied the perfusion rate and the withdrawal rate of the catheter. To record these profiles some parameters are to be set such as the size of the catheter, the perfusion rate of the catheter and the rate at which the catheter is withdrawn through the urethra. I used one size catheter and varied the perfusion and withdrawal rate. The shape of the urethral pressure profiles measured in the model urethra was comparable to those in patients. However, I found that MUCP depended significantly on the perfusion rate and the withdrawal rate of the catheter. MUCP increased with increasing perfusion and rate and decreased with increasing withdrawal rate. Only a limited number of combinations of the two gave results comparable to LPP. From these results I concluded that, for application of UPP as an objective measure of continence in the clinic, both the perfusion rate and the withdrawal rate of the catheter need to be carefully chosen and standardized. However, the weak correlation between MUCP and LPP found in patients can be explained as being the result of the fact that the model urethra cannot contract like the urethra *in vivo* can, as muscular components have not been included. The dynamic viscoelastic properties caused by muscle contraction in the urethra *in vivo* could lead to different pressure values, which can contribute to the aforementioned correlation being rather weak. Additionally, when applying the model results to clinical use of UPP, it should be considered that the optimal combination of perfusion and withdrawal rate in the model urethra might not give the most accurate results in the human situation. However, despite the differences between our model urethra and the human male urethra, the comparability of the shape of the pressure profile with those of patients show that the model developed is a realistic biophysical model of the human urethra. That is why I have used this model to further study the relation between recorded sound and the degree of obstruction.

To study the relation between the recorded sound and the degree of obstruction in detail, subject of my second research question, I used the previously developed biophysical model urethra as a bench model¹⁶. I applied a large range of degrees of obstruction to this model urethra with the Bladder Outlet Obstruction Index (BOOI) ranging from –17 to +118. sound was recorded at 12 positions downstream of the obstruction. Results showed that three parameters, derived from the sound frequency spectrum, were uniquely and monotonically related to the degree of obstruction. Therefore it can be said that the relation between the recorded sound and the degree of obstruction is as follows: “The weighted average frequency of the sound frequency spectrum and the standard deviation around this weighted average frequency are negatively and monotonically related to the degree of obstruction whereas the skewness is positively and monotonically related to the degree of obstruction.” These findings thus show that in my realistic model of the urethra the degree of obstruction can be derived from a sound recording at the model wall. The standard deviation of the power spectrum classified the model urethra as obstructed or unobstructed conform the guidelines of the International Continence Society¹

with a success rate of 89%. Therefore, perineal sound recording could possibly be used as a non-invasive method for clinically diagnosing BOO caused by an enlarged prostate. My experience with the model urethras and the experiments I have performed allowed me to construct a measurement setup that can be used to apply perineal sound recording in patients. With this setup I studied the variability and repeatability of perineal sound recording in a population of healthy male volunteers. In this population I found that variation in measurements within volunteers was significantly smaller than variation in measurements between volunteers. This leads to the conclusion that based on perineal sound recording the volunteers could be distinguished. Furthermore, the repeatability of perineal sound recordings in each volunteer was comparable to the repeatability of the maximum flow rate. The conclusions that can be drawn in relation to the variability and repeatability in our population of volunteers lead to a partial answer to my third research question in that perineal sound recording can be applied in the clinic but further clinical validation is necessary to establish the diagnostic value of this method when diagnosing BOO in patients with LUTS. Also, perineal sound recording is very promising as a cheap and simple diagnostic method for BOO in patients with LUTS but further clinical testing will be necessary in order to develop this method into a commercially available device.

In the current field of non-invasive urodynamics the method of perineal sound recording has two major advantages over the other methods. First of all, perineal sound recording does not require any manipulation or interruption of the urinary flow during voiding whereas the condom-catheter, the penile-cuff method and the penile compression-release technique do. Secondly, it measures a primary effect of an enlarged prostate, i.e. turbulence in the urinary stream, whereas changes in bladder wall thickness may or may not be caused by BOO. Perineal sound recording can, however, be compared to Doppler flowmetry. The flow velocity measured with Doppler flowmetry is a property of the urinary stream, which is similar to the turbulence measured in perineal sound recording. The ratio of velocities in the prostatic urethra and the bladder neck is, in fact, a primary effect of an enlarged prostate. However, one drawback of Doppler flowmetry is that it involves expensive ultrasound equipment whereas perineal sound recording only requires a simple and cheap microphone to be attached to the perineum. A second drawback of Doppler flowmetry is that it requires a highly accurate positioning of the transducer to properly image the urinary flow, which involves the use of a robotic arm. The microphone used with perineal sound recording can easily be attached to the perineum and it does not require accurate positioning.

On the other hand, despite the promising results in the model urethra and the healthy male volunteers, one still has to bear in mind that the recorded sound was only found to be related to the degree of obstruction in a biophysical model of the male urethra. In actual humans, anatomical properties of the obstruction or the viscoelastic properties of the urethra may, of course, vary (length, stiffness, shape etc) and model urethras with different viscoelastic properties showed that variation of those properties did influence the produced noise. How this variation influences the generation of sound exactly is yet unknown. Therefore, despite the promising results from the volunteer study, measurements in patients will be necessary in order to establish the diagnostic value of perineal sound recording. In this thesis I have shown that in a realistic biophysical model of the urethra the recorded sound is uniquely and monotonically related to the degree of obstruction. Furthermore, I have shown that sound recordings in volunteers from a healthy volunteer

population are repeatable. And I have shown that volunteers can be distinguished based on a sound recording with a microphone placed at the perineum. Based on these findings an alternative, cheap and patient friendly non-invasive method to diagnose BOO in patients with LUTS is suggested: Perineal sound recording.

Urodynamic outlook

I have shown that under controlled circumstances sound recorded downstream of an obstruction are significantly and monotonically related to the degree of obstruction. I have also shown that this method is repeatable within volunteers in a volunteer-population and that measurements between volunteers differ significantly. The next step is to apply perineal sound recording to a population of patients. These patients must be diagnosed using the invasive pressure-flow study as the 'golden standard' for assessment of the degree of obstruction in patients with LUTS. Before these patients undergo a pressure-flow study they usually do a free-flow measurement. It is this free-flow measurement that can easily be combined with the perineal sound recording method. This way, developed parameters can be compared to standard measures for urethral resistance which will allow for an assessment of the clinical applicability of the method.

Several invasive and non-invasive methods have been developed to diagnose BOO^{1,4-8,16,20} but a significant disadvantage of these methods is that most of them only diagnose the presence of an obstruction in the lower urinary tract but not the location of the obstruction. Even perineal sound recording and Doppler flowmetry only give an indication of whether the obstruction is located at the prostatic urethra or not. The only way to establish the actual location of an obstruction is by applying Urethral Pressure Profilometry (UPP), i.e. by retracting a catheter from the bladder through the urethra and simultaneously recording the pressure in this catheter along the urethra. When this pressure increases dramatically this indicates that an obstruction is present at the location in the urethra. However, this method is invasive and is also notoriously unreliable²¹⁻²⁵. A better approach for a detailed assessment of the location of an obstruction might be the measurement of the dynamic behavior of the lower urinary tract during voiding using transperineal or transabdominal ultrasound imaging (elastography). Originally, elastography was developed for the detection of stiffer masses in soft tissue, i.e. tumors. The method is based on measuring the strain in tissue upon mechanical stimulation, e.g. compression of breast tissue with a carcinoma *in situ*. Ultrasonic data are acquired before and after compression and analytical techniques, e.g. cross-correlation of images before and after compression, are used to calculate the strain in different areas of the breast tissue. The resulting strain image is called an elastogram. Konofagou *et al.*^{26,27} applied elastography in the field of cardiology with the purpose of detecting cardiac dysfunction. Strain in the cardiac muscle, induced by the pumping of blood, was imaged to assess the mechanical function of the muscle. Elastographic imaging has also been studied to assess atherosclerotic plaques using intravascular ultrasound (IVUS)²⁸. In this study, the movement of the arterial wall, which is caused by the variation in blood pressure, is monitored and from the resulting elastograms of the arterial wall the plaques and their elastic properties could be derived. A similar technique can be applied to assess the location of an obstruction in the urethra. During voiding, the urinary flow through the urethra exerts

radial pressure to the urethral tissue which induces strain in the bladder neck, the prostatic urethra and further downstream the urethra. By using motion-estimation software, this strain can possibly be monitored. Sections of the urethra with less strain upon voiding than the surrounding tissue would implicate little relaxation in those sections. That way, the degree of resistance of the urethra along its length could be mapped.

Whenever a general practitioner has used the cheap and simple method of perineal sound recording to diagnose a possible prostatic obstruction in a patient with LUTS, the patient could then be referred to a diagnostic center for further detailed research, e.g. using elastographic imaging of the lower urinary tract.

Literature

1. D.J. Griffiths, K. Höfner, R. van Mastrigt, H.J. Rollema, A. Spångberg, and D.M. Gleason. Standardization of terminology of lower urinary tract: pressure-flow studies of voiding, urethral resistance and urethral obstruction. *Neurourology and Urodynamics*, 16:1–18, 1997.
2. H.C. Klingler, S. Madersbacher, B. Djavan, G. Schatzl, M. Marberger, and C.P. Schmidbauer. Morbidity of the evaluation of the lower urinary tract with transurethral multichannel pressure-flow studies. *Journal of Urology*, 159(1):191–194, 1998.
3. D. Porru, G. Madeddu, G. Campus, I. Montisci, R.M. Scarpa, and E. Usai. Evaluation of morbidity of multi-channel pressure-flow studies. *Neurourology and Urodynamics*, 18(6):647–652, 1999.
4. J.J.M. Pel and R. van Mastrigt. The variable outflow resistance catheter: a new method to measure bladder pressure noninvasively. *Journal of Urology*, 165:647–652, 2001.
5. D.J. Griffiths, D. Rix, M. MacDonald, M.J. Drinnan, R.S. Pickard, and P.D. Ramsden. Noninvasive measurement of bladder pressure by controlled inflation of a penile cuff. *Journal of Urology*, 167:1344–1347, 2002.
6. M.P. Sullivan and V.S. Yalla. Penile urethral compression-release maneuver as a non-invasive screening test for diagnosing prostatic obstruction. *Neurourology and Urodynamics*, 19:657–669, 2000.
7. H. Ozawa, H. Kumon, T. Yokoyama, T. Watanabe, and M.B. Chancellor. Development of noninvasive velocity flow video urodynamics using doppler sonography. part ii: clinical application in bladder outlet obstruction. *J Urol*, 160(5):1792–6, 1998.
8. C. Manieri, S. S. Carter, G. Romano, A. Trucchi, M. Valenti, and A. Tubaro. The diagnosis of bladder outlet obstruction in men by ultrasound measurement of bladder wall thickness. *J Urol*, 159(3):761–5, 1998.
9. T. Idzenga, J.J.M. Pel, R.A. Baldewsing, and R. Mastrigt. Perineal noise recording as a non-invasive diagnostic method of urinary bladder outlet obstruction: a study in polyvinyl alcohol and silicone model urethras. *Neurourology and Urodynamics*, 24(4):381–8, 2005.
10. T. Idzenga, J.J.M. Pel, and R. van Mastrigt. A biophysical model of the male urethra: Comparing viscoelastic properties of polyvinyl alcohol urethras to male pig urethras. *Neurourology and Urodynamics*, 25(5):451–460, 2006.
11. Jr. Feldner, P.C., L.R. Bezerra, R.A. de Castro, M.G. Sartori, E.C. Baracat, G.R.

- de Lima, and M.J. Girao. Correlation between valsalva leak point pressure and maximal urethral closure pressure in women with stress urinary incontinence. *Int Urogynecol J Pelvic Floor Dysfunct*, 15(3):194–7, 2004.
12. M.T. McLennan, C.F. Melick, and A.E. Bent. Leak-point pressure: clinical application of values at two different volumes. *Int Urogynecol J Pelvic Floor Dysfunct*, 11(3):136–41, 2000.
 13. C.W. Nager, J.A. Schulz, S.L. Stanton, and A. Monga. Correlation of urethral closure pressure, leak-point pressure and incontinence severity measures. *Int Urogynecol J Pelvic Floor Dysfunct*, 12(6):395–400, 2001.
 14. T. Idzenga, J.J.M. Pel, and R. van Mastrigt. Fluid perfused urethral pressure profilometry and valsalva leak point pressure: a comparative study in a biophysical model of the urethra. *World J Urol*, 25(4):423–9, 2007.
 15. T. Idzenga, D.J. Kok, J.J.M. Pel, R. van Mastrigt, and K.P. Wolffenbuttel. Is the impaired flow after hypospadias correction due to increased urethral stiffness? *Journal of Pediatric Urology*, 2(4):299–303, 2006.
 16. T. Idzenga, J.J.M. Pel, and R. van Mastrigt. Towards an acoustic non-invasive diagnosis of urinary bladder outlet obstruction. *IEEE Transactions on Biomedical Engineering*, Submitted, 2007.
 17. A.J. van Koevinge and R. van Mastrigt. A relation between the sound produced by urethral turbulence in patients and objectively assessed subvesical obstruction. *Neurourology and Urodynamics*, 10:442–443, 1991.
 18. H. Teriö. Acoustic method for assessment of urethral obstruction: a model study. *Medical and Biological Engineering and Computing*, 29:450–456, 1991.
 19. W.E. Bradley, B.P. Brockway, and G.W. Timm. Auscultation of urinary flow. *Journal of Urology*, 118:73–75, 1977.
 20. P. Abrams, L. Cardozo, M. Fall, D. Griffiths, P. Rosier, U. Ulmsten, P. van Kerrebroeck, A. Victor, and A. Wein. The standardisation of terminology of lower urinary tract function: report from the standardisation sub-committee of the international continence society. *Neurourol Urodyn*, 21(2):167–78, 2002.
 21. R. Bruskewitz and S. Raz. Urethral pressure profile using microtip catheter in females. *Urology*, 14(3):303–7, 1979.
 22. D.J. Griffiths. The pressure within a collapsed tube, with special reference to urethral pressure. *Phys. Med. Biol.*, 30(9):951–963, 1985.
 23. R.S. Anderson, A.M. Shepherd, and R.C.L. Feneley. Microtransducer urethral profile methodology: variations caused by transducer orientation. *Journal of Urology*, 130:727–731, 1983.
 24. W. Schaefer. Some biomechanical aspects of continence function. *Scand J Urol Nephrol Suppl*, (207):44–60; discussion 106–25, 2001.
 25. P. Abrams, L. Cardozo, S. Khoury, and A. Wein, editors. *Incontinence: Basics & Evaluation, Chapter 11*, volume 1. Health Publication Ltd, 2005.
 26. E.E. Konofagou. Quo vadis elasticity imaging? *Ultrasonics*, 42(1-9):331–6, 2004.
 27. E.E. Konofagou, J. D'Hooge, and J. Ophir. Myocardial elastography—a feasibility study in vivo. *Ultrasound Med Biol*, 28(4):475–82, 2002.
 28. R.A. Baldewsing, J.A. Schaar, C.L. de Korte, F. Mastik, P.W. Serruys, and A.F. van der Steen. Intravascular ultrasound elastography: A clinician's tool for assessing vulnerability and material composition of plaques. *Stud Health Technol Inform*,

113:75–96, 2005.

Summary

Summary

Elderly men often develop Lower Urinary Tract Symptoms (LUTS), such as a weak urinary stream, frequent (nocturnal) voiding and incomplete emptying of the bladder. The two most probable causes for these symptoms are a weakly contracting bladder muscle or an enlarged prostate resulting in Bladder Outlet Obstruction (BOO). Enlargement of the prostate (Benign Prostatic Enlargement or BPE) is very common in elderly men. More than two thirds (68%) of men over the age of fifty have histological evidence of BPE. At present, to diagnose BOO an invasive pressure flow study is recommended, i.e. measurement of urinary flow rate in combination with invasive measurement of bladder pressure during voiding using a catheter inserted via the urethra. This method is time-consuming, expensive and uncomfortable to the patient. The urethral catheter may induce urethral trauma and urinary tract infection. I studied perineal sound recording as an alternative, non-invasive method to diagnose BOO. The method of perineal sound recording is based on turbulence in the urinary stream caused by an obstruction (enlarged prostate) of the urethra. The pressure variations at the urethral wall (as a result of the turbulence) are recorded using a cheap and simple contact-microphone placed at the perineum (between scrotum and rectum).

In **Chapter 2** I confirmed the hypothesis that the sound recorded downstream of an obstruction in a biophysical model of the urethra (made from a 10% aqueous solution of PolyVinyl Alcohol (PVA cryogel)) is related to the degree of obstruction. To test possible factors contributing to variation in recorded sound I used three model urethras with different viscoelastic properties and recorded sound at three different positions downstream of the obstruction. I applied three different degrees of obstruction and found that the average amplitude of the recorded sound and the weighted average frequency of the sound frequency spectrum were significantly related to the degree of obstruction. Furthermore, they were significantly related to the microphone position and the viscoelastic properties of the model urethra. Based on these results perineal sound recording shows good potential as an alternative method for diagnosing BOO. However, the microphone position and the viscoelastic properties of the model urethra need to be taken into account.

To account for the latter I developed in **Chapter 3** a biophysical model of the human male urethra with realistic viscoelastic properties. I made various model urethras from PVA cryogel with different viscoelastic properties and compared them to those of the male pig urethra, which is physiologically comparable to the male human urethra. I measured the viscoelastic properties by applying strain to the urethral wall in a stepwise manner, injected a known volume of water in a closed urethra and recorded its pressure response. I fitted the step-response of a mechanical model to this pressure response and derived the

viscoelastic properties from the coefficients of the fitted step-response. A uniform model urethra that was freeze-thawed three times, with a Y-shaped flow channel, was found to best represent the male pig urethra. This model was considered the most realistic model of the human male urethra.

In **Chapter 4** I used the model urethra as a bench model in pediatric urology. A low flow rate without clinical symptoms is commonly found in boys after hypospadias (a birth defect that involves an abnormally placed urinary opening) correction. Urethral calibration usually shows no abnormalities. I investigated whether this flow rate impairment might be caused by increased neo-urethral wall-stiffness. From PVA cryogel I constructed two models of the urethra, a hypospadias model and a control model. Both models had a constant and equal inner diameter and equal viscoelastic properties. The hypospadias model had a less compliant distal segment mimicking the distal neo-urethra after hypospadias correction. In both models flow rate was recorded as a function of bladder pressure. In a physiological range of bladder pressures (10-130 cm H₂O) the mean flow rate (± 1 s.e.m.) in the hypospadias model was 2.8 ± 0.3 ml/s, significantly lower ($p < .05$) than in the control model (5.4 ± 0.6 ml/s). Shortening of the hypospadias model showed some increase in flow rate, however not statistically significant. In the control model this also did not cause significant variation in flow rate. These results showed that a low compliant segment of a urethral model reduced the flow rate. Extrapolating these results to asymptomatic boys with a low urinary flow rate after hypospadias correction might justify a watchful waiting policy.

In **Chapter 5** I used this model urethra to study the correlation between Maximum Urethral Closure Pressure (MUCP) and Valsalva Leak Point Pressure (LPP) to validate the model clinically, i.e. to compare its behavior to that of the male human urethra *in situ*. In patients this correlation is weak at best ($r = 0.22-0.50$) with different values used for perfusion and withdrawal rate of the catheter in measuring MUCP. I applied differently sized pressure zones and different degrees of resistance to the model urethra by stepwise inflating three types of blood pressure cuff placed around the model. At each degree of resistance I measured detrusor LPP, an *in vitro* equivalent of Valsalva LPP. Subsequently, I recorded the urethral pressure profile using a water-perfused 5F end-hole catheter at four withdrawal rates and five perfusion rates and calculated MUCP. I tested the dependence of LPP on the pressure zone length and MUCP on the perfusion rate, the withdrawal rate and the pressure zone length using Analysis of Variance (ANOVA) and tested the correlation between LPP and MUCP. The urethral pressure profiles were found to be similar to those measured in patients. However, MUCP significantly depended (ANOVA, $p < .01$) on perfusion rate, withdrawal rate and pressure zone length. MUCP increased with increasing cuff pressure, increased with increasing perfusion rate, and decreased with increasing withdrawal rate. LPP did not depend significantly on the pressure zone length (ANOVA, $p = 0.80$) and increased linearly with increasing cuff pressure. In our model urethra MUCP only accurately reflected urethral resistance for a very limited number of combinations of perfusion rate and withdrawal rate. LPP reflected urethral resistance independent of the type of pressure zone.

After validation of the developed model urethra I studied in **Chapter 6** the relation between recorded sound and the degree of obstruction in more detail using the validated model urethra. I applied a wide range of degrees of obstruction: Bladder Outlet Obstruction Index (BOOI) ranged from -17 to $+118$. In patients BOOI less than 20 indicates

non-obstructed. The patient is diagnosed as obstructed when BOOI is higher than 40. If BOOI is between 20 and 40 the patient is diagnosed as equivocal and further testing is advised. I recorded sound at 1 to 12 cm downstream from the obstruction and found that the average amplitude was not uniquely and monotonically related to the degree of obstruction and therefore the average amplitude is not suitable for use as a measure for the degree of obstruction. The sound frequency spectrum (characterized by its weighted average frequency, standard deviation and skewness), however, was uniquely and monotonically related to the degree of obstruction. The weighted average frequency and the standard deviation decreased with increasing degree of obstruction and the skewness increased. Of the latter three parameters the standard deviation was found to be the best predictor of BOO (89% correct classification). These findings show that the degree of obstruction can be derived from a sound recording at the wall of our model urethra.

In **Chapter 7** I studied the applicability of perineal sound recording in a population of 16 healthy male volunteers. I studied the variability and repeatability of perineal sound recording as a possible non-invasive method for diagnosing BOO. The volunteers had a flat age-distribution (22-62 years), a median International Prostate Symptom Score (IPSS) of 1 (range: 0-18) and voided at least ten times. From each perineal sound recording the frequency spectrum was calculated and characterized by its weighted average frequency, standard deviation and skewness. For each parameter the variability within volunteers was significantly smaller than the variability between volunteers (Kruskal-Wallis, $p < .05$), therefore volunteers could be distinguished based on a perineal sound recording. And for each parameter more than one volunteer was significantly different from three or more volunteers (Dunn's test, $p < .05$). The repeatability of the three parameters was comparable to that of the maximum flow rate. From these findings and the three parameters being uniquely and monotonically related to the degree of obstruction I conclude that perineal sound recording is a promising method for a simple, quick non-invasive diagnosis of BOO and clinical validation is strongly indicated.

Samenvatting

Samenvatting

Bij ouder wordende mannen neemt de prostaat gemiddeld toe in volume (goedaardige prostaatvergroting of BPE). De prostaat zit net onder de blaas en omsluit de plasbuis. Een vergrote prostaat kan zo de plasbuis dichtknijpen en dit kan leiden tot plasklachten, zoals een zwakke urinestroom, frequent (ook 's nachts) plassen en het gevoel de blaas niet volledig leeg te plassen. Een tweede mogelijke oorzaak voor dezelfde plasklachten kan een zwak werkende blaasspier zijn. De huidige meest gebruikte methode om te onderzoeken of de plasklachten veroorzaakt worden door een vergrote prostaat of een zwakke blaasspier is het meten van de blaasdruk tezamen met de urinestroom. Om de blaasdruk te meten wordt een katheter via de plasbuis in de blaas gebracht. Dit is een tijdrovend en pijnlijk onderzoek en erg onprettig voor de patiënt. Bovendien kan de katheter infecties en verwondingen veroorzaken in de lagere urinewegen. Als een alternatief voor deze methode wordt in dit proefschrift het perineaal meten van geluid tijdens het plassen gepresenteerd. De methode is gebaseerd op wervelingen (turbulentie) in de urinestroom die veroorzaakt worden door de vernauwing in de plasbuis door een vergrote prostaat. Deze wervelingen veroorzaken drukveranderingen op de wand van de plasbuis en die kunnen op hun beurt bij mannen als geluid worden opgenomen met een microfoon tegen het perineum (tussen scrotum en rectum) tijdens het plassen. In dit proefschrift laat ik in een model zien dat de graad van vernauwing uit het aldus opgenomen geluid is af te leiden. En ik laat een toepassing zien in een groep vrijwilligers.

Ik heb in **Hoofdstuk 2** in een aantal modellen, gemaakt van een oplossing van het polymeer PolyVinyl Alcohol (PVA), de hypothese getest dat het opgenomen geluid gerelateerd is aan de graad van vernauwing. Hierin zijn een aantal factoren onderzocht die mogelijk een invloed hebben op het geluid: de graad van vernauwing, de viscoelastische eigenschappen en de afstand tussen microfoon en vernauwing. In drie modellen met verschillende viscoelastische eigenschappen heb ik drie graden van vernauwing aangebracht. Vervolgens heb ik in deze modellen op drie afstanden van de vernauwing het geluid gemeten tijdens stroming van water door het model. Mijn bevinding was dat de amplitude en het frequentie spectrum (gemiddelde gewogen frequentie) van het geluid beiden statistisch significant van de graad van vernauwing afhingen, echter nog niet dat de ene uit de andere berekend kan worden. De amplitude en het frequentie spectrum bleken echter ook afhankelijk te zijn van de viscoelastische eigenschappen en de positie van de microfoon.

Vanwege de laatste afhankelijkheid heb ik in **Hoofdstuk 3** een realistisch model ontwikkeld met viscoelastische eigenschappen die vergelijkbaar zijn met die van de menselijke plasbuis. Om de eigenschappen van de laatste te bepalen heb ik de plasbuis van

het mannetjes varken gebruikt. Varkens hebben veel fysiologische overeenkomsten met de mens. Van een groot aantal verschillende modellen heb ik de viscoelastische eigenschappen gemeten en vergeleken met de varkensplasbuis. Dit heb ik gedaan door een klein volume water in een zeer kort tijdsbestek in de afgesloten plasbuis te injecteren. Hierdoor werd de druk in de plasbuis stapsgewijs verhoogd. Hoe de wand dan wordt opgerekt is afhankelijk van de viscoelastische eigenschappen. Deze eigenschappen zijn af te leiden uit het verloop van de druk in de plasbuis na injectie. Aan de drukresponsie in de plasbuis werd de responsie van een mechanisch model gefit, zodat ik uit de fit-coëfficiënten de viscoelastische eigenschappen kon berekenen. Het model dat de meeste overeenkomsten met de varkensplasbuis vertoonde heb ik verder gebruikt als het meest realistische model van een menselijke plasbuis.

In jonge patiënten met hypospadie wordt er vaak na een hypospadie-correctie nog steeds een zwakke urinestroom gevonden. Hypospadie is een aangeboren afwijking waarbij de locatie van de urine uitstroom-opening afwijkt, bijvoorbeeld halverwege de penis en niet aan het uiteinde. Dit wordt veelal gecorrigeerd door in het overige deel van de penis een nieuw stuk plasbuis te maken. De oorzaak van de zwakke urinestroom na correctie is echter onbekend. Een hypothese is dat de zwakke urinestroom wordt veroorzaakt doordat het nieuwe stuk plasbuis een verhoogde stijfheid heeft. In **Hoofdstuk 4** heb ik twee modellen gemaakt met identieke stijfheid en inwendige diameter. Een van de modellen, het hypospadie-model, had een stukje met verhoogde stijfheid, dat het nieuwe stuk plasbuis nabootst. In beide modellen heb ik de urinestroom gemeten als functie van de blaasdruk. In een fysiologische range van blaasdrukken (10-130 cm H₂O, ter vergelijking in patiënten worden blaasdrukken gemeten tussen de 10 en 180 cm H₂O) was de gemiddelde urinestroom (± 1 sem) in het hypospadie-model 2.8 ± 0.3 ml/s. Dit was significant lager dan de urinestroom in het controle model (5.4 ± 0.6 ml/s). Bij het inkorten van beide modellen was er geen significante verandering in de urinestroom. Deze resultaten laten zien dat een nieuwe stukje plasbuis met verhoogde stijfheid de oorzaak kan zijn voor een zwakke urinestroom. Bij asymptomatische jongens met een zwakke urinestroom is dan een 'watchful waiting' beleid gerechtvaardigd.

Voor een klinische validatie van het ontwikkelde model heb ik in **Hoofdstuk 5** het model vergeleken met de menselijke plasbuis *in situ* met behulp van de Valsalva lekdruk en het urethrale drukprofiel onder variërende omstandigheden. Bij het meten van de Valsalva lekdruk wordt de druk in buikholte geleidelijk verhoogd door bijvoorbeeld tegen de rug van de hand te blazen (Valsalva manoeuvre). De druk waarbij de persoon urine verliest is de lekdruk (Leak Point Pressure of LPP). Het urethrale drukprofiel wordt gemeten door een katheter door de plasbuis terug te trekken en op elke positie de druk in de plasbuis te meten. De maat daarvoor is de druk die nodig is om een vloeistof met een constant debiet (perfusiesnelheid) door de katheter te laten stromen. Het maximale verschil tussen de druk in de plasbuis en die in de blaas is dan de maximale openingsdruk (Maximum Urethral Closure pressure of MUCP). Beide methoden geven een maat voor de maximale blaasdruk die de plasbuis kan weerstaan zonder lekkage. In patiënten is de correlatie tussen de twee methoden echter mager ($r = 0.22-0.50$) en bovendien wordt MUCP gemeten met verschillende waarden voor de perfusie- en terugtrekingsnelheid van de gebruikte katheter. Om deze magere correlatie onder de loep te nemen heb ik in het model verschillende graden van weerstand aangebracht door verschillende cuffs rondom het model aan te brengen en de druk hierin in stappen te verhogen. Bij elke druk in de cuff

heb ik LPP gemeten en het urethraal drukprofiel bij verschillende perfusie snelheden en terugtreksnelheden. De urethrale drukprofielen in het model hadden veel overeenkomst met de drukprofielen gemeten in patiënten. Echter, mijn bevinding was dat de berekende MUCP afhankelijk was van zowel de perfusie snelheid als de terugtreksnelheid. MUCP nam toe bij een toename in cuff-druk en perfusie snelheid en af wanneer de katheter sneller door het model wordt getrokken. LPP nam toe met een toename in cuff-druk. Bij slechts een gelimiteerd aantal combinaties van perfusie- en terugtreksnelheid was het urethraal drukprofiel een realistische maat voor de weerstand in het model. Deze parameters dienen dus zorgvuldig gekozen worden. LPP was een betere maat voor de weerstand.

Met het aldus gevalideerde model van de plasbuis heb ik in **Hoofdstuk 6** de relatie tussen gemeten geluid en de graad van vernauwing in detail bestudeerd. In het model heb ik een grote range van vernauwingen gecreëerd met een kleine cuff om het model door de druk in deze cuff in stappen te verhogen. De graad van vernauwing werd uitgedrukt in de Bladder Outlet Obstruction Index (BOOI). Deze index is samengesteld uit het drukverschil tussen begin en eind van het model (incl. de cuff) minus twee maal de urinestroom door het model. Patiënten met een BOOI-waarde kleiner dan 20 worden gediagnosticeerd als niet-geobstrueerd en met een waarde groter dan 40 als geobstrueerd. Bij een BOOI-waarde tussen 20 en 40 wordt de patiënt verder onderzocht. In het model varieerde deze index van -17 tot $+118$. Ik heb vervolgens geluid gemeten op 1 tot 12 cm afstand van de vernauwing. De amplitude van het geluid was niet uniek and monotoon gerelateerd aan BOOI. Bij een toename in BOOI stijgt de amplitude gevolgd door een daling. Bij een lage amplitude kan BOOI dus zowel hoog als laag zijn. Daarom is deze parameter niet bruikbaar als maat voor de vernauwing van de plasbuis. Het frequentie spectrum van het geluid (gekaracteriseerd door de gewogen gemiddelde frequentie, de standaard deviatie en de 'skewness' van het spectrum) was echter wel uniek en monotoon gerelateerd aan de graad van vernauwing. Bij een toename in BOOI daalden de gemiddelde frequentie en de standaard deviatie en bij een toenemende BOOI-waarde nam de skewness van het spectrum toe. De standaard deviatie was van deze drie de beste voorspeller voor een verhoogde blaasuitgangswaerstand. In 89% van de gevallen classificeerde deze parameter het model correct als geobstrueerd/niet-geobstrueerd. Deze resultaten laten zien dat in een model van de plasbuis de graad van vernauwing kan worden afgeleid uit een geluidsoptname met een microfoon tegen de modelwand tijdens het 'plassen'.

De mogelijkheid van toepassing van deze methode in patiënten voor diagnose van een prostaat vernauwing heb ik in **Hoofdstuk 7** getest in een groep vrijwilligers. Deze bestond uit 16 vrijwilligers tussen 22 en 62 jaar. Als indicatie van zijn urologische conditie heeft iedere vrijwilliger een Internationale Prostaat Symptoom Score (IPSS) enquête ingevuld. Een IPSS-score tussen 0 en 7 geeft aan dat de persoon geen tot lichte klachten heeft, tussen 8 en 19 matige tot milde klachten en tussen 20 en 35 ernstige klachten. De mediane IPSS score was 1 (variërend tussen 0 en 18). Elke vrijwilliger plaste ten minste 10 keer met een microfoon tegen het perineum gedrukt. In deze groep was de variatie van de in het voorgaande genoemde parameters binnen een vrijwilliger significant kleiner dan de variatie tussen de vrijwilligers (Kruskal-Wallis, $p < .05$). Op basis van het opgenomen geluid kon er dus een onderscheid gemaakt worden tussen de vrijwilligers. Bovendien geldt voor iedere parameter dat deze in een aantal vrijwilligers significant verschillend was van dezelfde parameter in drie of meer andere vrijwilligers (Dunn's test, $p < .05$).

Samenvatting

Verder is de variatie van de drie parameters tussen metingen in een enkele vrijwilliger vergelijkbaar met die van de maximale urinestroom.

De algemene conclusie van het onderzoek gepresenteerd in dit proefschrift is dat het geluid opgenomen stroomafwaarts van een vernauwing in een model plasbuis gerelateerd is aan de graad van vernauwing. Drie parameters, afgeleid uit het frequentiespectrum van het geluid, zijn uniek en monotoon gerelateerd aan de graad van vernauwing. Dit betekent dat uit een geluidsopname in de model plasbuis de graad van vernauwing berekend kan worden. Verder is het mogelijk om een onderscheid te maken tussen verschillende vrijwilligers op basis van een geluidsmeting. Het perineaal meten van geluid tijdens plassen is dus een veelbelovende methode voor een snelle en simpele diagnose van een vernauwing in de plasbuis door een vergrote prostaat bij mannen met plasklachten. Klinische validatie van deze methode wordt ten zeerste aangeraden.

Nawoord

Nawoord

Het zit erop

Allereerst wil ik u, de lezer, van harte bedanken voor de tijd die u heeft genomen om dit proefschrift van begin tot eind te lezen. Het is een interessante ontdekkingstocht geweest, althans voor mij. Dit proefschrift zou echter niet tot stand zijn gekomen als ik het alleen had willen doen, er zit een bijdrage van velen in. Hoe ga je te werk als je alle mensen wil bedanken die hebben bijgedragen? Dit zijn er veel, dus voor deze mensen: collega's, vrienden en passende vrijwilligers van harte bedankt! Er zijn echter een aantal personen die ik in het bijzonder wil bedanken.

Te beginnen met diegenen die het mogelijk hebben gemaakt dat ik aan dit avontuur kon beginnen: mijn ouders. Bedankt voor de fundering Bouwe en Maya.

Het avontuur werd mogelijk gemaakt door mijn promotor, jij zette de grote lijnen uit. Deze lijnen waren in het begin voornamelijk rood. De manuscripten die ik aan jou gaf voor correctie kwamen rood terug. De door mij getikte letters waren niet meer terug te vinden: het omstreden rode-pen proces. Geleidelijk werd dit minder, ik heb hier blijkbaar iets van geleerd en ben meer gestructureerd gaan werken. Bedankt Ron.

Toen ik hieraan begon kwam ik onwetend van de universiteit en was onbekend met onderzoek bij de afdeling Urologie van een academisch ziekenhuis. Dan heb je iemand nodig die je wegwijs maakt in het doen van urologisch onderzoek. Bedankt Johan.

Voor het schaven aan het engels in dit proefschrift wil ik mijn zusje hartelijk bedanken, een studie Engels kan toch goed van pas komen. Bedankt Marianne.

Tenslotte blijft er nog een persoon over. Annika, we zijn tezamen aan dit avontuur begonnen, jij aan jouw onderzoek en ik aan het mijne. Ik kon aan jouw onderzoek geen touw vastknopen en jij niet aan het mijne, maar de problemen waar we in ons onderzoek tegenaan liepen begrepen we des te beter. Bedankt voor het klankbord, we zullen dit avontuur tezamen afmaken.

Hartelijk bedankt,

Tim.

Curriculum vitae

Curriculum Vitae

Tim Idzenga werd op 5 februari 1977 geboren te Nijmegen. Het eerste jaar van zijn Gymnasium volgde hij op het Stedelijk Gymnasium te Nijmegen. In het begin van het tweede jaar verhuisde hij naar Zwolle en vervolgde zijn opleiding aan het Gymnasium Celeanum te Zwolle. Na in 1995 aldaar zijn diploma te hebben behaald begon hij aan de studie Technische Natuurkunde aan de Universiteit Twente te Enschede. Als onderdeel van het curriculum heeft hij een stage-opdracht gedaan bij het Gray Cancer Institute te London, UK onder leiding van Prof. Boris Vojnovic. Op 19 Maart 2003 rondde hij de studie Technische Natuurkunde bij de leerstoel Biofysische Technieken. Op 1 April van datzelfde jaar begon hij als promovendus bij de afdeling Urologie, sector Furore van het Erasmus MC te Rotterdam. Daar heeft hij onder leiding van Prof. dr. ir. Ron van Mastrigt het onderzoek uitgevoerd dat in dit proefschrift staat beschreven.

